Optimal Power Control in DFIG Turbine Based Wind Farm Considering Wake Effect and Lifetime

Tian, Jie

DOI (link to publication from Publisher):
10.5278/vbn.phd.eng.00010

Publication date:
2017

Document Version
Publisher's PDF, also known as Version of record

OPTIMAL POWER CONTROL IN DFIG TURBINE BASED WIND FARM CONSIDERING WAKE EFFECT AND LIFETIME

BY
JIE TIAN

DISSERTATION SUBMITTED 2017

AALBORG UNIVERSITY
DENMARK

OPTIMAL POWER CONTROL IN DFIG TURBINE BASED WIND FARM CONSIDERING WAKE EFFECT AND LIFETIME

by

Jie Tian

AALBORG UNIVERSITY
DENMARK

Dissertation submitted 2017

.

Thesis submitted: April 9, 2017
PhD supervisor: Prof. ZHE CHEN,
Aalborg University
Assistant PhD supervisor: Dr. CHI SU, Prof. FREDE BLAABJERG,
Aalborg University
Prof. HONGHUA XU,
Chinese Academy of Sciences

PhD committee: Prof. WEI-JEN LEE,
University of Texas at Arlington
Prof. BIKASH CHANDRA PAL,
Imperial College London
Prof. FILIPE MIGUEL FARIA DA SILVA,
Aalborg University

PhD Series: Faculty of Engineering and Science, Aalborg University

ISSN (online): 2446- 1636
ISBN (online): 978-87-7112-942-7

Published by:
Aalborg University Press
Skjernvej 4A, 2nd floor
DK – 9220 Aalborg Øst
Phone: +45 99407140
aauf@forlag.aau.dk
forlag.aau.dk

Printed in Denmark by Rosendahls, 2017

CV

Jie Tian received the B.Eng. and M.Sc. degrees from the Institute of Electrical Engineering, Yanshan University, China, in Jul, 2005 and Jan, 2011 respectively. He is now a PhD candidate with the Department of Energy Technology, Aalborg University, Aalborg, Denmark. He is working on the advanced coordinative control of the wind energy conversion system.

He worked as a Laboratory Technician in the Institute of Electrical Engineering, Yanshan University from Jul, 2005 to Jan, 2012 and as a Research Assistant in the Department of Energy Technology, Aalborg University from Sep, 2016 to Dec, 2016.

ENGLISH SUMMARY

In recent years, the large scale wind farm is increasingly integrated into the power grid worldwide and trends to move from onshore to offshore. In a wind farm, due to the wake effect, the upstream wind turbine causes the power loss to its downstream wind turbines. According to a filed survey in large scale offshore wind farm, the power loss due to the wake effect may reach up to approximately 15% of the total power output from the whole wind farm. The widely implemented active power control method in the Doubly Fed Induction Generator (DFIG) wind turbine based wind farm is the Maximum Power Point Tracking (MPPT), by which each individual turbine generates the maximum active power seen from a single wind turbine without the consideration of the wake effect in the wind farm.

The DFIG based wind turbine has two degrees of freedom for active power control, which are the pitch angle and the tip speed ratio. According to the wake models, the power loss of the downstream wind turbine due to the wake effect is also determined by the pitch angle and tip speed ratio of the upstream wind turbine. As the first main contribution of this PhD thesis, considering the wake effect, a Maximum Power Generation (MPG) active power control method is proposed to maximize the total active power of the wind farm, by optimizing the pitch angle and tip speed ratio of all the wind turbines in the wind farm. To implement the optimized pitch angle and tip speed ratio, optimized pitch angle curves and active power curves are generated for each individual wind turbine at various wind directions.

Due to the expensive installation and maintenance in the offshore wind farm, the reliability issues in the wind turbine system became more and more important. According to a filed survey, the electrical parts of the wind turbine system have the maximum failure probability than the other components, which indicates the power converters have shorter lifetime expectancy than other components. The lifetime expectancy of the power converter is highly depending on the operation condition of the wind turbine, which indicates the lifetime expectancy of the power converter is also determined by the pitch angle and tip speed ratio of the wind turbine. In consequence, the lifetime expectancy of the wind turbine is also determined by the pitch angle and tip speed ratio of the wind turbine. Besides, the energy production of the wind farm is determined by both the active power and the operation time. As the secondary main contribution of this PhD thesis, considering the wake effect and the lifetime expectancy, a Maximum Energy Production (MEP) active power control method is proposed to maximize the total energy production of the wind farm, by optimizing the pitch angle and tip speed ratio of all the wind turbines in the wind farm. With the optimized pitch angle and tip speed ratio, optimized pitch angle curves and active power curves are generated for each individual wind turbine at various wind directions.

The DFIG wind turbine has some amount of reactive power capability, which depends on the active power generation of the wind turbine, both from the stator side of the generator and the Grid Side Converter (GSC). In case that the DFIG wind turbine is employed to provide reactive power to support the grid voltage control, the conventional reactive power dispatch method assigns the total reactive power requirement on the wind farm to each wind turbine in positive proportion to their respective reactive power capability. Considering that the reactive power also determines the lifetime expectancy of the wind turbine, as the third main contribution of this PhD thesis, an optimal reactive power dispatch method is proposed to improve the lifetime of the wind turbine, based on the wake effect analysis and the lifetime estimation.

DANSK RESUME

I de seneste år, er de store skala vindmølleparker i stigende grad integreret i elnettet på verdensplan og tendenser til at flytte fra landet til havet. I en vindmøllepark, på grund af kølvandet effekt, forårsager de opstrømsvindmøller effekttab til de nedstrømsvindmøller. Ifølge en undersøgelse indgivet fra de store skala havmølleparker, effekttab på grund af kølvandeffekten kan nå op til ca. 15% af den samlede effekt fra den hele vindmøllepark. Det populærte implementeret aktiveeffektstyring metode i Doubly Fed Induction Generator (DFIG) vindmølle baseret vindmøllepark er Maximum Power Point Tracking (MPPT), hvorved hver enkelt turbine frembringer den maksimale aktive effekt, set fra en enkelt vindmølle uden vederlaget af kølvandet effekt i vindmølleparken.

DFIG vindmøllerne har to frihedsgrader for den aktive effektstyring, som er stigningsvinklen og det spids shastighedsforhold. Ifølge kølvandsmodeller, er effekttabet i nedstræmsvindmøllens på grund af kølvandet effekten også bestemt af stigningsvinklen og tiphastighedsforhold af de opstrømsvindmøller. Som den første vigtigste bidrag i denne PhD-afhandling, overvejer kølvandet effekt, er en Maximum Power Generation (MPG) aktive effekt kontrolmetode foreslået at maksimere den totale aktive effekt af vindmølleparken, ved at optimere banen vinkel og drikkepenge hastighed forholdet alle vindmøllerne i vindmølleparken. At gennemføre den optimerede pitchvinkel og tiphastighedsforhold, er optimeret stigningsvinkel kurver og aktive effektkurver genereres for hvert enkelte vindmølle ved forskellige vindretninger.

På grund af den dyre installation og vedligeholdelse i havmølleparken, pålidelighed spørgsmål i vindmøllesystemet blev mere og mere vigtigt. Ifølge en indleveret undersøgelse, de elektriske dele af vindmøllesystemet har den maksimale uheldsandsynlighed end de andre komponenter, der angiver effektkonvertere har kortere forventet levetid end andre komponenter. Den forventede levetid af effektkonverteren er stærkt afhængig af driftssituation af vindmøllerne, der angiver den forventede levetid effektkonverteren bestemmes også af stigningsvinklen og tiphastighedsforhold af vindmøllerne. Som konsekvens, er den forventede levetid af vindmøllen også bestemt af stigningsvinklen og tiphastighedsforhold af vindmøllen. Desuden er den energi produktion af vindmølleparken bestemt af både den aktive effekt og driftstid. Som det sekundære vigtigste bidrag i denne PhD-afhandling, overvejer kølvandet effekt og den forventede levetid, er en Maximum Energy Production (MEP) aktive effekt kontrolmetode foreslået at maksimere den samlede energiproduktion af vindmølleparken, ved at optimere banen vinkel og drikkepenge hastighed forholdet mellem alle de vindmøller i vindmølleparken. Med den optimerede pitchvinkel og tiphastighedsforhold, er optimeret stigningsvinkel kurver og aktive effektkurver genereres for hvert enkelte vindmølle ved forskellige vindretninger.

DFIG vindmøllerne har mængde af reaktiv effekt kapacitet, som afhænger af den aktive effekt generation af vindmøllen, både fra statoren af generatoren og Grid Side Converter (GSC). I tilfælde af at DFIG vindmøllen anvendes til at tilvejebringe reaktive effekt til at understøtte elnettet spændingsstyring, tildeler den konventionelle reaktive effekt afsendelse metode den samlede reaktive effekt behov på vindmølleparken til hver vindmølle i positiv forhold til deres respektive reaktive effektkapacitet. I betragtning af at den reaktive effekt bestemmer også den forventede levetid af vindmøllen, som den tredje vigtigste bidrag af denne PhD afhandling, foreslås en optimal reaktive effekt afsendelse metode til at forbedre levetiden af vindmøllen, baseret på kølvandseffekt analysen og levetidsestimeringen.

ACKNOWLEDGEMENTS

Firstly, I would like to thank the Sino-Danish Center for Education and Research as well as the Department of Energy Technology, Aalborg University, Denmark and the Institute of Electrical Engineering, University of Chinese Academy of Sciences, China for their financial support of the research work documented in this thesis.

I am indebted to my supervisor Prof. Zhe Chen and my co-supervisor Dr. Chi Su from the Department of the Energy Technology, Aalborg University, for their consistent understanding, support and guidance throughout the entire period of this project. The enlightening discussions with them and encouraging comments from them contribute tremendously to the success of my PhD Meanwhile, I would like to express my deepest appreciation to my co-supervisors Prof. Frede Blaabjerg from the Department of the Energy Technology, Aalborg University and my co-supervisor Prof. Honghua Xu from the Institute of Electrical Engineering, Chinese Academy of Science, for their guidance and expertise.

I would also sincerely thank my colleagues Dr. Xiao Liu, Dr. Elsayed Abulanwar, Dr. Xionfei Wang, Dr. Yunqian Zhang, Dr. Rongwu Zhu, Dr. Chengxi Liu, Dr. Yongheng Yang, and Dr. Ge Xie for their inspiring suggestions and generous help. Special thanks go to Dr. Dao Zhou, Prof. Mohsen N. Soltani and Dr. Jiakun Fang, for their valuable technical assistance and professional discussions. Many thanks go to Prof. Zhe Zhang from Technical University of Denmark, Denmark, Prof. Haishun Sun from Huazhong University of Science and Technology, China and Prof. Jinghua Li from Guangxi University, China, who gave me practical tips.

I would thank Corina Gregersen, Eva Janik and Tina Lisbeth Larsen for their assistants in many ways. I am also thankful to many others who have followed and contributed to this project.

Last but not least, I want to thank my family and friends for their endless love, care and support.

Jie Tian / 田杰

April, 2017

Aalborg University,

Aalborg Øst, Denmark

TABLE OF CONTENTS

TABLE OF FIGURES

CHAPTER 1. INTRODUCTION

1.1. PROJECT BACKGROUN AND MOTIVATION

In the last decade, the clean and climate friendly wind power was increasingly integrated into the power grid. In 2015, 63 GW new wind power capacity was installed worldwide [1]. The total 433 GW installed wind power capacity worldwide was meeting close to 4% of the world's electricity demand [1]. The wind power has taken the largest share of the new electricity source in Europe, the United States and Canada, and the second share in China [1]. In 2016, the wind power reached to 42.2% of national electricity demand in Denmark, while the wind power targets in Denmark are 50% by 2020 and 84% by 2035 [1] and [2]. In May 2016, the renewable electricity met the 100% electricity demand for four days in Portugal [1].

Besides the fast integration of the wind power into the grid, in order to save the cost of wind power generation, the centralized large scale wind farms have been developed and installed in many countries [3]. To reduce the environment impact and to obtain even better wind conditions, another progress in the wind power technology is the movement of wind farms from onshore to offshore [3]. In Denmark, the development of large scale offshore wind farms had been started from 2002 with the commissioning of 160 MW Horns Rev offshore wind farm [4]. In 2014, the United Kingdom has observed the increase of 22% of its offshore wind farm capacity and Germany has reached half of its 2020 offshore target of 6.5 GW [1]. By 2015, the offshore wind power of 12 GW was operating in 13 countries [1].

With the fast development of the large scale wind farm, the wake effect in the wind farm became an important issue [5]. The wake in the wind farm is normally invisible. In Fig. 1.1, the cloud photo in Horns Rev offshore wind farm in Denmark shows the wake shape [6]. In the wind farm, the obvious effect of the wake is the power loss caused by the upstream wind turbine in its downstream wind turbines [5]. In the offshore wind farm, with the distance between two adjacent wind turbines of 4-8 rotor diameters, the power loss due to the wake effect can be 5-15% of the wind farm active power [7]. In the Horns Rev offshore wind farm, the distance between two adjacent wind turbines is 7 rotor diameters [4]. The downstream wind turbines lose 20% or 30% of their active power, and sometimes even more [6].

In modern wind farms, the popular and widely installed wind turbines are the variable speed wind turbine, including the Doubly Fed Induction Generator (DFIG) based wind turbine and the Permanent Magnet Synchronous Generator (PMSG) based wind turbine [8]. The variable speed wind turbine has two degrees of freedom

for active power control, which are the pitch angle and tip speed ratio [8]. The widely implemented active power control method in modern wind farms is the Maximum Power Point Tracking (MPPT), by which each individual wind turbine generates the maximum active power seen from the single wind turbine without the consideration of the power loss in the wind farm due to the wake effect [3].

Fig. 1.1. Wake effect on the Horns Rev offshore wind farm in Denmark [6].

To evaluate the power loss due to the wake effect in the wind farm, many wake models have been developed [5] and [9]. It is indicated that the power loss caused by the upstream wind turbine in its downstream wind turbines depends on the pitch angle and tip speed ratio of the upstream wind turbine [3], [5] and [10]. Compared with the MPPT method, by changing the pitch angle and tip speed ratio of the upstream wind turbine, the active power of the upstream wind turbine will be reduced [3] and [10]. However, the downstream wind speed can be increased, which results in the active power increase of the downstream wind turbine [3] and [10]. Very probably, the total active power of all the wind turbines can be increased [3] and [10]. Consequently, it is promising to reduce the power loss due to wake effects and thus to increase the total active power of the wind farm by developing optimal active power control method seen from the wind farm level considering the wake effect [3] and [10].

Besides the wake effect, with the wind farm moving from onshore to offshore and due to the expensive offshore installation and maintenance, the reliability issues in the wind turbine system also became more and more important [11]. According to the experiences of 15 years on 1500 wind turbines distributed in different areas in Germany, reported by Berthold Hahn et al. from Institut für Solare Energieversorgungstechnik (ISET), Kassel, Germany, the malfunctions concerned on the half mechanical components and half electrical components are shown in Fig. 1.2 [12]. It can be observed the electrical system has the highest failure rate of 23%, which indicates the power converter in the wind turbine has the smaller lifetime expectancy than the other components. The lifetime expectancy of the wind turbine can be increased by increasing the lifetime expectancy of its power converter [11].

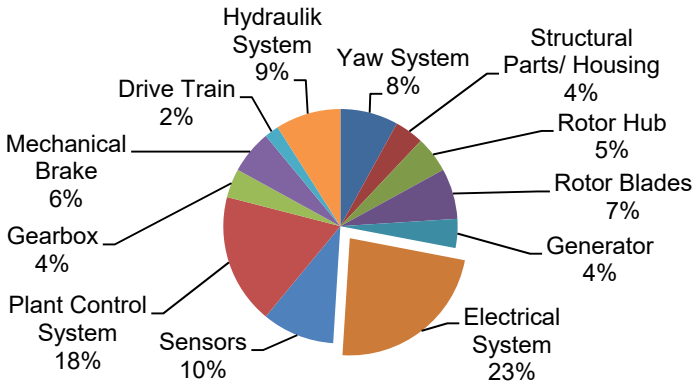

Fig. 1.2. Share of the wind turbine main components on total number of failures [12].

It is not possible to calculate the exact lifetime of the power converter in years. Instead, the lifetime is expressed in terms of the B10 lifetime, which is the number of cycles during which 10 percent of the total number of modules fails [13]. The B10 lifetime of the power converter is highly depending on the operation condition of the wind turbine, which indicates the B10 lifetime of the power converter is determined by the pitch angle, tip speed ratio and reactive power of the wind turbine [11]. In [14], the B10 lifetime of the Grid Side Converter (GSC) and the Rotor Side Converter (RSC) are calculated and compared at difference operation condition of the DFIG wind turbine. It is found that, in case that the wind turbine is controlled by the MPPT method and no reactive power generation, the B10 lifetime of the RSC is much less than the B10 lifetime of the GSC. Consequently, the lifetime of the wind turbine can be increased by increasing the lifetime of its RSC [11].

The energy production of the wind farm relates to the active power and the lifetime of each wind turbine [11]. The active power of the upstream wind turbine and the

power loss of the downstream wind turbine are all determined by the pitch angle and tip speed ratio of the upstream wind turbine [11]. Besides, in case of no reactive power generation, the lifetime of the DFIG wind turbine also can be increased by optimal control its pitch angle and tip speed ratio [11]. Consequently, it is expected to develop some optimal active power control methods in order to maximize the total energy production of the wind farm by improving the active power and the lifetime expectation of the wind farm considering the wake effects [11].

Required by the modern grid codes, a large scale wind farm must be equipped with the reactive power control function to support the primary grid voltage control [9, 10]. Moreover, the wind farm also can be employed to support the secondary voltage control of the power grid, where the voltage reference at the Point of Common Coupling (PCC) of the wind farm or the reactive power reference for the wind farm are sent out from the Automatic Voltage Control (AVC) of the power system [17] and [18]. The DFIG wind turbine has some amount of reactive power capabilities both from the stator side of the generator and from the Grid Side Converter (GSC) [19] and [20]. Consequently, the DFIG wind turbine can be employed as continuous reactive power source besides its active power generation [2] and [19].

The reactive power capability of the DFIG wind turbine depends on the wind turbine active power [19]. Due to the wake effect, there is a significant difference of active power among the wind turbines, which results in the difference of reactive power capability among the wind turbines [2]. In case of the wind turbines providing reactive power to support the grid voltage control, a typical reactive power dispatch method in the wind farm is essentially to dispatch the reactive power requirement to each wind turbine in proportion to its reactive power capability [21]. By this method, the lifetime of the upstream wind turbine may be shorter than the industrial standard which is expected to be longer than 25 years, while the downstream wind turbine has an overly long lifetime [2]. Based on the B10 lifetime estimation, the lifetime can be traded off among the wind turbines by optimal dispatching the reactive power among the wind turbines [2].

1.2. PROJECT OBJECTIVES

Under the circumstance as described in the previous section, considering the wake effect and the lifetime estimation, it is highly expected to develop some optimal control methods in the wind farm level to increase the total active power of the wind farm, to improve the lifetime of wind turbines, and to increase the energy production of the wind farm [2], [3] and [11]. The main objectives of this PhD project are listed as follows:

- Model the DFIG wind turbine and its power controller.

- Based on the wake model, analyze the wind speed deficit and power loss in the wind farm equipped with DFIG wind turbines.
- Considering the wake effect in the wind farm, develop optimal active power control method to maximize the total active power of the wind farm.
- Estimate the B10 lifetime of the power converter in the DFIG wind turbine in terms of the wind speed, pitch angle, tip speed ratio and reactive power.
- Analyze the wake effect on the lifetime estimation of DFIG wind turbines in the wind farm.
- Considering the wake effect and lifetime estimation, develop optimal active power control method to maximize the total energy production of the wind farm.
- Analyze the reactive power capability of DFIG wind turbine.
- Based on the wake model and the lifetime estimation, develop optimal reactive power dispatch method to improve the lifetime of DFIG wind turbines in the wind farm.

1.3. LIMITATIONS

The limitations in this PhD thesis are listed as follows:

- In the last few decades, wake models have been developed ranging in complexity. Generally speaking, the wind velocity profile in wind farm can be accurately calculated with the Computation Fluid Dynamics (CFD) method which solves the complete Navier-Stokes Equation [22]. Because of the complexity of the Navier-Stokes Equation and its large time consumption especially in a large scale wind farm, there is a gap between the engineering solutions and the completely CFD models [23]. In this PhD thesis, the Katic wake model based on the momentum theory and is currently embedded in the industrial software WAsP [24], is adopted. The more accurate wake models with small computation complexity developed in the future can be adopted in the proposed optimal power control methods in this Ph.D thesis.
- The proposed optimal power control methods in this Ph.D thesis are studied in the wind farm with typical regular layout and at the wind directions where the wind turbines in one row along the wind direction will not cause the power loss to the wind turbines in other rows. In the wind farm with irregular layout, the proposed method is also applicable. However, the methods to reduce the computation complexity especially in large scale wind farms should be adopted.
- In this PhD thesis, the lifetime of the wind turbine is represented by the B10 lifetime of RSC. The B10 lifetime of the other parts in the wind turbine system may be taken into account in the future works.
- In this PhD thesis, the over-excited reactive power generated from the stator side of the generator is assumed. In case that the wind turbine generates under-excited reactive power from the stator side of the

generator, its B10 lifetime of the RSC may be further increased. Moreover, the GSC can also provide the reactive power generation. At the lower over-excited reactive power generation of the wind turbine, the GSC can share some amount of B10 lifetime consumption with the RSC. In the future work, the under-excited reactive power generated from the stator side of the generator and the reactive power generation from the GSC will be taken into account.

1.4. OUTLINE OF THE THESIS

This PhD thesis contains 7 chapters and will be organized as follows:

Chapter 1 Introduction

This chapter briefly introduces the project background, motivation, main objectives, limitations and publications.

Chapter 2 Modeling of the wind turbine

This chapter focuses on the modeling of single wind turbine. An overview of wind turbine technologies is given. The active power control scheme of the DFIG wind turbine is presented. The reactive power capability of the DFIG wind turbine is evaluated. And, the lifetime of DFIG wind turbine is estimated.

Chapter 3 Modeling of the wind farm

This chapter focuses on the modeling of the wake effect and its impact on the active power generation and lifetime estimation of each individual wind turbines in the wind farm.

Chapter 4 Maximum Power Generation (MPG) in wind farm considering wake effect

In this chapter, an optimal active power control method MPG is proposed to maximize the total active power of the wind farm considering the wake effect.

Chapter 5 Maximum Energy Production (MEP) in wind farm considering wake effect and wind turbine lifetime

In this chapter, an optimal active power control method MEP is proposed to maximize the total energy production of the wind farm taking into account the wake effect in the wind farm and the wind turbine lifetime.

Chapter 6 Optimal reactive power dispatch method in wind farm considering wake effect and wind turbine lifetime

In this Chapter, an optimal reactive power dispatch method is proposed to improve the wind turbine lifetime taking into account the wake effect in the wind farm and the wind turbine lifetime.

Chapter 7 Conclusions and future work

This chapter concludes the thesis, summarized the main contributions of this research work, and gives recommendations on the future research works based on the results acquired from this project.

1.5. LIST OF PUBLICATION

- Conference Papers (During PhD):

  [C.1] J. Tian, C. Su, and Z. Chen, "Reactive power capability of the wind turbine with doubly fed induction generator," in *Proc. of 39th IEEE Industrial Electronics Society Conf.,* pp. 5310–5315, 2013. (Published)

  [C.2] J. Tian, C. Su, M. Soltani and Z. Chen, "Active power dispatch method for a wind farm central controller considering wake effect," in *Proc. of 40th IEEE Industrial Electronics Society Conf.,* pp. 5450–5456, 2014. (Published)

  [C.3] J. Tian, D. Zhou, C. Su, F. Blaabjerg and Z. Chen, "Wake effects on lifetime estimation in DFIG-based wind farms," in *Proc. of IEEE International Future Energy Electronics Conf. 2017 - ECCE Asia,* 2017. (Accepted)

  [C.4] J. Tian, D. Zhou, C. Su, F. Blaabjerg and Z. Chen, "Maximum energy yield oriented turbine control in PMSG based wind farm," *International Conference on Renewable Power Generation,* 2017. (Abstract submitted)

- Journal Papers (During PhD):

  [J.1] J. Tian, D. Zhou, C. Su, Z. Chen and F. Blaabjerg. "Reactive power dispatch method in wind farms to improve the lifetime of power converter considering wake effect," *IEEE Trans. Sustainable Energy,* Sep. 2016. (E-Pub Ahead of Print)

  [J.2] J. Tian, D. Zhou, C. Su, F. Blaabjerg and Z. Chen. "Optimal control to increase energy production of wind farm considering wake effect and

lifetime estimation," *Applied Sciences,* vol. 7, no. 1, Jan. 2017. (Published)

[J.3] J. Tian, D. Zhou, C. Su, M. Soltani, Z. Chen and F. Blaabjerg. "Wind turbine power curve design for optimal power generation in wind farms considering wake effect" *Energies,* vol. 10, no. 3, Feb. 2017. (Published)

CHAPTER 2. MODELING OF THE WIND TURBINE

This chapter focuses on the modeling of single wind turbine. Firstly, an overview of wind turbine technologies is given, followed by the introduction to the active power control scheme of the Doubly Fed Induction Generator (DFIG) wind turbine. Afterwards, the reactive power capability of the DFIG wind turbine is evaluated. Finally, the lifetime of DFIG wind turbine is estimated.

2.1. OVERVIEW OF THE WIND TURBINE TECHNOLOGY

Over many years, different types of wind turbines have been developed [8]. Wind turbine can be classified into Horizontal Axis Wind Turbine (HAWT) and Vertical Axis Wind Turbines (VAWT) based on the orientation of their spin axis [8]. The wind turbine can also be classified into the fixed speed wind turbine and variable speed wind turbine based on the rotor speed control strategy [8]. The configuration of the Wind Energy Conversion System (WECS), can be classified into the fixed speed WECS without power converter interface, the variable speed WECS using the reduced capacity converters and the variable speed full capacity converter operated WECS [8].

In the VAWT, the orientation of the spin axis is perpendicular to the ground [8]. The generator and gearbox are normally placed in the base of the turbine on the ground [8]. In the HAWT, the orientation of the spin axis is parallel with the ground [8]. The rotor blade and nacelle are elevated to a height with the tower to reach better wind condition [8]. The nacelle houses the gearbox, the generator, and, in some designs, the power converters [8]. “Compared with the VAWT, the HAWT features higher wind energy conversion efficiency due to the blade design and access to the stronger wind, but needs a stronger tower to support the heavy weight of the nacelle thus its installation cost is higher. On the contrary, the VAWT has the advantage of lower installation costs and easier maintenance due to the ground-level gearbox and generator installation, but its wind energy conversion efficiency is lower due to the weaker wind on the lower position of the blades and limited aerodynamic performance of the blades. In addition, the rotor shaft of VAWT is long, making it prone to mechanical vibrations. It is these disadvantages that hinder the practical application of VAWT for large scale wind energy conversion. HAWT dominate today’s wind market, especially in large commercial wind farms.” [8].

The four main types of wind turbines based on their rotor speed control strategies and WECS configurations in today’s global market are illustrated in the following. All of them are HAWT. The fixed speed wind turbine has advantages of low

manufacturing and maintenance costs as well as reliable operation, but disadvantage of lower energy conversion efficiency. “On the contrary, the variable speed wind turbine increases the energy conversional efficiency and reduces the mechanical stress caused by the wind gusts. It also reduces the wear and tear on the gearbox and bearings, expanding the lifetime and reducing the maintenance requirements. The main drawback of the variable speed wind turbine is the need for a power converter interface to control the generator speed, which adds cost and complexity to the system.” [8].

Type A: Fixed speed wind turbine without power converter interface

As it is shown in Fig 2.1, the fixed speed wind turbine is based on the Squirrel Cage Induction Generator (SCIG) without a power converter interface. “At different wind speed, the generator speed varies in an extremely small range determined by the gear box ratio, the grid frequency and the number of poles of the generator. The maximum conversion efficiency can be achieved only at a given wind speed. A soft starter to limit high inrush currents during system start up is usually used, but the soft starter is bypassed by a switch after the system is started. A three-phase capacitor bank is required to compensate the reactive power drawn by the induction generator.” [8].

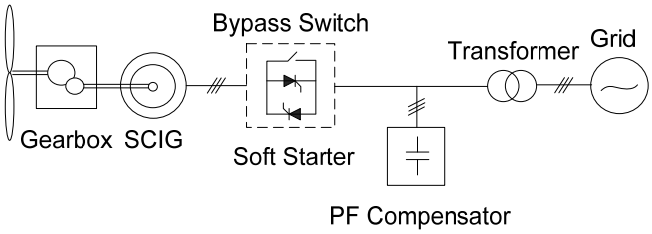

Fig. 2.1. Fixed speed wind turbine without power converter interface [8].

This wind energy system features simplicity, low manufacturing/maintenance costs, and reliable operation. The main drawbacks include [8]:

- The maximum conversion efficiency can be achieved only at a given wind speed, and the system efficiency degrades at other wind speeds.
- The highly fluctuating output power causes disturbances to the power system.

Despite its disadvantages, this wind energy system is still widely accepted in industry with a rated power up to several megawatts [8].

Type B: Variable rotor resistance based variable speed wind turbine with reduced capacity power converter

The variable speed wind turbine with reduced capacity converter is feasible with Wound Rotor Induction Generators (WRIG) [8]. One of the control diagrams for the WRIG wind turbine is shown in Fig. 2.2 [8]. The rotor speed of the generator can be adjusted by changing the rotor resistance, which affects the torque/speed characteristic of the generator [8]. Operating at variable speed, the energy conversion efficiency can be increased, with the power loss on the resistance [8]. As the rotor speed is typically limited to about 10% above the synchronous speed of the generator, this configuration also requires a soft starter and reactive power compensation [8]. The rotor resistance is normally made adjustable by a power converter [8].

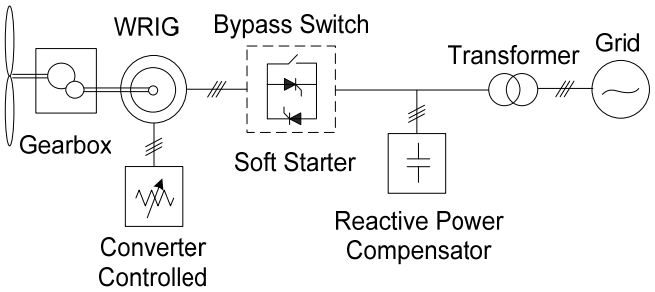

Fig. 2.2. Variable rotor resistance based variable rotor speed wind turbine with reduced capacity power converter [8].

Type C: Doubly Fed Induction Generator (DFIG) based variable speed wind turbine with reduced capacity power converters

Another configuration for the variable speed wind turbine with reduced capacity power converters is the Doubly Fed Induction Generator (DFIG) based wind turbine, as it is shown in Fig. 2.3 [8]. The rotor speed of the wind turbine is controlled by the four quadrant power converter system [8]. The active power and the reactive power can be generated through both the stator side of the generator and rotor side of the generator [8]. There is no need for the soft starter and the reactive power compensation [8]. The power converters just need to process the slip power in the rotor circuit, which is approximate of 30% of the rated power, results in the reduced converter cost in comparison to the wind energy conversion system using full capacity converters [8].

“The use of the converters also allows bidirectional power flow in the rotor circuit and increases the speed range of the generator. This system features improved overall power conversion efficiency, extended generator speed range (±30%), and enhanced dynamic performance compared to the fixed speed WECS and the variable resistance configuration. These features have made the DFIG wind energy system widely accepted in today's market.” [8].

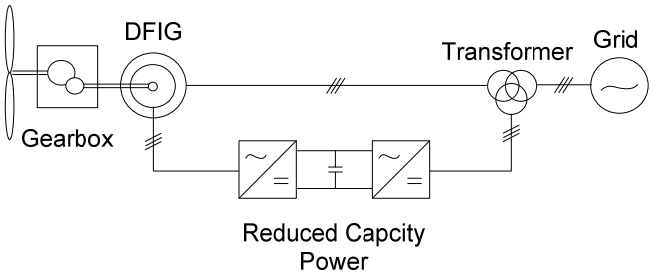

Fig. 2.3. DFIG based variable speed wind turbine with reduced capacity power converters [8].

Type D: Variable speed wind turbine with full capacity power converters

The configuration of the variable speed wind turbine with full capacity power converter is shown in Fig. 2.4 [8]. Squirrel cage induction generators, wound rotor synchronous generators, and permanent magnet synchronous generators (PMSG) have all found applications in this type of configuration with a rated power up to several megawatts [8]. "As the wind turbine is connected to the grid via the power converters, the power rating of the converter is normally the same as that of the generator. With the use of the power converter, the generator is fully decoupled from the grid, and can be operated in full speed range. This also enables the system to perform reactive power compensation and smooth the grid connection. The main drawback is a more complex system with increased costs." [8].

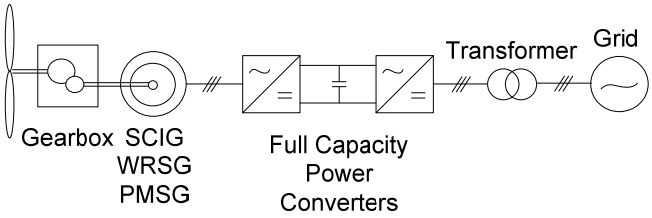

Fig. 2.4. Variable speed wind turbine with full capacity power converters [8].

"It is noted that this wind energy system can be operated without the need for a gearbox if a low speed synchronous generator with a large number of poles is used. The elimination of the gearbox improves the efficiency of the system and reduces initial costs and maintenance. However, a low speed generator has a substantially larger diameter to accommodate the large number of poles on the perimeter, which may lead to an increase in generator and installation costs." [8].

This PhD thesis focuses on the optimal control of the wind turbine to reduce the power loss due to the wake effect in the wind farm and to improve the lifetime of

wind turbine. The wind farm equipped with the wildly installed DFIG wind turbines is studied. The optimization in the wind farm equipped with the PMSG wind turbines will be studied in the future work.

2.2. ACTIVE POWER CONTROL SCHEME OF THE DFIG WIND TURBINE

The DFIG wind turbine has two degrees of control freedom for active power control, which are the pitch angle and tip speed ratio [8]. In DFIG wind turbine based wind farms, the widely implemented active power control method is the Maximum Power Point Tracking (MPPT), by which the wind turbine extracts the maximum mechanical power when wind speed is low [8].

According to the aerodynamic model, the extracted mechanical power can be calculated by [8],

$$P_m = \frac{1}{2}\rho\pi R^2 C_p(\beta,\lambda)v^3 \tag{2.1}$$

where v is the wind speed, ρ is the air density, R is the length of the blades and C_p is the power conversion coefficient, which is a function of the blade pitch angle β and the tip-speed ratio λ. The tip-speed-ratio λ is defined as [8],

$$\lambda = \frac{\omega_r R}{v} \tag{2.2}$$

where ω_r is the turbine rotor speed expressed in radians.

At a specific wind speed, according to (2.1), the mechanical power is determined by the power coefficient [3] and [10]. The power coefficient is a function of the pitch angle and tip speed ratio [3] and [10]. The power coefficients of the NREL 5 MW DFIG wind turbine in terms of the pitch angle and tip speed ratio are shown in Fig. 2.5 [25]. It can be observed, the maximum power coefficient of 0.4852 is obtained at the pitch angle of 0° and the tip speed ratio of 7.55 [3] and [10]. Consequently, controlled at the pitch angle of 0° and tip speed ratio of 7.55, the NREL 5 MW DFIG wind turbine can extract the maximum mechanical power from the wind [3] and [10].

The parameters of the NREL 5 MW DFIG wind turbine are shown in Table 2.1 [25]. With the MPPT method implemented, the active power curve of the NREL 5 MW DFIG wind turbine is shown in Fig. 2.6 [3]. Due to the minimum and maximum rotor speed limit of 6.9 rpm and the 12.1 rpm, the active power curve is divided into 4 control regions [25] and [3]. In Region2 (wind speed from 7 m/s to 11 m/s), the

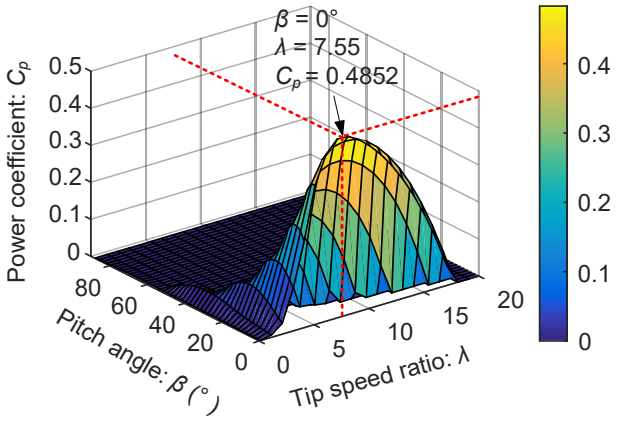

Fig. 2.5. Power coefficient of the NREL 5 MW DFIG wind turbine [25].

Table 2.1. Parameters of NREL 5 MW wind turbine [25].

Parameter	**Value**
Rated Power	5 MW
Rotor Diameter	126 m
Cut-in, Rated, Cut-out Wind Speed	3 m/s, 11.4 m/s, 25 m/s
Min. and Max. rotor Speed	6.9 rpm, 12.1 rpm
Gearbox Ratio	97:1
Number of Pole-pairs	3
Synchronous Frequency	50 Hz
Electrical Generator Efficiency	94.4%

wind turbine is operated with MPPT, where the pitch angle is 0° and tip speed ratio is 7.55 [3] and [25]. In region 4, the active power reaches to the rated power of 5 MW at the wind speeds higher than 11.4 m/s [3] and [25]. In region 1 and region 3, the rotor speed increases with the wind speed linearly [3], [25], [26] and [27]. In region 1, region 2 and region 3, the pitch angle is 0° [3], [8] and [25]. In region 4, the pitch angle is increased to limit the wind turbine output power at the rated value [3], [8] and [25].

One of the active power control scheme is shown in Fig. 2.7 [28], where the pitch angle the generator torque are separately controlled by the pitch angle controller and generator torque controller [28]. The tip speed ratio is changed automatically with the generator torque [28]. This scheme doesn't need to measure the wind speed

[28]. Instead, the generator speed is measured and used to calculate the pitch angle and torque references [28]. The pitch angle and generator torque curve in terms of the generator speed can be obtained from Fig. 2.6, where the generator torque is calculated by [8],

$$T_{em} = \frac{60P_m}{2\pi n\omega_r} \tag{2.3}$$

where n is the gearbox ratio.

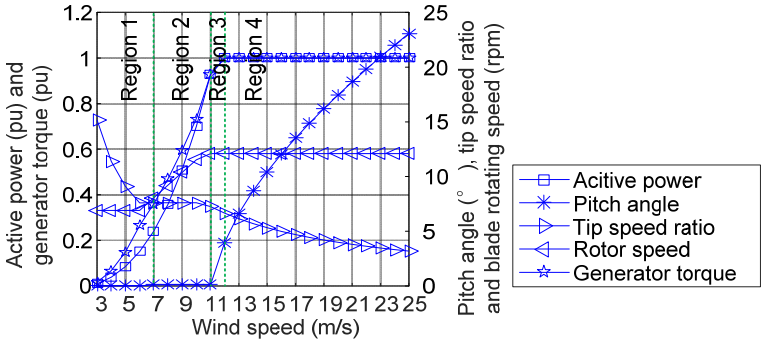

Fig. 2.6. Control parameters of the NREL 5 MW wind turbine, with the MPPT method implemented [3].

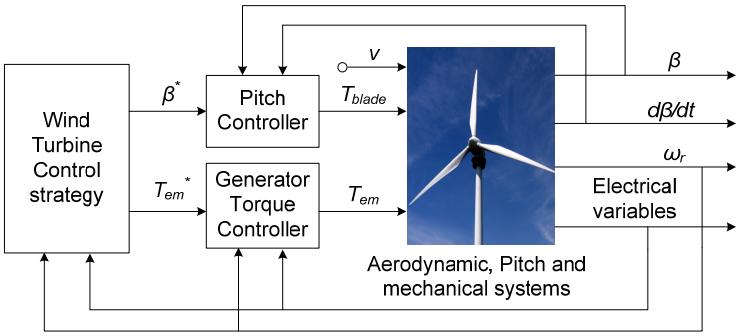

Fig. 2.7. Active power control scheme of the DFIG wind turbine [28].

2.3. REACTIVE POWER CAPBILITY OF THE DFIG WIND TURBINE

As it is shown in Fig. 2.8 [28], the DFIG can generate the reactive power both from the stator side of the generator and the Grid Side Converter (GSC) [19]. In this part,

by assuming the MPPT method implemented for active power control and limited by the maximum stator and rotor voltage and current, the reactive power capability of the NREL 5 MW DFIG wind turbine is analyzed and calculated [19].

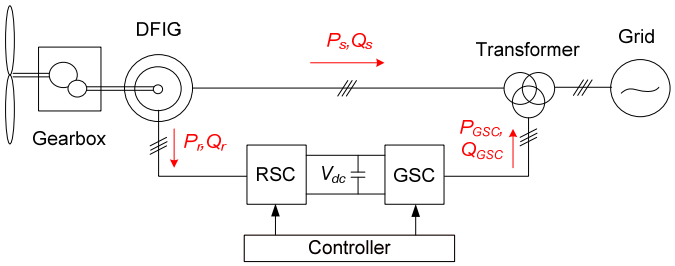

Fig. 2.8. Configuration of the DFIG wind turbine [28].

2.3.1. STEADY-STATE MODEL OF DFIG AND ITS POWER CONVERTER

The steady state model of the DFIG and its power converter is shown in Fig. 2.9 [8], where Z_{eq}/s is the equivalent impedance of the back-to-back converter.

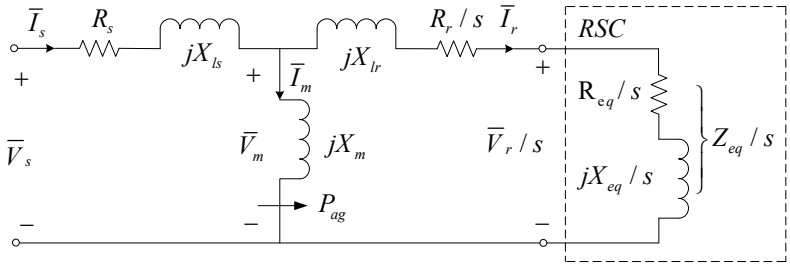

Fig. 2.9. Steady state model of the DFIG and its power converter [8].

When the stator operates at unity power factor，the air gap power P_{ag} can be calculated by [8] ,

$$P_{ag} = 3(V_s - I_s R_s) I_s \tag{2.4}$$

where V_s is the rms stator voltage, I_s is the rms stator current, R_s is the stator winding resistance. According to the induction machine theory, the air gap power can also be calculated by [8],

$$P_{ag} = \frac{\omega_s T_m}{p} \tag{2.5}$$

where ω_s is the stator frequency, p is the number of pole pairs, and T_m is the mechanical torque which can be calculated by [8],

$$T_m = \frac{P}{\omega_g} \tag{2.6}$$

where P is the total generator active power from both the stator side and the rotor side, and ω_g is the generator rotating speed.

Combining (2.4), (2.5) and (2.6) yields [8],

$$I_s = \frac{V_s \pm \sqrt{V_s^2 - \frac{4R_s\omega_s P}{3p\omega_g}}}{2R_s} \tag{2.7}$$

When the stator operates with a leading or lagging power factor, the rms stator current can be calculated by [8],

$$I_s = \frac{\omega_s P}{3V_s p\omega_g \cos\varphi_s} \tag{2.8}$$

where φ_s is the stator power factor angle.

The voltage across the magnetizing branch can be calculated by [8],

$$\overline{V_m} = \overline{V_s} - \overline{I_s}(R_s + j\omega_s L_{ls}) \tag{2.9}$$

where, L_{ls} is the stator leakage inductance, when the stator operates at unity power factor, the stator voltage and current are given by [8],

$$\overline{V_s} = V_s\angle 0° \text{ and } \overline{I_s} = I_s\angle 180° \tag{2.10}$$

when the stator operates with a leading or lagging power factor, the stator voltage and current are given by [8],

$$\overline{V_s} = V_s\angle 0° \text{ and } \overline{I_s} = I_s\angle(180° + \varphi_s) \tag{2.11}$$

The magnetizing current can be calculated by [8],

$$\overline{I_m} = \frac{\overline{V_m}}{j\omega_s L_m} \tag{2.12}$$

where L_m is the magnetizing inductance.

The rotor current can be calculated by [8],

$$\overline{I_r} = \overline{I_s} - \overline{I_m} \tag{2.13}$$

The rotor voltage can be calculated by [8],

$$\overline{V_r} = s\overline{V_m} - \overline{I_r}(R_r + js\omega_s L_{lr}) \tag{2.14}$$

where R_r is the rotor winding resistance, L_{lr} is the rotor leakage inductance, the slip s can be calculated by [8],

$$s = \frac{\omega_s - p\omega_g}{\omega_s} \tag{2.15}$$

2.3.2. REACTIVE POWER CAPABILITY OF THE NREL 5 MW DFIG WIND TURBINE

The DFIG wind turbine can generate reactive power both from the stator side of the generator and the GSC [19]. In this subsection, the reactive power capability of the NREL 5 MW wind turbine limited by the maximum stator current and the maximum rotor current is calculated [19]. The parameter of 5 MW DFIG is given in Table 2.2 [8].

Based on the steady state model of the DFIG and its power converter as shown in Fig. 2.9, the active power and reactive power from the stator side of the generator can be calculated by [19],

$$P_s = 3V_s I_s \cos\varphi_s \tag{2.16}$$

$$Q_s = 3V_s I_s \sin\varphi_s \tag{2.17}$$

In (2.16), the active power from the stator side of the generator is determined by the wind speed and active power control strategy [3]. The stator voltage is determined by the grid operation states. To make sure the wind turbine can generates the rated power at the stator voltage of 0.9 pu, the maximum stator current is set to be 1.1 pu for steady state operation, where the base power is the rated mechanical power of

the generator, the base voltage is the rated stator voltage of the generator and the base current is the rated stator current [2]. With the MPPT method implemented for active power control, at the stator voltage of 1.0 pu and the maximum stator phase current of 1.1 pu, the maximum phase angle can be calculated by (2.16). Then, the maximum reactive power from the stator side of the generator limited by the maximum stator current of 1.1 pu can be calculated by (2.17) and is shown in Fig. 2.10(a).

Table 2.2. Parameters of the 5 MW DFIG [8].

Parameter	**Value**
Rated Mechanical Power	5.0 MW
Rated Stator Phase Voltage	548 V (rms)
Rated Rotor Phase Voltage	381 V (rms)
Rated Stator Current	2578 A (rms)
Rated Rotor Current	3188 A (rms)
Rated Stator Frequency	50 Hz
Number of Pole Pairs	3
Stator Winding Resistance, Rs	1.552 mΩ
Rotor Winding Resistance, Rr	1.446 mΩ
Stator Leakage Inductance, Lls	1.2721 mH
Rotor Leakage Inductance, Llr	1.1194 mH
Magnetizing Inductance, Lm	5.5182 mH

As expressed by (2.18), the maximum reactive power from the GSC is determined by the capacity of the GSC and the active power from the rotor side of the generator [19]. The active power from the rotor side of the generator is determined by the wind speed and the active power control strategy [19].

$$Q_{GSC\_\max} = \pm\sqrt{S_{GSC}{}^2 - P_r^2} \tag{2.18}$$

As the maximum stator current also determines the maximum active power from the rotor side of the generator and the active power from the stator side of the generator determines the reactive power capability from the GSC, the reactive power capability from the GSC is also determined by the maximum stator current [19]. Assuming the capacity of the GSC is 30% of the rated power, the maximum

reactive power from the GSC limited by the maximum stator current of 1.1 pu is shown in Fig. 2.10(b).

As the reactive power from the stator side of the generator and the active power from the rotor side of the generator also determine the rotor current, the reactive power capability from the stator side of the generator and from the GSC are also limited by the maximum rotor current [19]. The maximum reactive power from the stator side of the generator limited by the maximum rotor current can be obtained by combining (2.4)-(2.13) and (2.17). The maximum reactive power from the GSC limited by the maximum rotor current can be obtained by combining (2.4)-(2.14), (2.16) and (2.18). For the NREL 5 MW DFIG wind turbine, the reactive power capability from the stator side of the generator and from the GSC limited by the maximum rotor current of 1.1 pu is the same as limited by the maximum stator current of 1.1 pu as shown in Fig. 2.10.

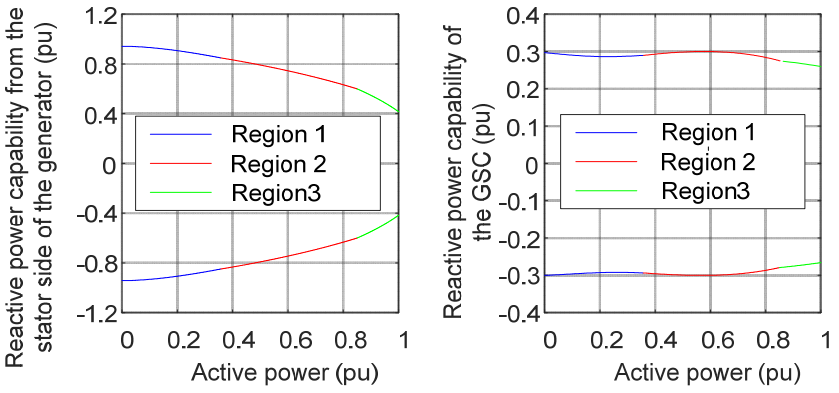

Fig. 2.10. Limited by the stator current of 1.1 pu: (a) The reactive power capability from the stator side of the generator; (b) The reactive power capability from the GSC.

2.4. LIFETIME OF THE DFIG WIND TURBINE

As the electrical system of the wind turbine has the highest failure rate among the wind turbine components [12] and the B10 lifetime of GSC is much higher than the RSC [14], in this thesis, the lifetime of DFIG wind turbine is presented by the B10 lifetime of RSC.

The power converter modules are subjected to a variety of temperature profiles [13] and [14]. The temperature profiles, which closely depends on the operation condition of the wind turbine, causes cyclic thermos-mechanical stress in all components and joints of the modules [13] and [14]. The magnitude and frequency

of the stress cycles determines the lifetime expectancy [13] and [14]. The flow chart to estimate the lifetime expectancy of RSC is shown in Fig. 2.11 [2], [13] and [14].

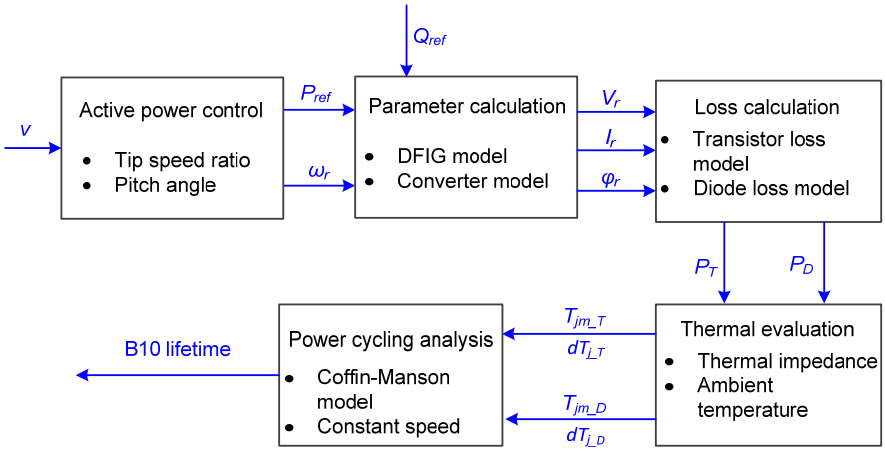

Fig. 2.11. Flow chart to estimate the B10 lifetime of rotor-side converter at wind speed v [2].

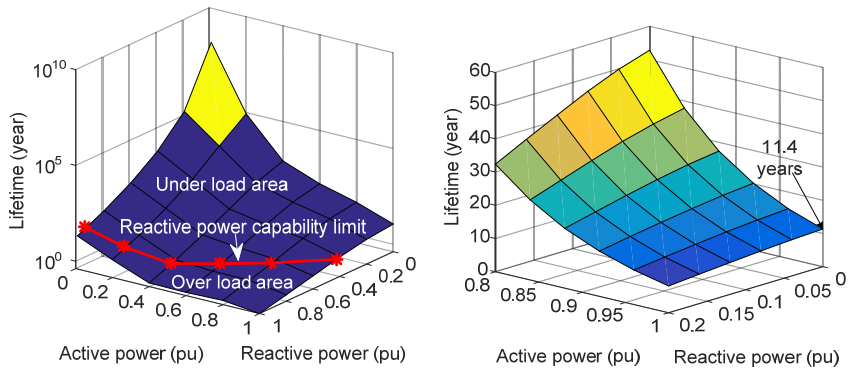

(a) *(b)*

Fig. 2.12. B10 lifetime of the NREL 5 MW DFIG wind turbine in terms of active power and reactive power: (a) Active power from 0 pu to 1 pu and the reactive power from 0 pu to 1 pu; (b) Active power from 0.8 pu to 1 pu and the reactive power from 0 pu to 0.2 pu [2].

The lifetime estimation starts with the calculation of the active power reference and the rotor speed, which are determined by the active power control method and the aerodynamic model [2], [13] and [14]. The reactive power reference is required by the power grid and given to the wind farm controller [2] and [18]. The operation

parameters of the power converter can be estimated by the model of the DFIG and its converter model as presented in Section 2.3.1 [2]. The power loss can be calculated by the transistor loss model and diode loss model, which consist of the conduction loss and switching loss [2], [13] and [14]. The two most important reliability indicators, which are the mean junction temperature T_{jm} and the junction temperature fluctuation dT_j, relate to the thermal impedance and ambient temperature [2], [13], [14]. Finally, the lifetime of the power converter can be estimated by the Coffin-Manson model [2], [13], [14] and [29].

With the MPPT method implemented for active power control, the lifetimes of the NREL 5 MW DFIG wind turbine in terms of constant active powers and reactive powers are shown in Fig. 2.12 [2]. In Fig. 2.12 (a), the under load and over load area respectively denote the reactive power is larger and smaller than the reactive power capability [2]. In Fig. 2.12 (b), it can be observed the B10 lifetime is 11.4 years at the active power of 1 pu and reactive power of 0 pu [2].

2.5. SUMMARY

This chapter focuses on the modelling and evaluation of the DFIG wind turbine. Firstly, the overview of the wind turbine technology is given. Then, the torque scheme and MPPT control method of the DFIG wind turbine is presented. The DFIG wind turbine has two degrees of control freedom for active power control, which are the pitch angle and tip speed ratio. With the torque control scheme implemented, the active power is controlled by the pitch angle controller and the generator torque controller with the measurement of the generator speed. The pitch angle-generator speed and generator torque-generator speed curves can be generated from the active power-wind speed, tip speed ratio-wind speed and rotor speed-wind speed curves. The tip speed ratio is changed automatically with the generator torque.

Afterwards, based on the steady state model of the DFIG and its power converter, the reactive power capability of the NREL 5 MW DFIG wind turbine is calculated. The reactive power capability of the DFIG wind turbine is determined by the stator voltage, active power control method, maximum stator current, maximum rotor voltage and maximum rotor current.

Finally, the lifetime of the NREL 5 MW DFIG wind turbine is estimated. The lifetime of the DFIG wind turbine can be represented by the B10 lifetime of the RSC, which is determined by the wind speed, active power control method and the reactive power generation.

CHAPTER 3. MODELING OF THE WIND FARM

This chapter starts with an overview of the wake effect and wake models in the wind farm. This is followed by the case studies of the wind speed deficit and the power loss of each wind turbine in typical wind farms due to the wake effect. Afterwards, the impacts of wake effect on the lifetime estimation of each wind turbine in wind farms are analyzed.

3.1. WAKE MODELS

3.1.1. OVERVIEW OF THE WAKE MODELS

In the last few decades, wake models with different levels of complexity have been developed [5] and [9]. Early attempts were presented by Templin in 1974 [30] and by Newman in 1977 [31]. These models are based on the boundary layer theory, where the wind turbine increases the roughness of the terrain is assumed [9]. As it is shown in Fig. 3.1 [36], the ambient wind speed has speed deficit and turbulence under the earth's boundary layer. The boundary layer is presented by its thickness δ, which depends on the apparent roughness of the terrain [35]. The wind speed inside the boundary layer varies logarithmically with the height [35]. Given the roughness of the terrain with wind turbines, the wind speed profile in the wake can be obtained [35]. These models were further developed by Bossanyi et al [32], Frandsen [33] and Emeis and Frandsen [34]. Even though it is not widely used on a commercial scale, it can still be useful when predicting the effects of large wind farms on resultant wind flow [35].

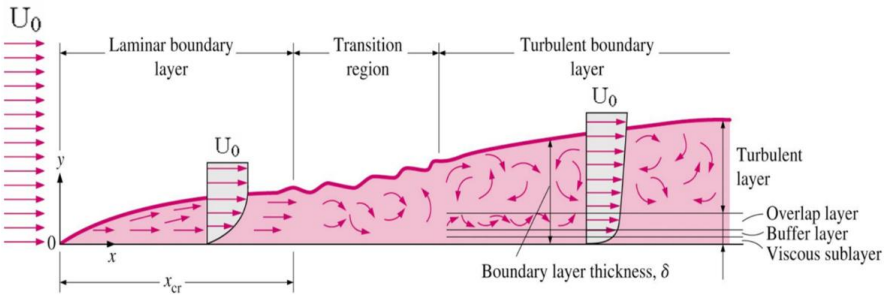

Fig. 3.1. Wind speed deficit and turbulence inside the earth's boundary layer caused by the apparent roughness of the terrain [36].

The wake model for a single wind turbine was presented by Lissaman in 1979 [37]. Based on the experimental and theoretical work, the initial wind speed deficit in the wake is calculated with the wind turbine thrust coefficient [37]. The wake width and expansion are governed by the ambient turbulence, the shear generated turbulence and wind turbine generated turbulence [37]. The maximum wind speed at each downstream position is calculated based on the global momentum conservation [37].

A more simplified model of single wind turbine wake was presented by Katic in 1986 [38], which expended the previous work of Jensen in 1983 [39]. This model aims to give an estimation of the energy content represented by an average wind speeds at the positon of the downstream wind turbine [38]. The initial velocity deficit in the wake is calculated with the wind turbine thrust coefficient [38]. The wake width in positive proportional to the distance between the upstream wind turbine and the downstream wind turbine (known as 'top hat') is assumed [38]. Then, the wind speed at the position of the downstream wind turbine is calculated based on the momentum conservation theory [38]. This model is inaccurate in the near wake area (less than 4 wind turbine blade diameters), but the space between wind turbines in the wind farm is always larger than this distance and thus the model error can be neglected [38]. The Katic model is currently embedded in the industrial software WAsP developed by Risø, Technical University of Denmark (DTU) for site selection and wind farm Annual Energy Production (AEP) estimation [40].

A more recent model of single wind turbine wake, which is included in the European Wind Turbine Standard II [41], was completed by Larsen et al. in 1996[42]. Neglecting the ground blocking effect, the wake is assumed to be a free turbulent flow [42]. The wind speed in the wake can be adequately described by the boundary layer equation [42]. The mean wind speed deficit and the width of the wake at different distance from the wind turbine are calculated [42]. This model also gives the cost-efficient numerical procedure for determination of the turbulence spectrum with a semi-analytical solution, in which a set of simple empirical relations are used to predict the turbulence intensity and the turbulence length scale, by assuming that the dominating part of the downstream turbulence is associated with the shear layer and the ambient air flow turbulence [42].

Field wake model was originally presented by Sforza et al. [43]. In this model, the wind speed profile at all the position of the wind turbines are calculated, by which constant convection velocity, constant eddy diffusivity and parabolic approximation are assumed [43]. The wind speed deficit in the wind turbine wake was calculated based on the linearized conservation of momentum equation [43]. The field wake model was further developed by Taylor [44], Liu [45], Crespo [46], Ainslie [47] and more recently Magnusson [48]. All these models calculate the wind speed profile in the wind turbine wake by solving the Navier-Stokes Equation with assumptions and simplifications. In these models, the turbulent mixing contribution

from the shear layer and ambient turbulence is descried by an eddy viscosity turbulence model.

Generally speaking, the wind velocity profile can be accurately calculated with the Computation Fluid Dynamics (CFD) method which solves the complete Navier-Stokes Equation. Because of the complexity of the Navier-Stokes Equation and its large time consumption especially in large-scale wind farms, the CFD models with engineering solutions all have simplified the Navier-Stokes Equation and its parameters to reduce the computation burden. Thus, there is a gap between the engineering solutions and the complete CFD models [49].

In [49], the authors compared the wind farm models in complexity among the wake models mentioned above, which are the WAsP in which the Katic wake model is implemented, the moderately complex WindFarm in which the Ainslie wake model is implemented, the WAKEFARM, and the complete CFD model. All these models have estimation error in different levels. The estimation error varies with the ambient wind speed and wind farm air condition. It is hard to say which model is more accurate than the others. Because of the issues related to the wake measurement and the specific objectives of various wake models, more effort should be made to understand the wake and to modify the wake models to improve the prediction accuracy [5]. With the increasing of computation capability, it is tended to the modification and investigation of CFD wake models and many institutes and projects are underway of the development of CFD wake models [5]. In this thesis, to simplify the problem, the simplified Katic model which is widely implemented in the industrial is adopted to estimate the energy contents at the position of downstream wind turbines with the average ambient wind speed.

3.1.2. KATIC WAKE MODEL

This PhD thesis mainly concerns the power loss due to the wake effect in the wind farm. Compared with the CFD model, the Katic wake model calculates the power loss at the position of downstream wind turbine straightforwardly with small calculation complexity instead of illustrating the wind profile in the overall wind farm field with large calculation complexity. To simplify the problem, the Katic wake model is adopted throughout this PhD thesis to estimate the wind speed distribution in the wind farm

In a wake caused by a single turbine, the Katic model presents the downstream energy contents by a constant wind speed [38]. As it is shown in Fig. 3.2 [11], the wind speed of the upstream wind turbine is the same as the ambient wind speed u. As the downstream wind speed deficit relates to the wind turbine operation condition, the wind turbine thrust coefficient C_t, which is a function of the pitch angle β and tip-speed-ratio λ, is introduced [38]. The initial wind speed deficit $1-u_r/u$ can be expressed by [38],

$$1-\frac{u_r}{u}=\frac{1}{2}(1-\sqrt{1-C_t(\beta,\lambda)}) \tag{3.1}$$

where, u_r is the initial wind speed behind the wind turbine in the wake.

The wake starts with the blade diameter D and expands linearly with a decay constant k, which is known as the 'top hat' profile [38]. At the distance of X, the wake diameter expands to $D_w=D+2kX$ [38]. Inside the wake, at any distance, the wind speed v is assumed to be constant at any point of the wake disc [38]. The constant wind speed at the distance of X is predicted by the momentum conversation theory, which can be expressed by [38],

$$D^2u_r+(D_w{}^2-D^2)u=D_w{}^2v \tag{3.2}$$

Combining (3.1) and (3.2), the wind speed deficit at the distance of X in the wake can be derived and expressed by [38],

$$1-\frac{v}{u}=\frac{1-\sqrt{1-C_t(\beta,\lambda)}}{(1+2kX/D)^2} \tag{3.3}$$

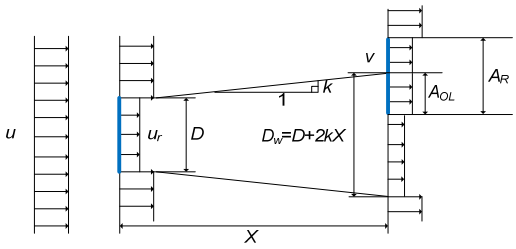

Fig. 3.2. Katic wake model [11].

Due to the simplification that the downstream wake diameter expands linearly with the decay constant, the wind speed deficit cannot be calculated accurately with a fixed decay constant implemented at all the downstream distances [38]. Normally, the decay constant is adjusted to fit the data at the distance larger than about four diameters [38]. As the distance between two wind turbines in actual wind farms is larger than four diameters, the results are generally in agreement with the real measurement [38]. Recommended in the Wind Atlas Analysis and Application Program-WAsP help facility [24], the decay constant is 0.075 for onshore wind farms and 0.04-0.05 for offshore wind farm.

When the downstream wind turbine is partly in the wake, the equivalent wind speed deficit can be expressed by [24],

$$1-\frac{v}{u}=\left(1-\sqrt{1-C_t(\beta,\lambda)}\right)\left(\frac{D}{D+2kx}\right)^2\frac{A_{OL}}{A_R} \tag{3.4}$$

where A_R is the blade sweep area. A_{OL} is the overlap area of the blade sweep area and the wake area.

When the j^{th} wind turbine is in multiple wakes, the wind speed deficit at the position of the j^{th} wind turbine 1-v_j/u is given by [38],

$$\left(1-\frac{v_j}{u}\right)^2=\sum_{i=1}^{n}\left(1-\frac{v_{ij}}{u}\right)^2 \tag{3.5}$$

where, the j^{th} wind turbine is in the wake of n wind turbines, v_j is the wind speed at the position of j^{th} wind turbine, and $1-v_{ij}/u$ is the wind speed deficit at the position of the j^{th} wind turbine caused by the i^{th} wind turbine, which can be calculated by (3.3).

3.2. POWER LOSS IN TYPICAL WIND FARMS DUE TO WAKE EFFECT

In this section, with the MPPT method implemented for active power control, the power losses due to the wake effect in typical wind farms based on NREL 5MW wind trubines are estimated by Katic wake model. The decay constant k of 0.04 for offshore wind farm is assumed. The thrust coefficient of the NREL 5 MW wind turbine is shown in Fig. 3.3 [25].

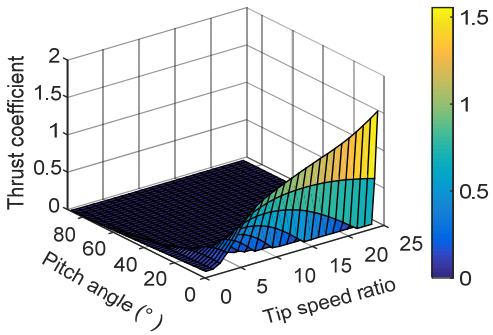

Fig. 3.3. Thrust coefficient of the NREL 5 MW DFIG wind turbine [25].

3.2.1. POWER LOSS IN A 2-TURBINE WIND FARM

In the wind farm with 2 NREL 5 MW wind turbines as it is shown in Fig. 3.4 [3],

the distance *XD* between the two wind turbines is 6.5 blade diameters. At the wind direction of 270°+φ, the overlap area between the wake area of WT_1 and the blade sweep area of WT_2, which is A_{OL_12}, is shown in Fig. 3.5 [3]. According to (3.4), the wind speed deficit of WT_2 at the ambient wind speed u can be calculated by,

$$1-\frac{v_2}{u}=\left(1-\sqrt{1-C_{t\_1}(\beta_1,\lambda_1)}\right)\left(\frac{D}{D+2kXD\cos(\varphi)}\right)^2\frac{A_{OL\_12}}{A_R} \tag{3.6}$$

where, v_2 is the wind speed of WT_2, C_{t_1} is the thrust coefficient of WT_1, β_1 and λ_1 are the pitch angle and tip speed ratio of WT_1.

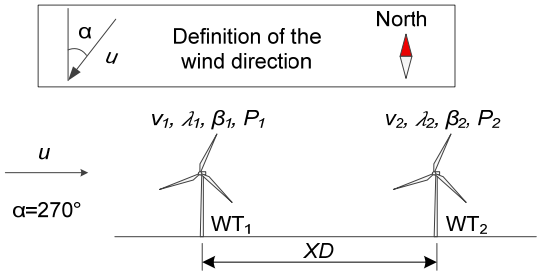

Fig. 3.4. Layout of the 2- turbine wind farm [3].

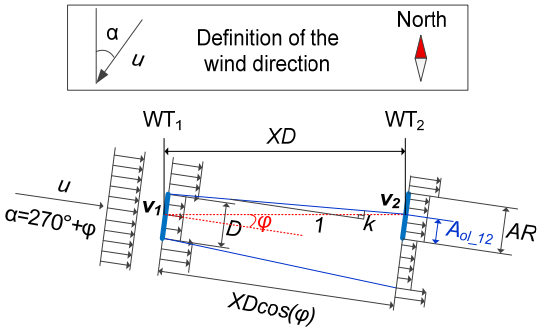

Fig. 3.5. The overlap area between the wake area of WT_1 and the blade sweep area of WT_2, which is A_{ol_12} [3].

At the wind directions of from 270° to 282° and the ambient wind speeds of 3 m/s to 25 m/s, the wind speeds of WT_2 are shown in Fig. 3.6(a) [3]. The wind speed of WT_2 at the wind direction of 270° is the same as at the wind directions of 273° and 276° [3]. At the wind direction of 270°, the active powers of WT_1 and WT_2 are shown in Fig. 3.6(b) [3]. With the wind direction increasing from 276° to 282°, the wind speed of WT_2 increases as the overlap area reduces [3]. At the wind direction

of 282°, the wind speed of WT_2 is the same as the ambient wind speed, as the overlap area reduces to 0 [3]. Generally, it is found that the power loss due to wake effects in the wind farm appears in the four symmetrical wind direction ranges of 270°-282°, 258°-270°, 78°-90° and 90°-102° [3].

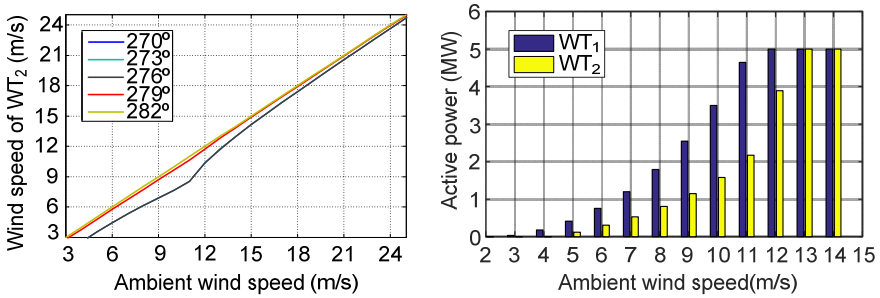

Fig. 3.6. (a) Wind speed of WT_2, at the wind directions from 270° to 282°. (b) Active power of WT_1 and WT_2 at the wind direction of 270°, the WT_1 and WT_2 has the same active power when the ambient wind speed is larger than 13 m/s [3].

3.2.2. POWER LOSS IN A 3-TURBINE WIND FARM

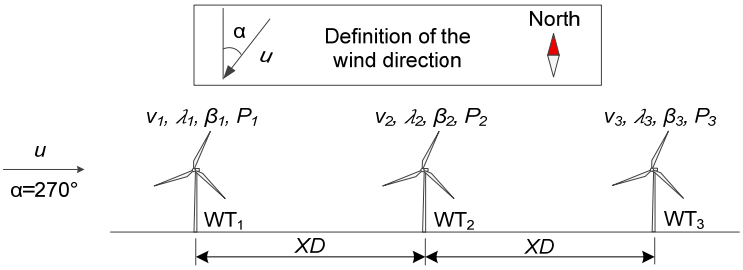

Fig. 3.7. Layout of the wind farm with 3 NREL 5 MW DFIG wind turbines in a line [3].

In the wind farm with 3 NREL 5 MW wind turbines as shown in Fig. 3.7 [3], the distance between the two adjacent wind turbines is 6.5 blade diameters. At the wind direction of 270°+φ, the overlap area between the wake area of WT_1 and the blade sweep area of WT_3, which is A_{ol_13}, and the overlap area between the wake area of WT_2 and the blade sweep area of WT_3, which is A_{ol_23}, are shown in Fig. 3.8 [3]. According to the Katic wake model, the wind speed deficit of WT_3 can be calculated by [3],

$$\left(1-\frac{v_3}{u}\right)^2=\left(1-\frac{v_{13}(\beta_1,\lambda_1)}{u}\right)^2+\left(1-\frac{v_{23}(\beta_2,\lambda_2)}{u}\right)^2 \tag{3.7}$$

where $1\text{-}v_3/u$ is the wind speed deficit of WT_3, $1\text{-}v_{13}/u$,$1\text{-}v_{13}/u$ are the wind speed deficit of WT_3 respectively caused by WT_1 and WT_2. The β_1, λ_1, β_2 and λ_2, are the pitch angle and tip speed ratio of WT_1 and WT_2. The wind speed deficit of WT_3 caused by WT_1 and WT_2 can be calculated by [3],

$$1-\frac{v_{13}(\beta_1,\lambda_1)}{u}=\left(1-\sqrt{1-C_{t\_1}(\beta_1,\lambda_1)}\right)\left(\frac{D}{D+4kXD\cos(\varphi)}\right)^2\frac{A_{ol\_13}}{A_R} \tag{3.8}$$

$$1-\frac{v_{23}(\beta_2,\lambda_2)}{u}=\left(1-\sqrt{1-C_{t\_2}(\beta_2,\lambda_2)}\right)\left(\frac{D}{D+2kXD\cos(\varphi)}\right)^2\frac{A_{ol\_23}}{A_R} \tag{3.9}$$

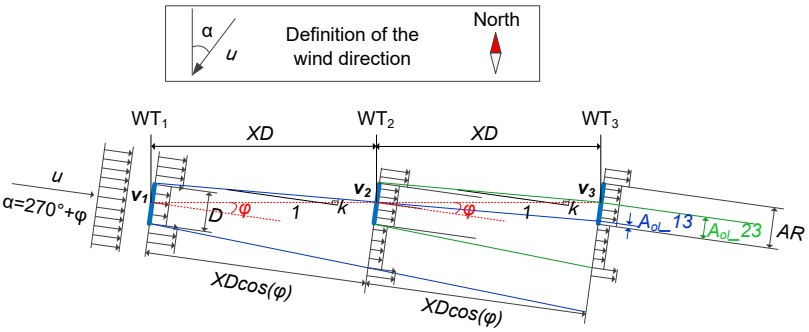

Fig. 3.8. Downstream wind speed deficit in multiple wakes in Katic wake model [3].

In Fig. 3.8 [3], the A_{ol_13} is smaller than A_{ol_23}, which indicates the range of wind direction in which WT_1 causes wind speed deficit to WT_3 is smaller than the wind direction range in which WT_2 causes wind speed deficit to WT_3. Consequently, the wind direction range in which the WT_3 has the wind speed deficit in the 3-turbine wind farm is the same as the wind direction range in which WT_2 has the wind speed deficit in the 2-turbine wind farm, which are the four symmetrical wind direction ranges of 258°-270°, 270°-282°, 78°-90° and 90°-102° [3].

In case that WT_1, WT_2 and WT_3 are controlled by the MPPT method, at the wind directions of from 270° to 282°, the wind speed of WT_3 is shown in Fig. 3.9(a) [3]. The wind speed of WT_3 at the wind direction of 270° is the same as at the wind direction of 273° [3]. It can be observed in Fig. 3.9(a) [3], at the wind direction of 270°, the wind speed of WT_3 has the maximum deficit. At the wind direction of 282°, there is no wind speed deficit [3]. At the wind direction of 270°, the active power of WT_1, WT_2 and WT_3 are shown in Fig. 3.9(b) [3]. It can be observed, WT_2 and WT_3 has large amount of power loss at the ambient wind speeds of from 3 m/s to 13 m/s [3].

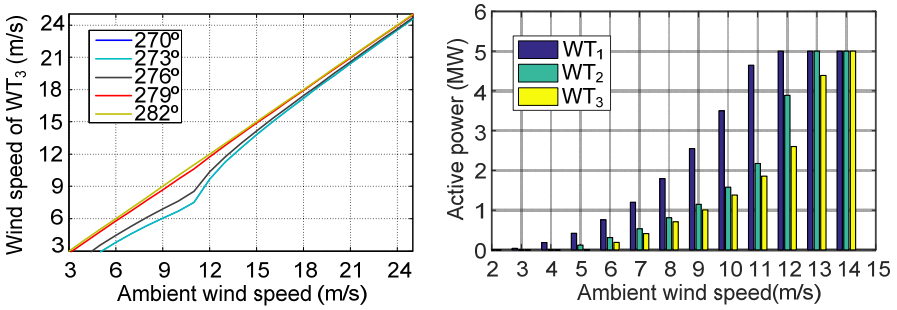

Fig. 3.9. At the wind direction of 270°: (a) Wind speed of WT_3; (b) Active power of WT_1, WT_2 and WT_3 [3].

3.2.3. POWER LOSS IN A 80-TURBINE WIND FARM

In the wind farm with 80 NREL 5 MW DFIG wind turbines as shown in Fig. 3.10 [3], the distance between adjacent wind turbines in the same row or in the same column is 6.5 blade diameters. The layout of the wind farm is the same as the Horns rev offshore wind farm in Denmark [4]. Estimated by the Katic wake model, the total active power of the wind farm are shown in Fig. 3.11 [3], where the wind directions from 1° to 360° and ambient wind speeds from 4 m/s to 14 m/s are taken into account. It can be observed that the wind farm has high power losses at the wind directions of around 41°, 90°, 131°, 172°, 221°, 270°, 311° and 352°, which are the symmetrical axis of the wind farm [3]. At the ambient wind speed of 10 m/s and at the wind direction of 270° and 311°, the wind speed and active power of all the wind turbines are shown in Fig. 3.12.

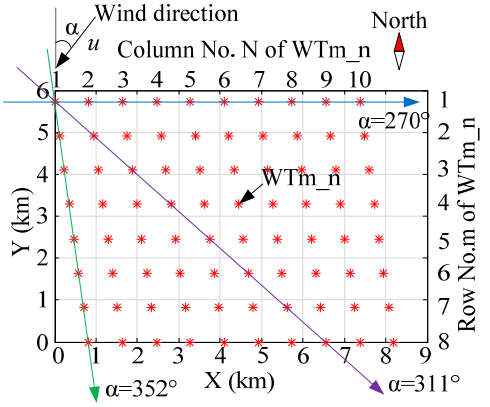

Fig. 3.10. Layout of the wind farm with 80 NREL 5 MW DFIG wind turbines [3].

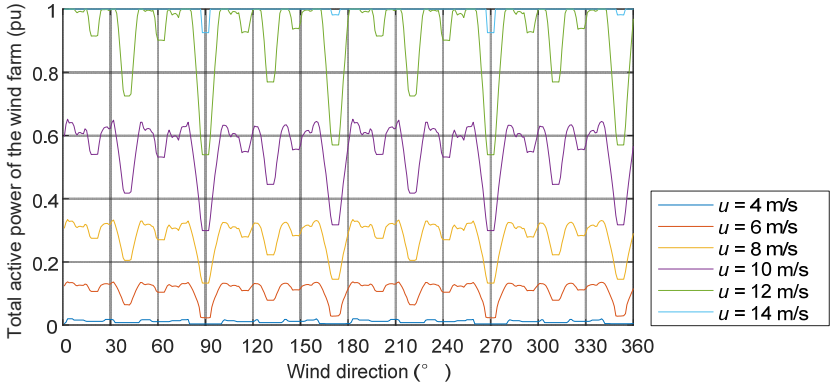

Fig. 3.11. At the wind directions of from 1° to 360° and ambient wind speeds of from 4 m/s to 14 m/s, the total active power of the wind farm [3].

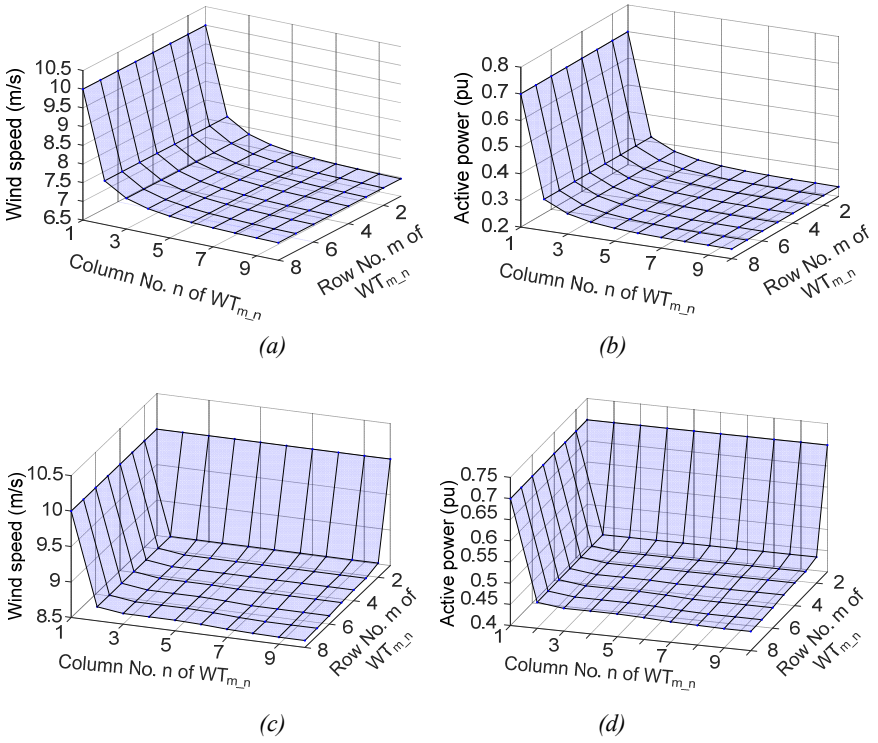

Fig. 3.12. At the ambient wind speed of 10 m/s: (a) Wind speed of all the wind turbines at the wind direction of 270°; (b) Active power of all the wind turbines at the wind direction of 270°; (c) Wind speed of all the wind turbines at the wind direction of 311°; (d) Active power of all the wind turbines at the wind direction of 311°.

3.3. WAKE EFFECT ON LIFETIME ESTIMATION IN DFIG WIND TURBINE BASED WIND FARM

As presented in section 2.4, the lifetime of the DFIG wind turbine depends on the wind speed, rotor speed, active power and reactive power. Due to the wake effect, wind turbines in a wind farm have different wind speeds and active powers, which results in the different lifetimes [50]. In this section, the lifetime of each wind turbine in typical wind farms is estimated considering the wake effect. The reactive power is assumed to be 0. Each wind turbine is controlled by the MPPT method.

In the wind farm with 10 NREL 5 MW DFIG wind turbine in a line as shown in Fig. 3.13 [3], at the wind direction of 270°, the wind speed and the active power generation of each wind turbine are shown in Fig. 3.14(a) and (b) [50], where the constant wind speeds from 3 m/s to 15 m/s with the resolution of 3 m/s are taken into account. In Fig. 3.14, the wind speed lower than the cut in wind speed of 3 m/s is not presented, as the wind turbine will be halted at the wind speed lower than 3 m/s. According to the lifetime in terms of the active power and reactive power as shown in Fig. 2.12, the B10 lifetime of each wind turbine are shown in Fig. 3.14 (c). In the 10-turbine wind farm, for opposite wind directions, the wind farm has the same power loss [50]. At the wind direction of 270°, the wind farm has the maximum power loss [50]. The active power, wind speed and B10 lifetime of each wind turbine at the wind directions from 270° to 280° with ambient speed of 12m/s, are shown in Fig. 3.15 [50].

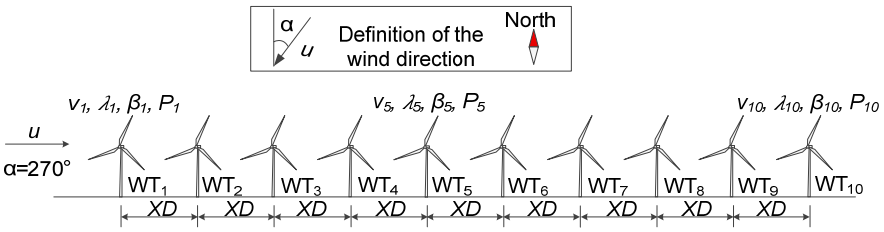

Fig. 3.13. Layout of the 10-turbine wind farm [3].

Considering the annual wind direction and wind speed distribution as shown in Fig.3.16(a) and (b) [2], which can be sort in to the wind direction and wind speed distribution as shown in Fig. 3.16(c) and (d) [2], the annual lifetime consumptions are shown in Fig. 3.17. In Fig. 3.16(c), the wind directions are separated into 36 rose sectors, with wind directions of 10° in each sector.

In the wind rose sector of 265°-275° and in the opposite wind rose sector of 85°-95°, the 10-turbine wind farm as shown in Fig. 3.13 has the power loss due to the wake effect [50]. In the wind rose sector of 265°-275°, in which the WT_1 has the largest lifetime consumption, the annual lifetime consumption of all wind turbines are

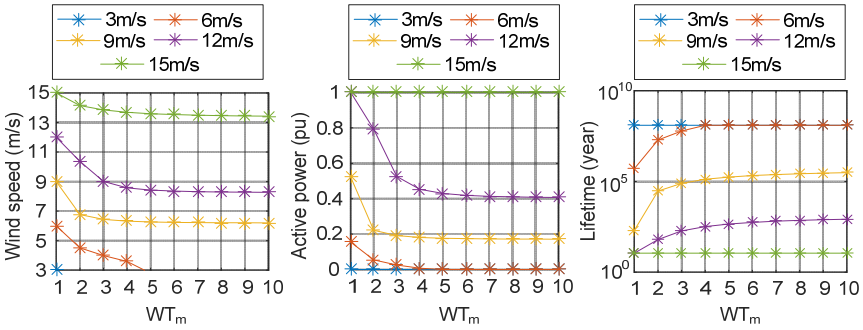

Fig. 3.14. In the 10-turbine wind farm, at the wind direction of 270: (a) Wind speed of each wind turbine; (b) Active power of each wind turbine; (c) B10 lifetime of each wind turbine [50].

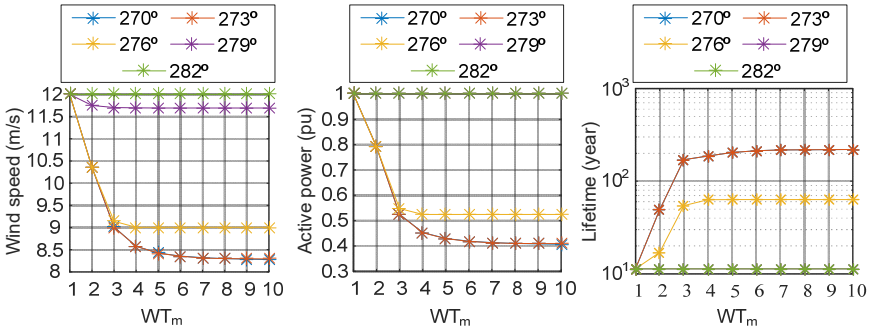

Fig. 3.15. In the 10-turbine wind farm, at the at the ambient wind speed of 12 m/s: (a) Wind speed of each wind turbine; (b) Active power of each wind turbine; (c) B10 lifetime of each wind turbine [50].

shown in Fig. 3.17(a). In the opposite wind rose sector of 85°-95°, in which the WT_{10} has the largest lifetime consumption, the annual lifetime consumption of all the wind turbines are shown in Fig. 3.17(b). By the superposition of the annual lifetime consumption in both the wind rose sectors of 265°-275° and 85°-95°, the annual lifetime consumption of all the wind turbines are shown in Fig. 3.17(c). It can be observed, even though the difference of lifetime consumption between WT_1 and WT_{10} are partly offset in the opposite wind rose sectors, there is still a difference of lifetime consumption between WT_1 and WT_{10} due to the difference of the wind speed in the two opposite wind rose sectors.

In the 10-turbine wind farm as shown in Fig. 3.13, by the superposition of the annual lifetime consumption in all the 36 wind rose sectors, the annual lifetime

consumption of all the wind turbines are shown in Fig 3.17(d). In the 80-turbine wind farm as shown in Fig 3.10, the annual lifetime consumption of all the wind turbines in all the 36 wind rose sectors are shown in Fig 3.17(e).

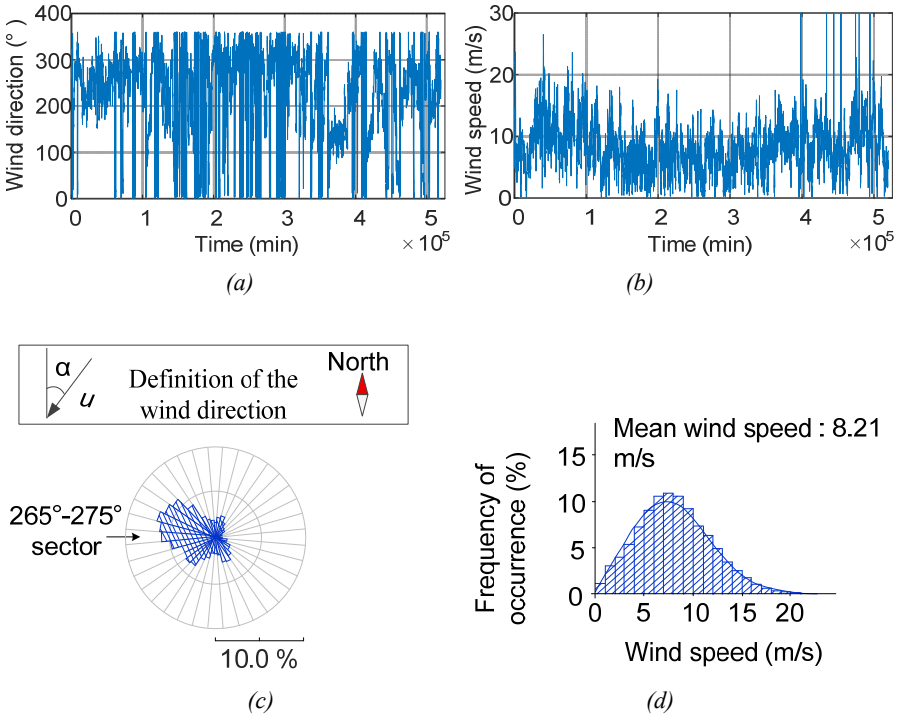

Fig. 3.16. (a) Annual wind direction. (b) Annual wind speed. (c) Annual wind direction distribution with the resolution of 10 degree in each sector. (d) Annual wind speed distribution [2].

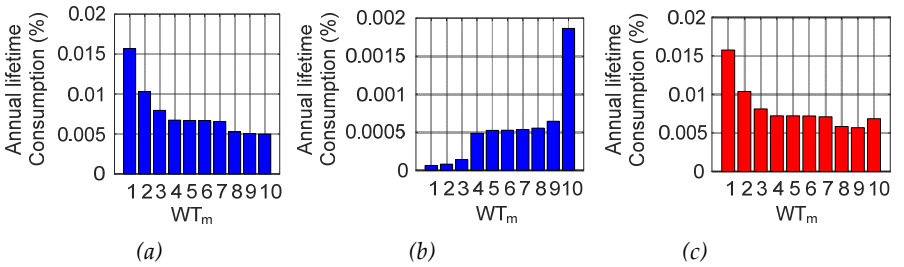

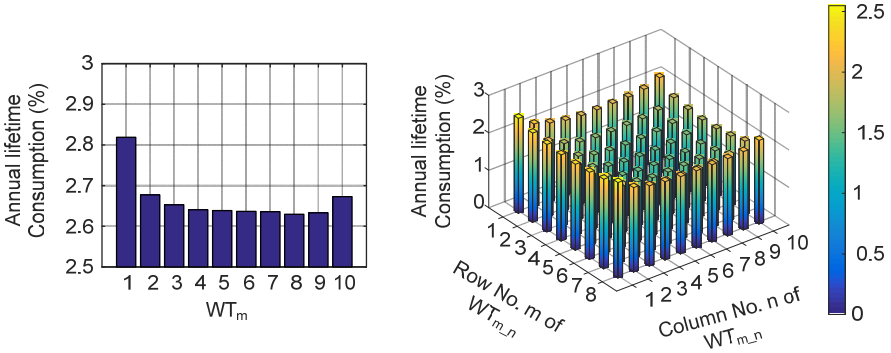

(d) *(e)*

Fig. 3.17. Annual lifetime consumption of all the wind turbines in the 10- turbine wind farm: (a) In the wind rose sector of 85°-95°; (b) In the wind rose sector of 265°-275°; (c) In the wind rose sectors of 85°-95° and 265°-275°; (d) In all the wind rose sectors. (e) Annual lifetime consumption of all the wind turbines in the 80-turbine wind farm.

3.4. SUMMARY

Accurately modelling the wake in the wind farm can be benefit to the reduction of wake loss and wind turbine load by optimizing the wind farm layout and wind farm control systems. Wake models have been developed in the past few decades in complexity from the most straightforward wake models to the complex CFD models. In these models the boundary layer theory and the conservation of the momentum are important theory implemented for the wake modeling. By many institutes, the wake models are still under development to improve the accuracy and to reduce the amount of computation. Among the wake models, it tends to develop the CFD models. In this PhD thesis, the objectives are to reduce the power loss of the downstream wind turbines due to the wake effect and to improve the lifetime of the downstream wind turbines by optimal control each wind turbine. The widely commercial used Katic model which estimates the average energy contents at the downstream wind turbines is adopted to estimate the wind speed at the position of the downstream wind turbines.

Based on the Katic wake model, the wind speed deficits and the power losses in typical wind farms from the most simple 2-turbine wind farm to the large scale 80-turbine wind farm are presented in this chapter. The wind speed deficits and power losses are determined by the ambient wind speed, the layout of the wind farm, the wind direction and the implemented active power control method. In the large scale 80-turbine wind farm, due to its layout, the highest wind speed deficits and power losses appear at the wind directions of around 41°, 90°, 131°, 172°, 221°, 270°, 311° and 352°, which are the symmetrical axis of the wind farm.

Due to the wind speed deficits and the power losses in the wind farm, the wind turbines in a wind farm have different lifetime expectation. Based on the analysis of the wind speed deficits and power losses at each wind directions, taking into account the annual ambient wind speed and wind direction distributions, the annual lifetime consumption of each wind turbine in the typical 10-turbine and the 80-turbine wind farms are presented. It can be concluded, due to the wake effect and depending on the annual wind profile, the wind turbines in a wind farm have different lifetime expectation. Due to the large wind speed which results in the large lifetime consumption, the upstream wind turbine has large lifetime consumption than the downstream wind turbine.

CHAPTER 4. MAXIMUM POWER GENERATION (MPG) IN WIND FARM CONSIDERING WAKE EFFECT

4.1. INTRODUCTION

The early attempt to reduce the power loss due to the wake effect in the wind farm was by developing new active power controller [51], by the boundary layer tunnel experiments [52] and by analysing the wind turbine load [53]. To estimate the power loss in the wind farm, many wake models have been developed [53] and [10]. At a given wind speed, the wind turbine active power is determined by its pitch angle and tip speed ratio [3], [10] and [15]. According to the wake models, the downstream power loss is also determined by the pitch angle and tip speed ratio of the upstream wind turbine [3] and [10]. Compared with the MPPT method, by changing the pitch angle and tip speed ratio of the upstream wind turbine, the active power of the upstream wind turbine will be reduced [3] and [10]. However, the downstream wind speed can be increased, which results in the increase of the active power of the downstream wind turbines [3] and [10]. As a consequence, it is expected to increase the overall active power generation of the wind farm [3] and [10].

In this Chapter, considering the wake effect, a Maximum Power Generation (MPG) active power control method is proposed to maximize the wind farm active power generation [3]. Firstly, the feasibility to increase the total active power of the wind farm by changing the pitch angle and tip speed ratio of the wind turbines in the wind farm compared with the MPPT method is implemented is presented in Section 4.2 [3]. Afterwards, the optimal pitch angle and tip speed ratio of each wind turbine are selected by the Particle Swarm Optimization (PSO) based optimization algorithm in Section 4.3 [10].

To implement the optimized pitch angle and tip speed ratio, in Section 4.4, the optimized pitch angle, active power and rotor speed curves in terms of the wind speed at the location of the wind turbine are generated for each individual wind turbine with the optimized pitch angle and tip speed ratio [3]. In case that the torque control scheme is implemented for the wind turbine active power control, the pitch angle and torque curve for each wind turbine in terms of the generator speed can be generated from the optimized pitch angle, active power and rotor speed curves in terms of the wind speed [3].

Considering the estimation error of the wake model, the maximum total active

power of the wind farm may not be able to be reached by the optimized control curves [3]. Especially, when there is a small power loss due to the wake effect in the wind farm, the total active power may be reduced compared with the MPPT method [3]. As the amount of power loss closely depends on the wind farm layout and the wind direction, the optimized control curves are separately generated at each wind directions, and the wind farm operator can trade off at which wind directions to implement the optimized control curves [3].

Moreover, the computation complexity to generate the optimal control curves for all the wind turbines at all the wind directions depends on the scale of the wind farm [3]. In Section 4.4, the optimal pitch angle and tip speed ratio of each wind turbine are selected by exhausted search method [3]. By this method, the total active power of the wind farm is compared among at all sets of pitch angle and tip speed ratio [3]. It is fond that, there is a small difference of the total active power of the wind farm in a large range of the pitch angel and tip speed ratio around the optimized pitch angle and tip speed ratio [3]. Besides, there is a small difference of the optimized pitch angle and tip speed ratio among the upstream wind turbines [3]. As a consequence, the optimized control curves of all the upstream wind turbines can be assumed to be the same [3]. Then, the optimization computation complexity can be reduced significantly [3]. The effectiveness of the proposed active power control method is verified in an 80-turbine wind farm with one year wind profile by simulation [3].

4.2. FEASIBILITY TO MAXIMIZE THE WIND FARM ACTIVE POWER GENERATION

In the 10-turbine wind farm as shown in Fig. 3.13, at the wind direction of 270° and the ambient wind speed of 10 m/s, in case that all the wind turbines are operating at the pitch angle of 0° and tip speed ratio of 7.55, the wind speed, the active power and the rotor speed of all the wind turbines are respectively shown in Fig. 4.1(a), (b) and (c) by the blue curves. It can be observed in Fig. 4.1(c), the rotor speed of all the wind turbines are in the range of from 6.9 rpm and 12.1 rpm, which are the up and down limit of the wind turbine rotor speed. In this case, all the wind turbines are controlled by the MPPT method.

If the pitch angle and tip speed ratio are changed to 4° and 6.9 respectively, the wind speed, the active power and the rotor speed of all the wind turbines are respectively shown in Fig. 4.1(a), (b) and (c) by the red curves. It can be observed in Fig. 4.1(c), the rotor speed of all the wind turbines are all in the range of from 6.9 rpm and 12.1 rpm, which indicates that the rotor speed will not be affected by the up and down limit of the wind turbine rotor speed.

Compared with the MPPT method, it can be observed in Fig. 4.1(b) the active

power of WT_1 is reduced. However, the active power of the wind turbines from WT_2 to WT_{10} are all increased. Overall, the total active power of the wind farm is increased from 15.3 MW to 18.1 MW, which accounts for 18.4% growth. Therefore, by optimizing the pitch angle and tip speed ratio of each wind turbine in the wind farm the total active power of the wind farm can be increased compared with the MPPT method [3].

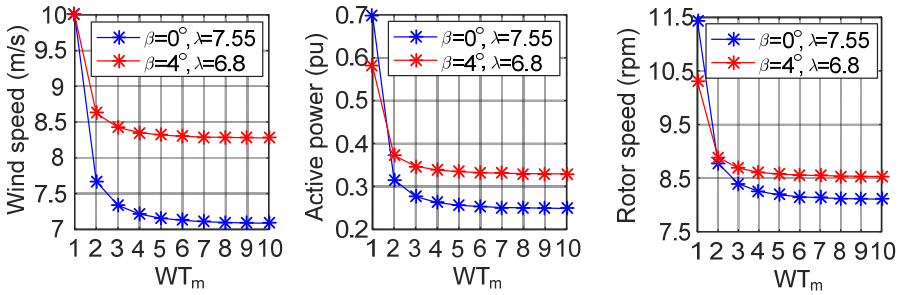

Fig. 4.1. Comparison between all the wind turbines are operating at the pitch angle of 0° and tip speed ratio of 7.55 (MPPT) and all the wind turbines are operating at the pitch angle of 4° and tip speed ratio of 6.8: (a) Wind speed; (b) Active power; (c) Rotor speed.

4.3. OPTIMIZATION BY THE PSO BASED ALGORITHM

According to the aerodynamic model, the active power of the wind turbine is determined by the pitch angle and tip speed ratio [10]. According to the wake model, the available power of the downstream wind turbine is determined by the pitch angle and tip speed ratio of the upstream wind turbine [10]. Consequently, the total active power of the wind farm is determined by the pitch angle and tip speed ratio of all the wind turbines [10]. In this section, the optimal pitch angle and tip speed ratio of all the wind turbines are selected by the Particle Swarm Optimization (PSO) based algorithm.

The Particle Swarm Optimization (PSO) is first developed by Kennedy and Eberhart in 1995. It deals with a swarm of particles that fly through the problem solution hyperspace [10]. The particle represents the optimization parameters [10]. The position of particle represents different value of the optimization parameters [10]. In iteration, particles change their position with a velocity, as presented by (4.1) and (4.2) [10],

$$V_i(t+1) = \omega \times V_i(t) + c_1 \times ran_1 \times (p_i - X(t)) + c_2 \times ran_2 \times (p_g - X_i(t)) \tag{4.1}$$

$$X_i(t+1) = X_i(t) + V_i(t+1) \tag{4.2}$$

where V is the velocity array, X is the position array, i is particle number, t is iteration number, c_1 and c_2 are acceleration coefficients, ran_1 and ran_2 are stochastic numbers ranged between 0 and 1, p_i is the historical best position of particle i, and p_g is the historical best position of the whole swarm [10]. The historical best position of the particle is obtained by comparing the objective function between the current iteration and the last iteration [10]. The historical best positon of the whole swarm can be obtained by comparing the objective function between the swarm of particles in the current iteration [10].

At a specific wind direction and a specific ambient wind speed, to maximize the total active power of the wind farm, the objective function can be expressed by [10],

$$\max(\sum_{i=1}^{i=n} P_i(v_i, \beta_i, \lambda_i)) \tag{4.3}$$

where, n is the number of the wind turbines in the wind farm, P_i is the active power of the i^{th} wind turbine WT_i, which is a function of the wind speed v_i, pitch angle β_i and tip speed ratio λ_i of WT_i and can be estimated by the aerodynamic model. The wind speed of WT_i, is determined by the ambient wind speed and the pitch angle and tip speed ratio of all its upstream wind turbines and can be calculated by the wake model [3]. The pitch angle and tip speed ratio of all the wind turbines are the control parameters of the optimization.

The constraints are as follow [10]:

$$\beta_{\min} \le \beta_i \le \beta_{\max} \tag{4.4}$$

$$\lambda_{\min} \le \lambda_i \le \lambda_{\max} \tag{4.5}$$

$$\omega_{r\_\min} \le \omega_{r\_WTi} \le \omega_{r\_\max} \tag{4.6}$$

$$P_i(\beta_i, \lambda_i) \le P_{rate} \tag{4.7}$$

$$V_{\min} \le V_i(t+1) \le V_{\max} \tag{4.8}$$

where β_i, λ_i, ω_{r_i} are the pitch angle, tip speed ratio and rotor speed of WT_i, β_{max}, λ_{max}, β_{min}, λ_{min}, ω_{r_max} *and* ω_{r_min} are the maximum and minimum value of the pitch angle, tip speed ratio and rotor speed, P_{rate} is the rated power, and V_{max} and V_{min} are the maximum and minimum value of the particle moving velocity $V_i(t+1)$ in the PSO program.

The flowchart to get the optimal pitch angle and tip speed of all the wind turbines by the PSO based optimization program is shown in Fig. 4.2 [10]. The elements in the position array of each particle are the pitch angle and tip speed ratio of all the wind turbines [10]. Firstly, the number of particles and the acceleration coefficients in velocity array is decided considering the operation range of the pitch angle and tip speed ratio and the computation complexity. The initial position array can be given as each wind turbine is controlled by the MPPT method [10]. The initial total active power of the wind farm for each particle can be calculated with the ambient wind speed and the initialized pitch angle and tip speed ratio of all the wind turbines by the aerodynamic model and the wake model [10]. Then, the initial best local position of each particle P_i and the initial best global position P_g can be obtained [10].

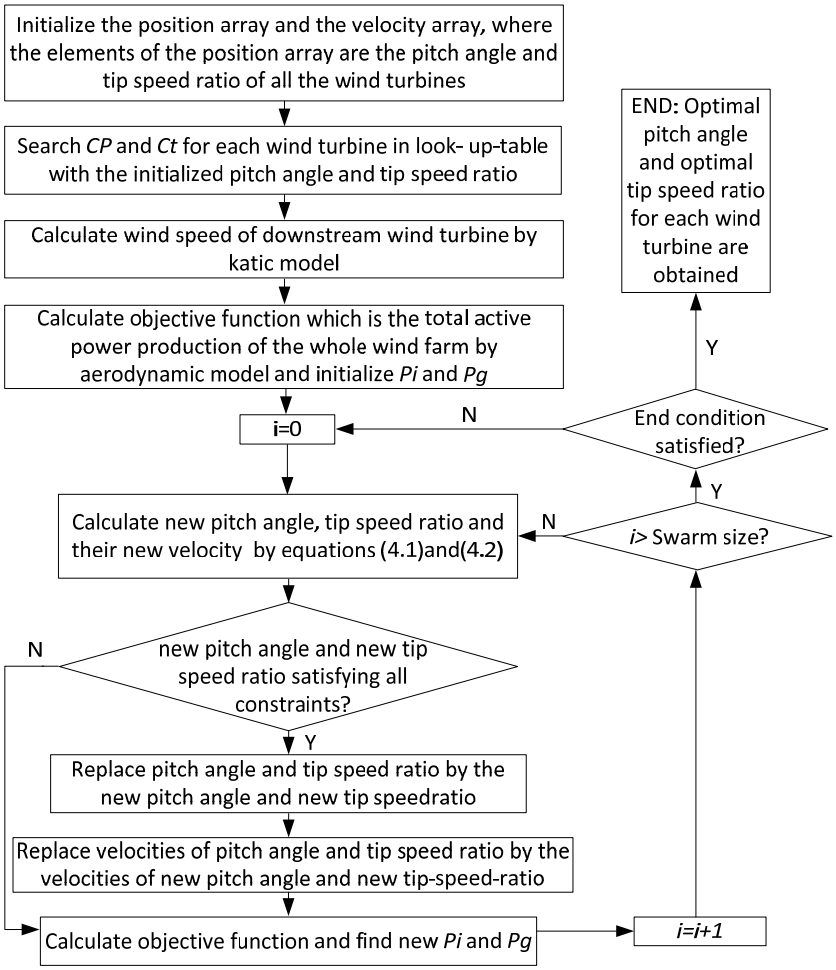

Fig. 4.2. Flow chart of the PSO iterations [10].

In the iterations, firstly, the pitch angle and tip speed ratio in the position array are changed according to (4.1) and (4.2) and limited by the constraints from (4.4) to (4.7) [10]. With the updated position of all the particles, the total active power of the wind farm of each particle can be calculated by aerodynamic model and the wake model [10]. By the comparison of the objective function (4.3) of each particle in current iteration and in the last iteration, the local best position of each particle can be updated [10]. Then, by the comparison of the objective function among the best local position of all the particles, the global best position of the whole swarm can be updated [10]. In a suitable number of iterations, the global best position of the whole swarm, which is the optimal pitch angle and tip speed ratio of all the wind turbines, can be obtained [10].

In the 10-turbine wind farm as shown in Fig. 3.13, at the wind direction of 270° and ambient wind speed of 10 m/s and 11.3 m/s, the optimized pitch angle and tip speed ratio of all the wind turbines obtained by the PSO based optimization algorithm are shown in Fig. 4.3(a) and (b). The optimized wind speed, active power and rotor speed of all the wind turbines are shown in Fig. 4.3(c), (d) and (e). Compared with the MPPT method, the pitch angle is increased, the tip speed ratio is decreased. The rotor speed is limited in the range from 6.9 rpm to 12.1 rpm which are the up and down rotor speed limit. At the ambient wind speed of 10 m/s, the active power of

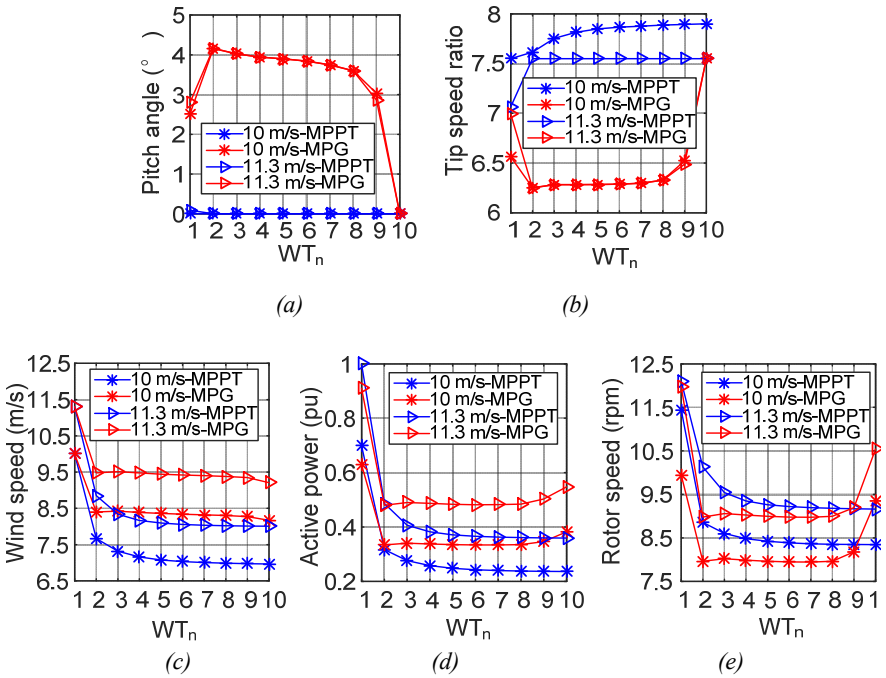

Fig. 4.3. Optimization results at 10 m/s and 11.3 m/s ambient wind speed.

WT_1 is reduced, but the active powers of WT_2 to WT_{10} are increased. Overall the total active power generation of the wind farm is increased from 15.3 MW to 18.0 MW, which is 17.6% increased.

Generally speaking, by the PSO method, the optimization results can be close to the optimal value infinitely. As the computation complexity and the optimization accuracy are all depending on the iteration number and the particle moving velocity, by trading off between the optimization computation complexity and the optimization accuracy, normally the exact optimal value may not be able to be obtained.

4.4. IMPLEMENTATION AND SIMPLIFICATION OF THE OPTIMIZATION IN TYPICAL WIND FARMS

To implement the optimized pitch angle and tip speed ratio, in this section, the optimal pitch angle, active power and rotor speed curves in terms of the wind speed are generated for each wind turbine [3]. In case that the generator torque control scheme is implemented for the wind turbine active power control, the optimized control curves can be transferred into the pitch angle and generator torque curves in terms of the generator rotor speed.

As the optimized pitch angle and tip speed ratio of each wind turbine depends on the ambient wind speed and the wind direction, the optimized control curves in terms of the wind speed are generated at each wind direction [3]. Moreover, the computation complexity of the optimization is large especially in large scale wind farms [3]. In this section, to implement and simplify the optimization in typical layout wind farms, the optimal pitch angle and tip speed ratio for each wind turbine are generated by the exhausted search method [3].

This section starts with the optimization in a 2-turbine wind farm [3]. As only the wake of the upstream wind turbine affects the total active power of the wind farm, the optimization computation complexity is small in the 2-trubine wind farm.

Then, in a 3 turbine wind farm, by the exhausted search method, the total active power of the wind farm is compared among all sets of pitch angle and tip speed ratio of all the wind turbines [3]. It is found that, there is a small difference of the total active power of the wind farm in a large range of pitch angel and tip speed ratio around the optimized pitch angle and tip speed ratio [3]. Besides, there is a small difference of the optimized pitch angle and tip speed ratio among the upstream wind turbines, while the last wind turbine along the wind direction should be controlled by the MPPT method as it doesn't cause the power loss due to the wake effect to the wind farm [3]. As a consequence, the optimized control curves of all the upstream wind turbines can be assumed to be the same [3]. This conclusion can be extended into the wind farm with more wind turbines installed in a line [3].

Then, the optimization computation complexity is reduced significantly [3].

Finally, the optimization and simplification are carried out in a typical large-scale wind farm with 80 NREL 5 MW DFIG wind turbines [3]. The improvement of the total active power of the wind farm by the proposed optimization method is verified with one year wind profile including the wind direction and wind speed distributions [3].

4.4.1. OPATIMIZATION AND IMPLEMENTATION IN A 2-TURBINE WIND FARM

In the wind farm with 2 NREL 5 MW DFIG wind turbines as shown in Fig. 3.4, the distance between two adjacent wind turbines is 6.5 blade diameters [3]. The decay constant k in the wake model is assumed to be 0.04. At the wind direction of 270°, to maximize the total active power of the wind farm, the WT_2 should be controlled by the MPPT method, as WT_2 will not cause the energy loss to the wind farm due to the wake effect [3]. At the ambient wind speed of 9 m/s, in case that WT_1 is operating at the pitch angle of 0°, the active power of WT_1, the wind speed of WT_2, the active power of WT_2 and the total active power of the wind farm in terms of the tip speed ratio of WT_1 are shown in Fig. 4.4 [3]. The wind speed of WT_2 is estimated by the Katic wake model.

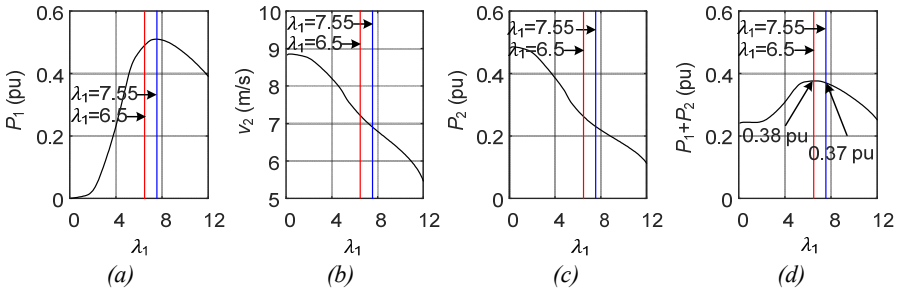

Fig. 4.4. Comparison between WT_1 operating at the tip speed ratio of 7.55 and 6.5, at the wind direction of 270° and ambient wind speed of 9 m/s: (a) The active power of WT_1, where the base value is 5 MW; (b) The wind speed of WT_2; (c) The active power of WT_2, where the base value is 5 MW; (d) The total active power of the wind farm, where the base value is 10 MW [3].

It can be observed in Fig. 4.4, if WT_1 is controlled by the MPPT method, where the tip speed ratio of WT_1 is 7.55, the active power of WT_1 get its maximum value [3]. The total active power of the wind farm is 0.37 pu [3]. Compared with the MPPT method, at the tip speed ratio of 6.5, the active power of WT_1 is reduced. However, the active power of WT_2 is increased. Totally, the active power of the wind farm is increased to 0.38 pu [3].

At the wind direction of 270° and ambient wind speed of 9 m/s, in case of WT_2 is controlled by the MPPT method, the total active power of the wind farm in terms of the pitch angle and tip speed ratio of WT_1 is shown in Fig. 4.5 [3]. It can be observed, if the WT_1 is controlled by the MPPT method, where pitch angle and tip speed ratio of WT_1 are 0° and 7.55 respectively, the total active power of the wind farm is 0.37 pu. If WT_1 is operating at the pitch angle and tip speed ratio of 1.8° and 6.9, the total active power of the wind farm is increased to 0.39 pu [3].

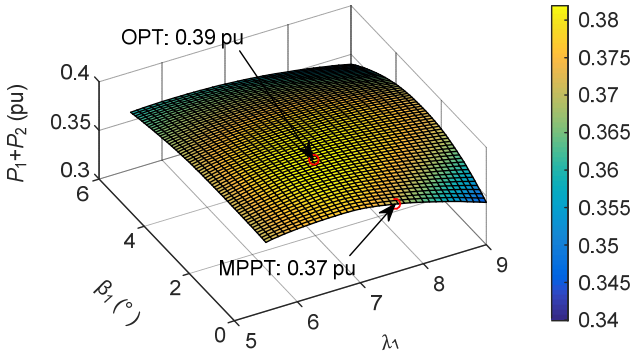

Fig. 4.5. Total active power of the wind farm in terms of the pitch angle and tip speed ratio of WT1, at 270° wind direction and 9 m/s ambient wind speed [3].

It can be concluded that the total active power of the wind farm can be maximized by optimizing the pitch angle and tip speed ratio of WT_1 [3]. By the exhausted search method, firstly, all the possible total active power of the wind farm at all sets of pitch angle and tip speed ratio of WT_1 are calculated, where the resolution of the pitch angle and tip speed ratio are 0.2° and 0.1 are taken into account [3]. Afterwards, the maximum total active power of the wind farm can be selected [3]. Finally, the corresponding optimal pitch angle and tip speed ratio of WT_1 can be obtained [3]. At the wind direction of 270° and the ambient wind speeds from the cut in wind speed 3 m/s to the cut out wind speed 25 m/s, the optimized pitch angle, tip speed ratio, active power and rotor speed of WT_1 in terms of ambient wind speed are shown in Fig. 4.6(a) [3].

At the wind direction of 270° and the ambient wind speeds from the cut in wind speed 3 m/s to the cut out wind speed 25 m/s, the active power of WT_1, the active power of WT_2 and the total active power of the wind farm are compared between the MPPT method and the proposed MPG method in Fig. 4.6(b) [3]. It can be observed that the total active power of the wind farm is increased at the ambient wind speeds from 7 m/s to 11 m/s [3].

At the wind directions of 270°, 276° and 282° and at the ambient wind speeds from the cut in wind speed 3 m/s to the cut out wind speed 25 m/s, the optimized pitch angle, tip speed ratio, active power and rotor speed of WT_1 in terms of ambient wind speed are shown in Fig. 4.7(a) [3]. The total active power of the wind farm is compared between the MPPT method and the proposed MPG method in Fig. 4.7(b) [3]. It can be observed in Fig. 4.7, at the wind direction of 282°, the optimized

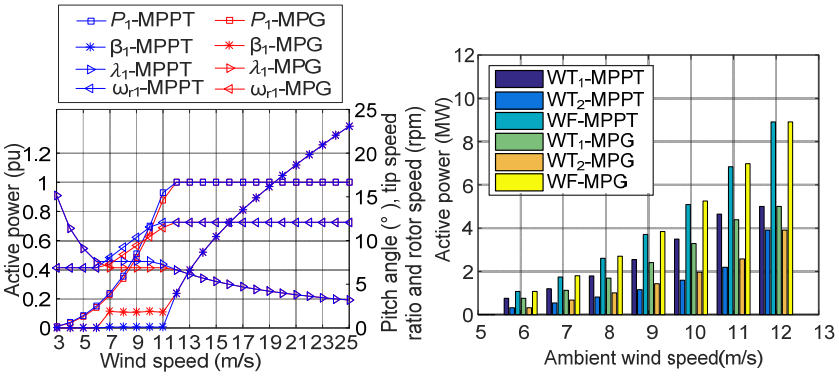

(a) (b)

Fig. 4.6. (a) At the wind direction of 270°, comparison of the pitch angle, tip speed ratio, blade speed and active power of WT_1 between the MPPT method and the proposed MPG method. (b) Comparison of the active power of WT_1, active power of WT_2, and the total active power of the wind farm, between the WT_1 is controlled by MPPT method and by the optimized method, at the wind direction of 270° [3].

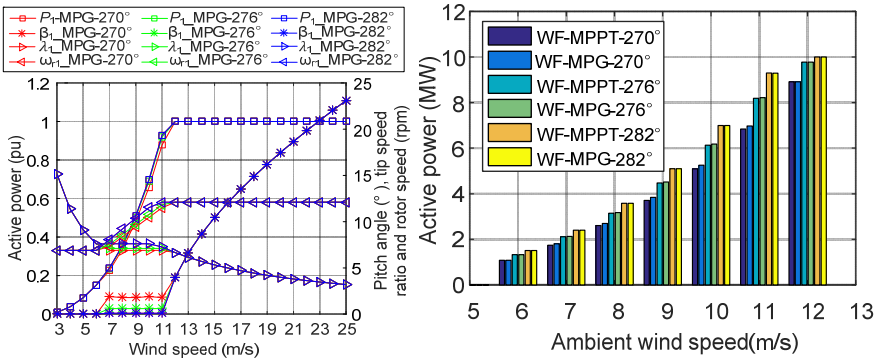

(a) (b)

Fig. 4.7. At the wind directions of 270°, 276° and 282°, and at the ambient wind speeds of from the cut in wind speed to the cut out wind speed 25 m/s, comparison between the WT_1 is controlled by the MPPT method and by the proposed MPG method: (a) Optimized pitch angle, tip speed ratio, rotor speed and active power of WT_1; (b) Total active power of the wind farm [3].

control curves of WT_1 and the total active power of the wind farm is the same as the WT_1 is controlled by the MPPT method. This is because there is no power loss in the wind farm due to the wake effect [3].

4.4.2. OPTIMIZATION AND IMPLEMENTATION IN A 3-TURBINE WIND FARM

In the wind farm with 3 NREL 5 MW DFIG wind turbines in a line as shown in Fig. 3.7, the distance between two adjacent wind turbines is 6.5 blade diameters [3]. The decay constant in the wake model of 0.04 is assumed [3]. At the wind direction of 270° and ambient wind speed of u, all the possible total active powers of the wind farm are shown in Fig. 4.8 [3]. The wind speed of WT_1 is the same as the ambient wind speed [3]. The wind speed of WT_2 and WT_3 can be estimated by the wake model [3]. The wind speed of WT_2 is determined by the pitch angle and tip speed ratio of WT_1 [3]. The wind speed of WT_3 is determined by the pitch angles and tip speed ratios of WT_1 and WT_2 [3]. The active power of WT_1, WT_2 and WT_3 can be calculated by the aerodynamic model [3].

At the wind direction of 270° (the definition of the wind direction is shown in Fig. 3.7), as WT_3 will not cause the energy loss to the wind farm due to the wake effect, to maximize the total active power of the wind farm, the WT_3 should be controlled by the MPPT method [3]. The pitch angle and tip speed ratio of WT_1 and WT_2 should be optimized [3]. By the exhausted search method, firstly, all the possible total active power of the wind farm are calculated at each set of pitch angle and tip speed ratio of WT_1 and WT_2 [3]. Afterwards, the maximum total active power of the wind farm can be selected [3]. Finally, the corresponding optimal pitch angle and tip speed ratio of WT_1 and WT_2 can be obtained [3].

At the wind direction of 270° and at the ambient wind speed of 11 m/s, obtained by the exhausted search method, the optimized pitch angle and tip speed ratio of WT_1 are 2.2° and 6.7 respectively [3]. The optimized pitch angle and tip speed ratio of WT_2 are 2.8° and 6.5 respectively [3]. At the wind direction of 270° and at the wind speeds from the cut in wind speed of 3 m/s to the cut out wind speed of 25 m/s, the optimized pitch angle, tip speed ratio, active power and rotor speed of WT_1 and WT_2 are shown in Fig. 4.9[3].

As shown in Fig. 4.9 [3], the optimized control curves of WT_1 and WT_2 are similar with a small difference. The feasibility to implement the same optimized control curves of WT_1 in WT_2 is analysis as follows:

By the exhausted search method, at the wind direction of 270° and at the ambient wind speed of 11 m/s, the active power of WT_1 and the wind speed of WT_2 in terms of pitch angle and tip speed ratio of WT_1 are shown in Fig. 4.10(a) and (b) [3]. The

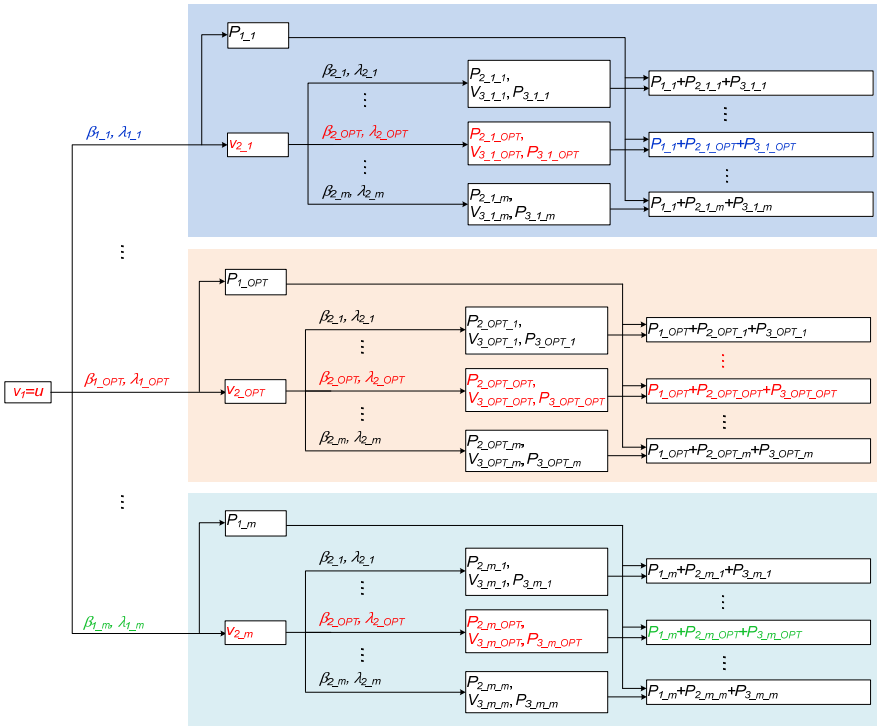

Fig. 4.8. Relationship of the variables in the wind farm with 3 wind turbines, at the wind direction of 270° [3].

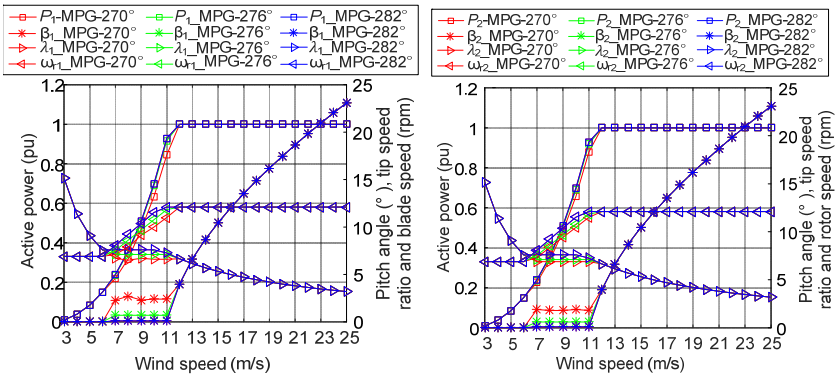

(a) (b)

Fig. 4.9. Optimized pitch angle, tip speed ratio, active power and rotor speed of: (a) WT_1; (b) WT_2 [3].

pitch angle of WT_1 is in the range of from 0° to 6° [3]. The tip speed ratio of WT_1 is in the range of from 5 to 9. Due to the 12.1 rpm rotor speed limit, the tip speed ratio of WT_1 is limited by 7.25 [3]. In case that WT_1 is operating at the pitch angle of 0° and tip speed ratio of 7.25 (MPPT), the active power of WT_2, the wind speed of WT_3, the active power of WT_3 and the total active power of the wind farm in terms of the pitch angle and tip speed ratio of WT_2 are shown in Fig. 4.10(c), (d), (e) and (f) respectively [3]. As it is shown in Fig. 4.10(f), the total active power of the wind farm is 0.58 pu [3]. In case that WT_1 is operating at the optimized pitch angle of 2.2° and tip speed ratio of 6.7, the active power of WT_2, the wind speed of WT_3, the active power of WT_3 and the total active power of the wind farm in terms of the pitch angle and tip speed ratio of WT_2 are shown in Fig. 4.10(g), (h), (i) and (j) respectively [3]. As it is shown in Fig. 4.10(j), the maximum total active power of the wind farm is 0.615 pu [3].

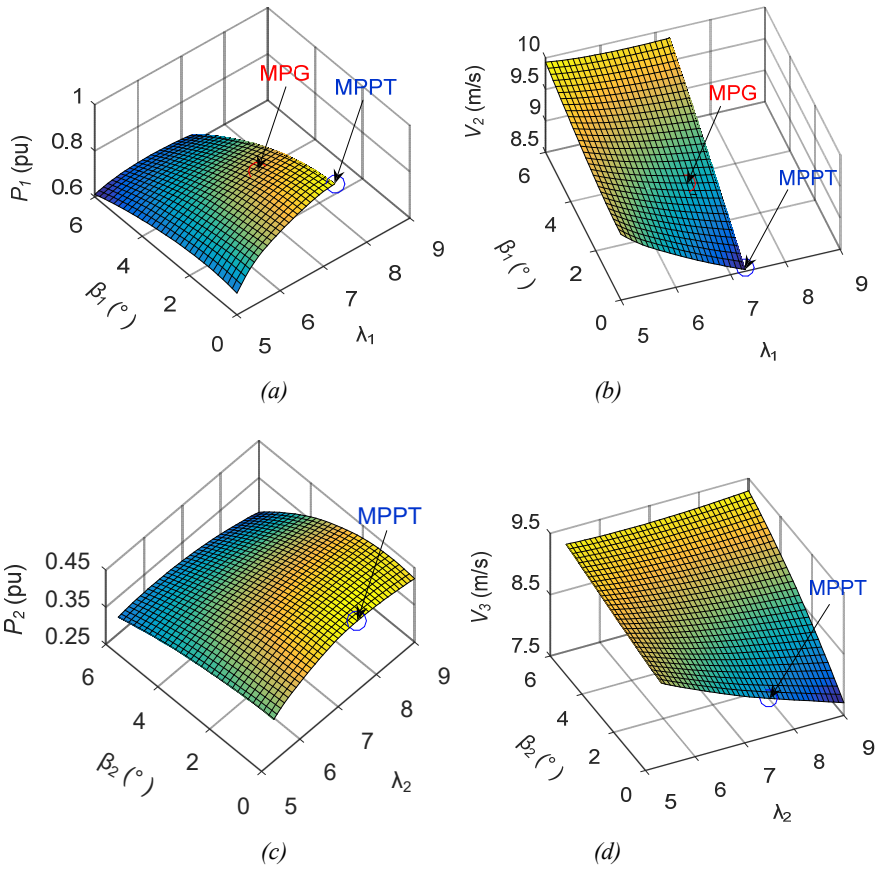

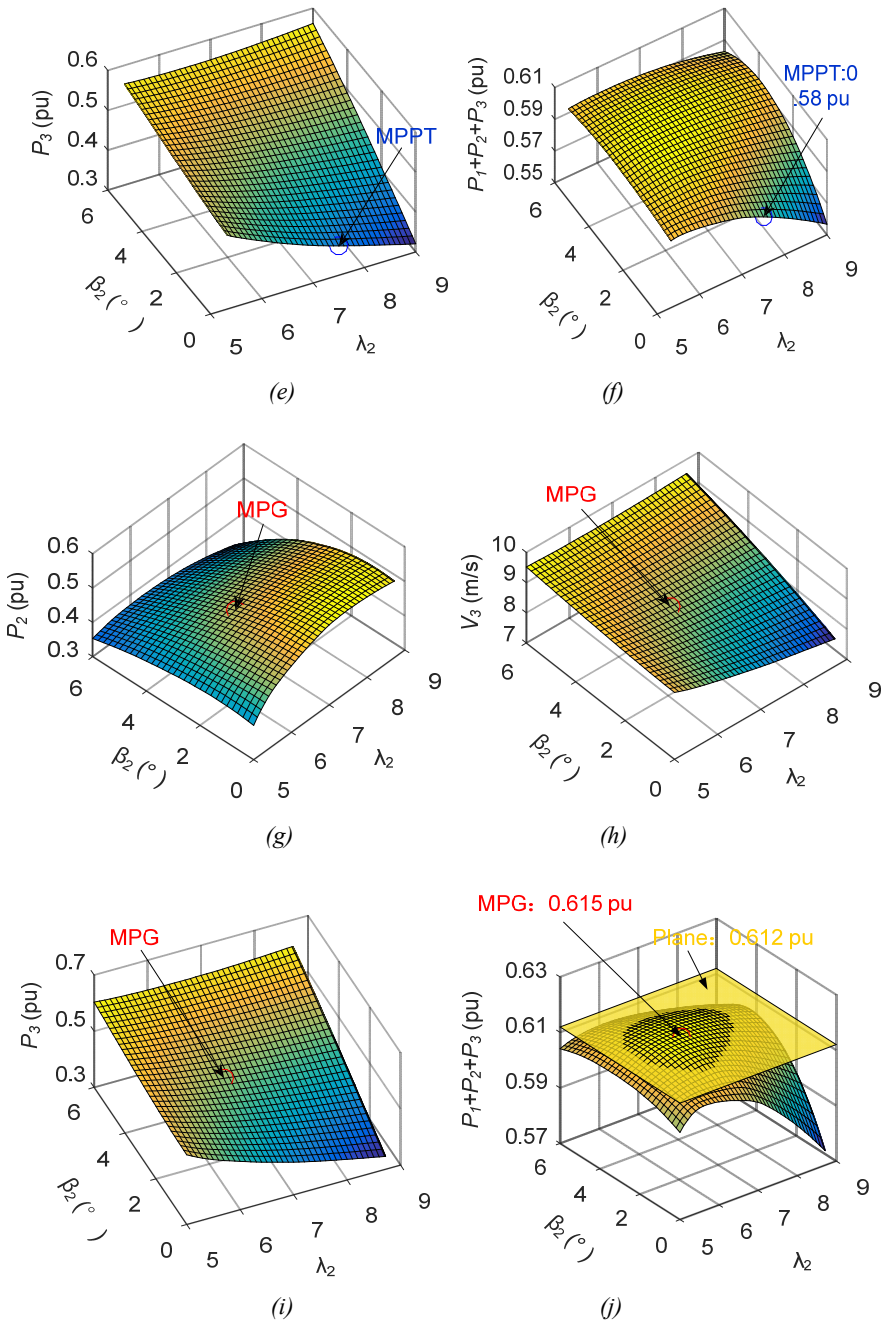

Fig. 4.10. At the wind direction of 270° and ambient wind speeds from 11 m/s: (a) The active power of WT_1; (b) The wind speed of WT_2 in terms of the pitch angle and tip speed ratio of

WT_1. In case of WT_1 is controlled by the MPPT method: (c) The active power of WT_2; (d) The wind speed of WT_3; (e) The active power of WT_3; (f) The total active power of the wind farm. In case of the WT_1 is operating at the optimized pitch angle and tip speed ratio: (g) The active power of WT_2; (h) the wind speed of WT_3; (i) The active power of WT_3; (j) The total active power of the wind farm [3].

As it is shown in Fig. 4.10(j), in a large range of pitch angles and tip speed ratios of WT_2, the total active power of the wind farm is larger than 0.612 pu [3]. Compared with the maximum total active power of the wind farm 0.615 pu, there is a small difference of 0.003 pu [3]. It is the same case at the other ambient wind speeds [3]. Consequently, at the wind direction of 270°, the optimized control curves of WT_1 can simply be implemented in WT_2 [3].

Furthermore, at the wind direction of 270°, the optimized control curves of WT_1 and WT_2 in the 3-turbien wind farm are similar as the optimized control curves of WT_1 in the 2-turbine wind farm and with a small difference [3]. Thus the optimized control curves of WT_1 in the 2-turbine wind farm can be implemented in WT_1 and WT_2 in the 3-turbien wind farm [3]. This conclusion can be extended into the wind farm with more wind turbines in a line, where the optimized control curves of WT_1 in the 2-turbine wind farm can simply be implemented in all the upstream wind turbines [3]. Consequently, the optimization computation complexity can be reduced significantly [3].

At the wind direction of 270° and ambient wind speeds from 6 m/s to 14 m/s, implement the optimized control curves of WT_1 in the 2-turbine wind farm in the WT_1 and WT_2 in the 3-turbine wind farm, the active power generation of each wind turbine and the total active power of the wind farm are shown in Fig. 4.11 [3]. It can be observed, the active power of the wind farm are increased from the ambient wind speeds from 6 m/s to 13 m/s [3].

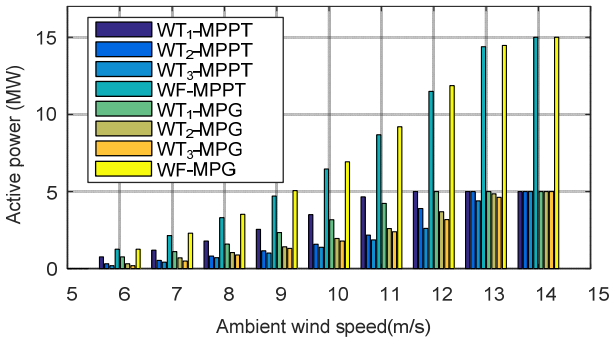

Fig. 4.11. At the wind direction of 270° and ambient wind speeds from 6 m/s to 14 m/s, comparison of the active power of WT_1, WT_2, WT_3 and the total active power of the wind farm between the MPPT method and the proposed MPG method [3].

4.4.3. OPTIMIZATION AND IMPLEMENTATION IN A 80-TURBINE WIND FARM

In the wind farm with 80 NREL 5 MW DFIG wind turbines as shown in Fig. 3.10, the computation complexity of the optimization is large, due to the large number of optimization parameters and the complexity of the downstream wind speed calculation in multiple wakes [3]. To simplify the optimization and implementation of the proposed MPG method, the optimization and implementation is carried out at the wind directions that the wind farm has large power loss, considering the reasons as follow [3]:

- The proposed MPG method generates the optimal control curves for each wind turbine in the wind farm at each wind direction.
- The optimization is feasible at the wind directions where the wind farm has power loss due to the wake effect.
- Due to estimation error of the wake model, the optimized control curves may not be able to increase the total active power of the wind farm at the wind directions that the wind farm has small power loss.
- As presented in Section 3.2.3, in the 80-turbine wind farm, the large power loss of the wind farm appears at the wind directions of around 41°, 90°, 131°, 172°, 221°, 270°, 311° and 352°. At these wind directions, the wind farm can be seen as isolated wind farms with wind turbines in a line. e.g. at the wind direction of 270°, the 80-turbine wind farm can be further simplified as 8 isolated 10-turbine wind farms as shown in Fig.3.13, as the wind turbine in one row will not cause the wind speed deficit to the wind turbines in other rows, due to the small decay constant in the Katic wake model.
- As discussed in Section 4.4.2, the optimized control curves of WT_1 in the 2-turbine wind farm obtained at the wind direction of 270° can simply be implemented in all the upstream wind turbines in the wind farm with wind turbines in a line with a small error which can be ignored. The last wind turbine along the wind direction is controlled by the MPPT method, as the last wind turbine will not cause the power loss due to the wake effect to the wind farm.

At the wind direction of 270°, the 80-turbine wind farm can be seen as 8 isolated 10-turbine wind farms as shown in Fig.3.13 [3]. With the optimized control curves of WT_1 in the 2-turbine wind farm implemented in WT_1-WT_9, and with the MPPT method implemented in WT_{10} in the 10-turbine wind farm, the total active powers of each isolated 10-turbine wind farm is shown with the yellow bar in Fig. 4.12 [3], where the ambient wind speed of from 6 m/s to 15 m/s are taken into account. Compared with all the wind turbines are controlled by the MPPT method, which is

shown with the blue bar in Fig. 4.12, the total active power of the wind farm can be increased in a large percentage [3]. At the other wind directions, where the wind farm has large power loss, the optimization and implementation can be carried out by the same method as at the wind direction of 270° [3].

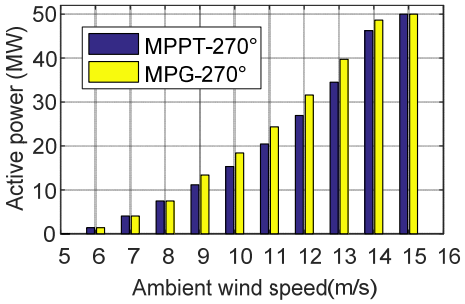

Fig. 4.12. Comparison of the total active power of the 10-turbine wind farm as shown in Fig. 3.4.1, between the MPG method and the MPPT method, at the wind direction of 270° [3].

With the one year wind profile as shown in Fig.3.16, the AEP of each wind turbine in the 80-turbine wind farm is compared between the MPPT method and the proposed MPG method in Table 4.1 and 4.2 [3]. In the wind rose sectors of 265°-275°, 85°-95°, 345°-355° and 165°-175° the AEP of the wind farm are increased by 11.02%, 19.2%, 15.2% and 12.7% respectively [3]. 13.6 GWh more AEP of the 80-turbine wind farm is increased [3]. Compared with the 124.4 GWh in case of all the wind turbines are controlled by the MPPT method, 1.09% is increased [3]. In case that the optimization is also implemented at other wind directions, this percentage will be larger [3].

Table 4.1. Comparison of the AEP (MWh) between the MPPT method and the proposed MPG method in the wind rose sectors of 265°-275° and 85°-95° [3].

AEP	265°-275° sector		85°-95° sector	
	MPPT	**MPG**	**MPPT**	**MPG**
WT_{m_1}	1356.6	1280.9	85.5	142.3
WT_{m_2}	977.8	949.7	86.8	130.7
WT_{m_3}	835.4	880.7	88.7	122.5
WT_{m_4}	760.8	840.4	90.5	123.4
WT_{m_5}	713.9	815.6	94.5	125.6
WT_{m_6}	689.1	798.6	99.1	128.8
WT_{m_7}	669.2	786.8	108.9	134.2

WT_{m_8}	658.7	780.4	127.1	143.3
WT_{m_9}	642.7	814.0	167.4	161.0
WT_{m_10}	631.2	859.3	288.4	262.8
WF	**63482.2**	**70450.4**	**9895.4**	**11795.4**
Increased	**11.0%**		**19.2%**	

Table 4.2. Comparison of the AEP (MWh) between the MPPT method and the proposed MPG method in the wind rose sectors of 345°-355° and 165°-175° [3].

AEP	345°-355° sector		165°-175° sector	
	MPPT	**MPG**	**MPPT**	**MPG**
WT_{1_n}	382.9	348.4	169.9	248.7
WT_{2_n}	234.1	232.1	173.0	233.8
WT_{3_n}	185.3	208.8	180.1	222.7
WT_{4_n}	162.5	195.5	187.7	228.1
WT_{5_n}	148.4	188.1	203.9	237.0
WT_{6_n}	142.3	183.4	230.1	252.0
WT_{7_n}	136.1	194.1	283.7	278.4
WT_{8_n}	134.0	207.0	435.2	400.0
WF	**15255.2**	**17573.2**	**18635.2**	**21006.9**
Increased	**15.2%**		**12.7%**	

4.5. SUMMARY

In this chapter, considering the wake effect, a MPG method is proposed to maximize the total active power of the wind farm. Firstly, the feasibility to increase the total active power of the wind farm is presented. Afterwards, the optimal pitch angle and tip speed ratio are selected by the PSO based optimization algorithm. The optimization is based on the downstream wind speed estimation by the wake model.

To implement the optimized pitch angle and tip speed ratio, optimal control curves are generated for each individual wind turbine. Considering the estimation error of the wake model, the maximum total active power of the wind farm may not be able to be reached, which indicates the optimized pitch angle and tip speed ratio are not accurate. Especially, at the wind direction where the wind farm has slight power loss due to the wake effect, the proposed MPG method may reduce the total active power generation of the wind farm compared with the MPPT method. However, at

the wind directions where the wind farm has large power loss, the total active power of the wind farm can be increased in a large proportion. As the amount of power loss closely depends on the wind farm layout and the wind direction, and the optimized control curves are separately generated at each wind directions, the wind farm operator can make a decision at which wind directions to implement the optimized control curves.

Especially in the large-scale wind farms, the computation complexity of the optimization is large, due to the large amount of optimization parameters and the complexity of the downstream wind speed calculated in multiple wakes. In Section 4.4, the optimal pitch angle and tip speed ratio are selected by exhausted search. By the analysis in the 2-turbine wind farm and 3-turbine wind farm, it can be concluded that the optimized control curves of the upstream wind turbine in the 2-turbine wind farm can be implemented in all the upstream wind turbines in the wind farm with more wind turbines installed in a line. The last wind turbine along the wind turbine should be controlled by the MPPT method, as the last wind turbine will not cause the power loss due to the wake effect to the wind farm. Thus, the optimization and implementation can be simplified.

Finally, the proposed MPG method is implemented in a large-scale 80-turbine wind farm with one year wind profile. In the wind rose sectors of 265°-275°, 85°-95°, 345°-355° and 165°-175° the AEP of the wind farm are increased by 11.02%, 19.2%, 15.2% and 12.7% respectively. Totally, 13.6 GWh more AEP is increased. Compared with the 124.4 GWh in case of all the wind turbines are controlled by the MPPT method, 1.09% is increased. In case that the optimization is also implemented at other wind directions where the wind farm has large power loss due to the wake effect, this percentage will be larger.

CHAPTER 5. MAXIMUM ENERGY PRODUCTION (MEP) IN WIND FARM CONSIDERING WAKE EFFECT AND WIND TURBINE LIFETIME

5.1. INTRODUCTION

In the DFIG wind turbine based wind farm, the commonly implemented active power control method is the Maximum Power Point Tracking (MPPT) [3], [8] and [11]. By the MPPT method, each wind turbine generates the maximum active power, by optimally controlling its pitch angle and tip speed ratio [3], [8] and [11]. According to the wind turbine aerodynamic model and the wake model, the active power generation of the wind turbine and the power loss of its downstream wind turbine due to the wake effect are both determined by the pitch angle and tip speed ratio of the upstream wind turbine [3] and [11]. In Chapter 4, considering the wake effect, a Maximum Power Generation (MPG) method is proposed. Compared with the MPPT method, by optimizing the pitch angle and tip speed ratio of the upstream wind turbine, the active power of the upstream wind turbine will be reduced [3] and [11]. However, the available active power of the downstream wind turbine will be increased [3] and [11]. Overall, the total active power of the wind farm can be increased [3] and [11].

The energy production of the wind farm relates to the active power and the lifetime of all the wind turbines in the wind farm [11]. As presented in Section 2.4, the lifetime of the power converter, which has the highest lifetime consumption than other components of the wind turbine and can be used to determine the lifetime of the wind turbine, is also determined by the pitch angle and tip speed ratio [11]. By the MPG method, the active power of the wind farm can be maximized, which results the maximum energy production of the wind farm in a specific period [11]. However, the lifetime of the power converter is not taken into account [11]. Consequently, the MPG method may not be able to reach the maximum energy production of the wind farm in its lifespan [11].

In this chapter, considering the wake effect and wind turbine lifetime, a Maximum Energy Production (MEP) method is proposed to maximize the total energy production of the wind farm in its lifespan, by optimizing the pitch angle and tip speed ratio of each wind turbine in the wind farm [11]. The energy production of the wind farm in its lifespan is calculated by the superposition of the energy

production of all the wind turbines in its individual lifespan [11]. Case studies are carried out in the 2-turbine wind farm [11]. Firstly, in Section 5.2, the energy production of the wind farm in all its lifespan is compared between the MPPT method and the MPG method [11]. Afterwards, in Section 5.3, the optimized pitch angle and tip speed ratio are selected for each wind turbine to maximize the energy production of the wind farm in all its lifespan by the proposed MEP method [11]. The optimized pitch angle curve and active power curve are generated with the optimized pitch angle and tip speed ratio to maximize the total energy production of the wind farm in all its lifespan [11].

5.2. COMPARISON OF THE WIND FARM ENERGY PRODUCTION BETWEEN THE MPPT METHOD AND THE MPG METHOD

In this section, the energy production of each wind turbine in its whole lifespan and the total energy production of the wind farm are compared between the MPPT method and the proposed MPG method in the 2-turbine wind farm as shown in Fig.3.4 [11].

A: Assuming constant wind direction of 270° and constant ambient wind speeds.

With MPPT method, the WT_1 and WT_2 are all controlled by the blue curves as shown in Fig. 4.6(a). With the MPG method, the WT_2 is controlled by the MPPT method, as WT_2 will not cause the power loss due to the wake effect to the wind farm [11]. Thus WT_2 is also controlled by the blue curves as shown in Fig. 4.6(a). The WT_1 is controlled by the optimized red curves as shown in Fig. 4.6(a). By the lifetime estimation method as presented in section 2.4, the lifetime of WT_1 and WT_2 are compared between the MPPT method and the MPG method in Fig. 5.1(a) [11], where the ambient wind speeds from 3 m/s to 25 m/s with the resolution of 1 m/s are taken into account.

In Fig. 5.1(a), the lifetime of the wind turbine is represented by the B10 lifetime of the power converter [11]. The B10 lifetime is the number of cycles during which 10 percent of the total number of modules fails [13]. Additionally, in case that the calculated value is larger than 30 years, the lifetime of the wind turbine is supposed to be determined by other components of the wind turbine rather than the power converter, and is limited at 30 years [11]. It can be observed, controlled by the MPG method compared with the MPPT method, the lifetime of WT_1 is increased and the lifetime of WT_2 is reduced at the ambient wind speeds from 9 m/s to 11 m/s [11].

At each constant wind speed between 3 m/s and 25 m/s, with the active power generation of each wind turbine as shown in Fig. 4.6(a) and with the lifetime of

each wind turbine as shown in Fig. 5.1(a), the energy production of each wind turbine in its whole lifespan and the total energy production of the wind farm are compared between the MPPT method and the MPG method in Fig. 5.1(b) [11]. It can be observed, controlled by the MPG method, the energy production of WT_1 in its whole lifespan is reduced at the ambient wind speeds from 7 m/s to 8 m/s and increased from 9 m/s to 11 m/s [11]. This is because, even though the active power of WT_1 is reduced, however the lifetime of WT_1 is increased [11]. The energy production of WT_2 in its whole lifespan and the energy production of the wind farm are increased from the ambient wind speeds from 7 m/s to 11 m/s [11].

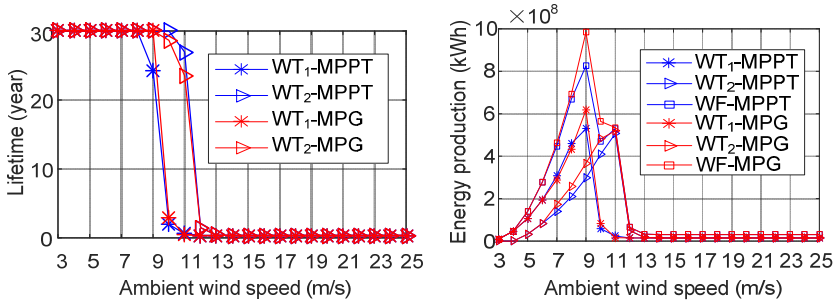

(a) *(b)*

Fig. 5.1. At the wind direction of 270°, comparison between the MPPT method and the MPG method of: (a) Wind turbine lifetime; (b) Energy Production [11].

B: Assuming constant wind direction of 270° and with an ambient wind speed distribution.

For a single wind turbine, assuming its active power is P_i and its lifetime is L_i at constant wind speed v_i, where i denotes different wind speeds, and assuming the wind speed distribution at the wind speed v_i is D_i with a wind speed distribution in its whole lifespan, the operation time of the wind turbine at the wind speed v_i can be expressed by L_iD_i [11]. The lifetime of the wind turbine can be expressed by ΣL_iD_i, and the energy production of the wind turbine in its whole lifespan can be calculated by $\Sigma P_iL_iD_i$ [11].

By assuming the constant wind direction of 270° and with an ambient wind speed distribution at the constant wind direction of 270° in the whole lifespan of the wind turbine as shown in Fig. 5.2(a) [11], the total energy production of the wind farm at each separate ambient wind speed are shown in Fig. 5.2(b) [11] and Fig. 5.3(a) [11]. In Fig. 5.2(b), it can be observed that the total energy production of the wind farm is increased mainly at the ambient wind speeds from 7 m/s to 10 m/s [11]. The total energy production of WT_1, WT_2 in its whole lifespan and the total energy production of the wind farm at all the ambient wind speeds are shown in Fig. 5.2(c)

[11]. It can be observed, they are increased by 3.1%, 15.2% and 8.7% respectively [11].

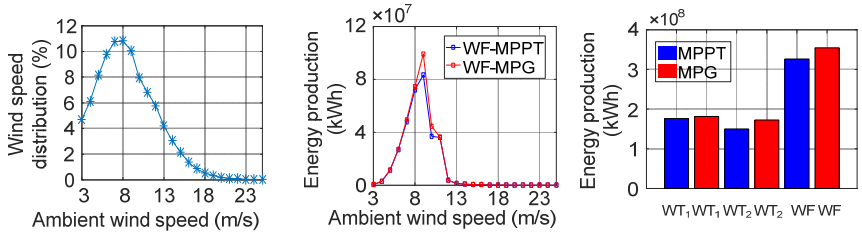

(a) *(b)* *(c)*

Fig. 5.2. (a) Field wind speed distribution. At the constant wind direction of 270°, comparison between the MPPT method and the MPG method: (b) Energy production of the wind farm at each separate ambient wind speed; (c) Total energy production of the wind farm at all ambient wind speeds [11].

C: Assuming constant wind direction of 276° and 282° with the same ambient wind speed distribution at each wind direction.

Compared with the MPPT method, the MPG method increases the active power of the wind farm at the wind directions where the wind farm has power loss due to the wake effect [11]. As presented in Section 3.2.1, the power loss due to the wake effect in the 2-turbine wind farm appears at the four symmetrical wind direction ranges of 270°-282°, 258°-270°, 78°-90° and 90°-102°. In other wind directions, as there is no power loss in the wind farm due to wake, the control curves of the MPG method are the same as MPPT method [11]. By assuming the constant wind direction of 276° and 282° in all the lifespan of the wind turbines and the same ambient wind speed distribution at each constant wind direction as shown in Fig. 5.2(a), the energy productions of the wind farm, at each constant wind direction and at each separate ambient wind speed, are shown in Fig. 5.3(a). It can be observed, the total energy production of the wind farm is increased in a small percentage at the constant wind direction of 282°, as there is a small power loss due to the wake effect in the wind farm at this wind direction.

D: Assuming wind direction distribution and ambient wind speed distribution.

Taking into account the wind direction distribution as shown in Fig. 5.3(b) [11] and the ambient wind speed distribution as shown in Fig 5.2(a), compared with the MPPT method, the total energy production of WT_1, WT_2 in its whole lifespan and total energy production of the wind farm are shown in Fig. 5.3(c) [11]. It can be observed, a small percentage of total energy production of the wind farm is

increased by the MPG method [11]. This is because Compared with the MPPT method, the MPG method increases the energy production of the wind farm at the four wind direction ranges of 270°-282°, 258°-270°, 78°-90° and 90°-102°. At other wind directions the wind farm has the same energy production compared between the MPPT method and the MPG method. Thus, the MPG method is not effective on the increase of the total energy production of the wind farm in which the power loss due to the wake effect is small [11]. In section 5.3, a Maximum Energy Generation (MEP) method is proposed to maximize the total energy production of the wind farm.

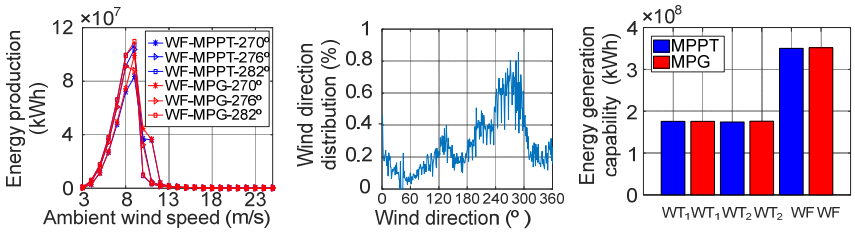

(a) *(b)* *(c)*

Fig. 5.3. (a) At the constant wind direction of 270°, 276° and 282°, comparison of the wind farm energy production at each separate ambient wind speed between the MPPT method and the MPG method, (b) Wind direction distribution, (c) Considering the wind direction distribution, comparison of the total energy production of the wind farm at all the wind directions and all the ambient wind speeds [11].

5.3. MAXIMIZATION OF THE WIND FARM ENERGY PRODUCTION

In this subsection, taking into account the wind turbine lifetime expectation, a Maximum Energy Generation (MEP) active power control method is proposed to maximize the total energy production of the wind farm, by optimizing the pitch angle and tip speed ratio of each wind turbine [11]. To implement the optimized pitch angle and tip speed ratio, the optimal pitch angle, active power and rotor speed curves are generated from the optimized pitch angle and tip speed ratio [11]. Case studies carried out in the 2-turbine wind farm as shown in Fig. 3.4.

5.3.1. OPTIMIZATION BY EXHAUSTED SEARCH METHOD

As the active power and the lifetime of a wind turbine, and the power loss of its downstream wind turbine are all determined by its pitch angle and tip speed ratio, the energy production of the wind farm can be maximized by optimizing the pitch angle and tip speed ratio of all the wind turbines in the wind farm [11]. In the 2-turbine wind farm as shown in Fig. 3.4, the objective function to maximize the

energy generation of the wind farm by selecting the optimal pitch angle and tip speed ratio of WT_1 and WT_2 can be formulated by [11],

$$Max(P_1(v_1,\beta_1,\lambda_1)L_1(v_1,\beta_1,\lambda_1)+P_2(v_2,\beta_2,\lambda_2)L_2(v_2,\beta_2,\lambda_2)) \quad (5.1)$$

where, P_1 and P_2 are the active power of WT_1 and WT_2, L_1 and L_2 are the lifetime of WT_1 and WT_2, v_1 and v_2 are the wind speed of WT_1 and WT_2, β_1 and β_1 are the pitch angle of WT_1 and WT_2, and λ_1 and λ_1 are the tip speed ratio of WT_1 and WT_2. The control parameters are the pitch angle and the tip speed ratio of WT_1 and WT_2 [11].

At the wind direction of 270°, the wind speed of WT_1 is the ambient wind speed, and the wind speed of WT_2 can be estimated by the wake model [11]. The active power and the lifetime of WT_1 and the wind speed of WT_2 are all determined by the wind speed, the pitch angle and the tip speed ratio of WT_1. The active power and the lifetime of WT_2 are all determined by the wind speed, the pitch angle and the tip speed ratio of WT_2 [11]. In summary, with the known pitch angle and tip speed ratio of each wind turbine, the active power, lifetime and wind speed of each wind turbine can be calculated [11]. At the wind direction of 270° and the ambient wind speed of u, all the possible total energy productions of the wind farm at all sets of pitch angle and tip speed ratio of all the wind turbines expressed by $P_{1\_m}L_{1\_m}+P_{2\_m}L_{2\_m}$ are shown in Fig. 5.4 [11].

In Fig. 5.4, m sets of pitch angle and tip speed ratio of WT_1 and m sets of pitch angle and tip speed ratio of WT_2 are assumed with a resolution [11]. By the exhausted search method, the total energy productions of the wind farm can be compared at sets of pitch angle and tip speed ratio of WT_1 and WT_2 [11]. Then, the maximum total energy generation of the wind farm can be obtained and the corresponding optimal pitch angel and tip speed ratio of WT_1 and WT_2 can be selected [11].

In Fig. 5.4, the maximum total energy production of the wind farm is $P_{1\_OPT}L_{1\_OPT}+P_{2\_OPT\_OPT}L_{2\_OPT\_OPT}$ and the corresponding optimal pitch angle and tip speed ratio of WT_1 and WT_2 are β_{1_OPT}, λ_{1_OPT}, β_{1_OPT} and λ_{1_OPT} [11]. At the optimal pitch angle and tip speed ratio of WT_1, the energy production of WT_1 and the wind speed of WT_2 are fixed values. Consequently, to maximize the total energy production of the wind farm, the optimal pitch angle and tip speed ratio of WT_2 is corresponding to the maximum energy production of WT_2 at the wind speed of WT_2 [11].

In case of the ambient wind speed is changed, the optimal pitch angle and tip speed ratio of WT_1 will be changed, and the wind speed of WT_2 will be changed [11]. However, the optimal pitch angle and tip speed ratio of WT_2 is still corresponding to the maximum energy production of WT_2 at the wind speed of WT_2 [11]. It can be

concluded that the optimal pitch angle and tip speed ratio of WT_2 is corresponding to the maximum energy production of WT_2 at the wind speed of WT_2 [11]. Thus, the optimal pitch angle and tip speed ratio of WT_2 can be selected at each wind speed of WT_2 from the cut-in wind speed to the cut-out wind speed [11]. Then the optimal control curves of WT_2 can be generated. With the optimized control curves of WT_2 implemented, the optimal pitch angle and tip speed ratio of WT_1 which corresponding to the maximum total energy production of the wind farm, can be selected [11]. In summary, the optimal pitch angle and tip speed ratio of WT_1 and WT_2 can be selected separately, and the optimal pitch angle and tip speed ratio of WT_2 should be selected prior to WT_1 [11].

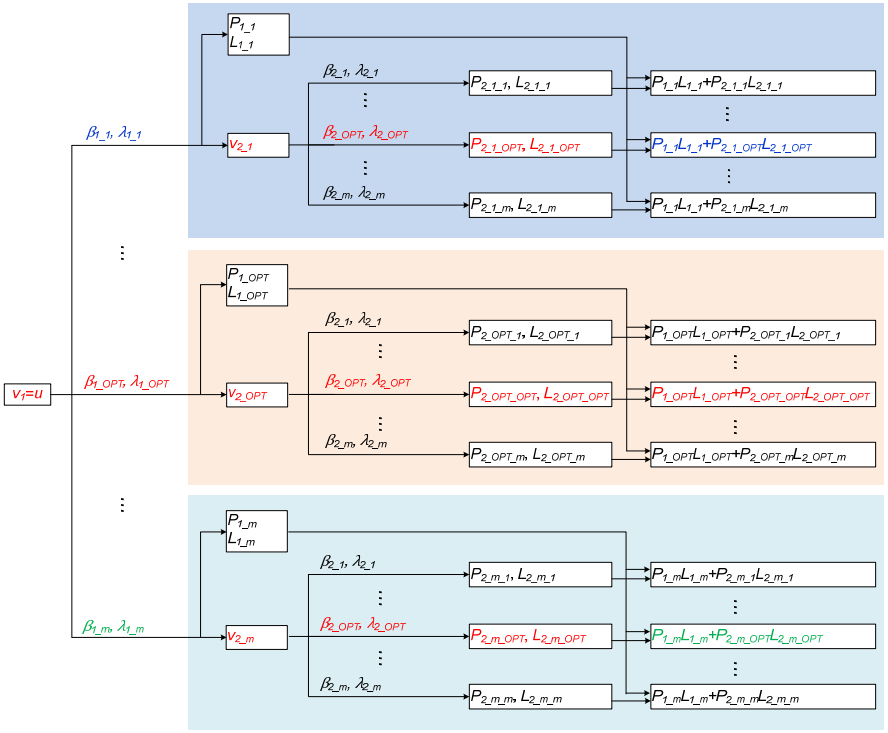

Fig. 5.4. Relationship of the variables in the 2-turbine wind farm, at the wind direction of 270° [11].

5.3.2. OPTIMAL CONTROL OF THE DOWNSTREAM WIND TURBINE IN A 2-TURBINE WIND FARM

As discussed in subsection 5.3.1, at the wind direction of 270°, to maximize the total energy production of the 2-turbine wind farm, the optimal pitch angle and tip

speed ratio of WT_2 can be selected separately from and prior to WT_1 [11]. The optimal pitch angle and tip speed ratio of WT_2 are corresponding to the maximum energy production of WT_2 at each wind speed of WT_2 [11]. In this section the optimal pitch angle and tip speed ratio of WT_2 are selected at the wind speeds from the cut-in wind speed to the cut-out wind speed, which can be used to generate the optimal control curves of WT_2 [11].

At the wind speeds of 7 m/s, 9 m/s and 11 m/s at the position of WT_2, the active power, the lifetime and the energy production of WT_2 in terms of the pitch angle and tip speed ratio of WT_2 are shown in Fig. 5.5 [11]. As shown in Fig. 5.5, at the ambient wind speed of 7 m/s, the lifetime, limited by factors other than the

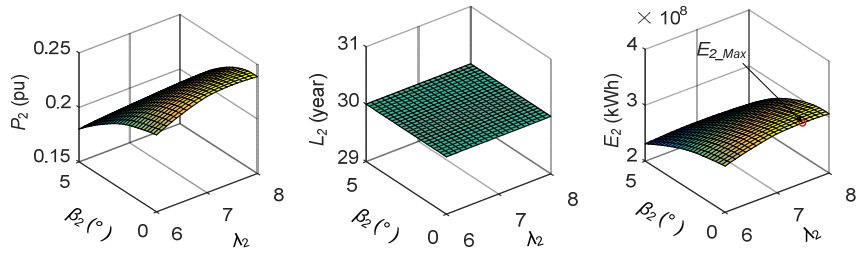

(a) 7 m/s wind speed at the position of WT2.

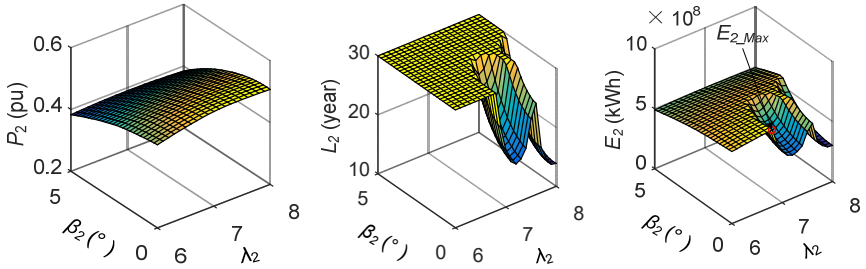

(b) 9 m/s wind speed at the position of WT2.

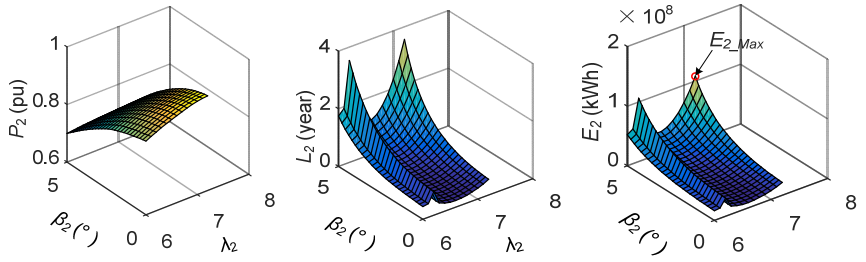

(c) 11 m/s wind speed at the position of WT2.

Fig. 5.5. The active power, lifetime and energy generation of WT_2 in terms of the pitch angle and tip speed ratio of WT_2 at the wind speed of: (a) 7 m/s; (b) 9 m/s; (c) 11 m/s [11].

converter lifetime, is 30 years [11]. In this case, the maximum energy production is obtained at the maximum active power, where the pitch angle and tip speed ratio of WT_2 are 0° and 7.5 [11]. At the ambient wind speed of 9 m/s, at parts of the pitch angle and tip speed ratio, the lifetime is smaller than 30 years because of the increased active power generation [11]. The maximum energy production is obtained at the pitch angle of 0° and the tip speed ratio of 6.8 [11]. At the ambient wind speed of 11 m/s, according to (2.2), the tip speed ratio should be limited by 7.2 because of the rotor speed limit of 12.1 rpm [11]. In consideration of the smoothness of the optimized pitch angle curve, the pitch angle is limited by 5°. Then, the maximum energy production is obtained at the pitch angle of 5° and tip speed ratio of 7.2 [11].

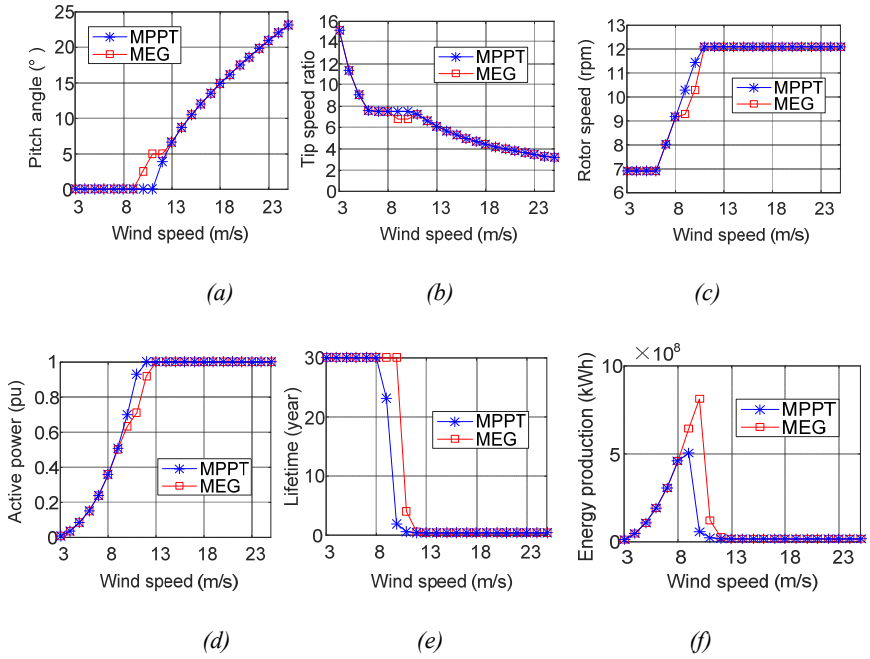

Fig. 5.6. At constant wind direction of 270° and constant wind speed in the whole year, comparison between the MPPT method and the MPG method of: (a) Pitch angle; (b) Tip speed ratio; (c) Rotor speed; (d) Active power; (e) Lifetime and (f) Energy production of WT_2 [11].

Compared with the MPPT method, the optimal pitch angle and tip speed ratio of WT_2 at the wind speeds from the cut-in wind speed of 3 m/s to the cut-out wind speed of 25 m/s are selected and shown in Figure 5.6(a) and (b) [11]. The corresponding rotor speed, active power, lifetime and energy production of WT_2 are

shown in Fig. 5.6(c), (d), (e) and (f) [11]. In Fig. 5.6, it can be observed, by increasing the pitch angle and reducing the tip speed ratio of WT_2, the active power of WT_2 is reduced, however the lifetime of WT_2 is increased, the energy production of WT_2 is respectively increased by 27.1%, 1274.8% and 409.1% at the wind speeds of 9 m/s, 10 m/s and 11 m/s [11].

The optimization of the pitch angle and tip speed ratio of WT_2 aims to maximize the total energy production of the wind farm at the ambient wind speed considering the wake effect and the wind turbine lifetime [11]. Due to the optimal pitch angle and tip speed ratio of WT_2 are also corresponding to the maximum energy production of WT_2 at the wind speed of WT_2, the optimization of the pitch angle and tip speed ratio of WT_2 just considers the wind turbine lifetime without the consideration of wake effect [11]. As shown in Fig. 5.6(f), compared with the MPPT method, the energy production of WT_2 can be increased by MEP method considering the wind turbine lifetime without the consideration of wake effect [11]. As a consequence, the energy production of the 2-turbine wind farm even can be increased by the MEP method at the wind directions where the wind farm has no power loss due to the wake effect [11].

5.3.3. OPTIMAL CONTROL OF THE UPSTREAM WIND TURBINE IN A 2-TURBINE WIND FARM

At the wind direction of 270°, the optimal control curves of WT_2 can be generated from the optimized pitch angle and tip speed ratio of WT_2 as shown in Fig. 5.6(a) and (b) [11]. The optimized control curves depend on which active power control scheme is implemented in the wind turbine control system [11]. In this section, at the wind direction of 270°, with the optimized control curves of WT_2 implemented, the optimal pitch angle and tip speed ratio of WT_1 are selected to maximize the total energy production of the wind farm [11].

At the ambient wind speed of 7 m/s, 9 m/s and 11 m/s, the wind speed of WT_2, the energy production of WT_2 and the total energy production of the wind farm in terms of the pitch angle and tip speed ratio of WT_1 are presented in Fig. 5.7 [11].

At the ambient wind speed of 7 m/s, the wind speed of WT_1 is 7 m/s. The wind speed of WT_2 is smaller than 7 m/s [11]. The lifetime of WT_1 and WT_2 are both 30 years, limited by factors other than the converter lifetime. In this case the maximum energy production of the wind farm is obtained at the maximum total active power of the wind farm [11]. As shown in Fig. 5.7(a), the maximum total energy production of the wind farm is 4.6×10^8 kWh. The corresponding optimal pitch angle and tip speed ratio of WT_1 are 1.8° and 6.9 [11].

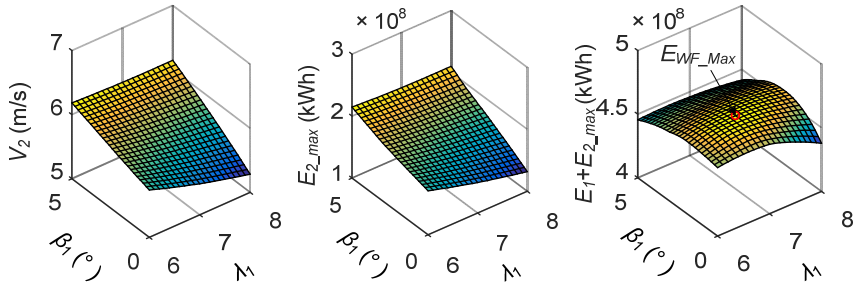

(a) At the ambient wind speed of 7 m/s.

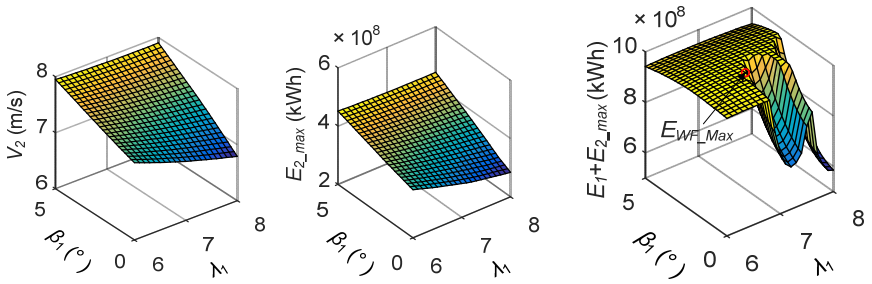

(b) At the ambient wind speed of 9 m/s.

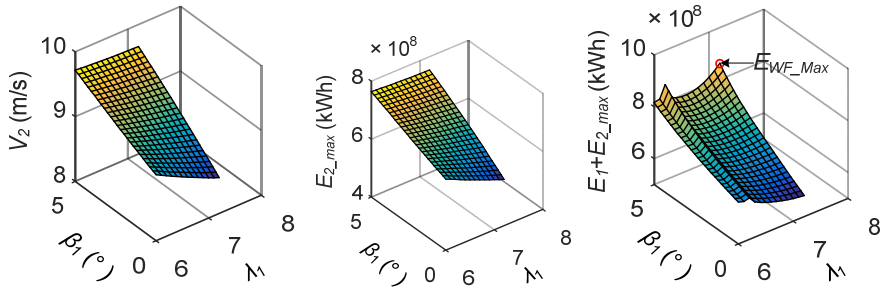

(c) At the ambient wind speed of 11 m/s.

Fig. 5.7. At wind direction of 270°, the wind speed of WT_2, the energy production of WT_2 and the total energy production of WT_1 and WT_2 in terms of the pitch angle and tip speed ratio of WT_1, at the ambient wind speed of: (a) 7 m/s; (b) 9 m/s; (c) 11 m/s [11].

At the ambient wind speed of 9 m/s, at parts of the pitch angle and tip speed ratio of WT_1 and WT_2, the lifetime of WT_1 and WT_2 are 30 years as shown in Fig 5.5(b) [11]. As shown in Fig. 5.7(b), the maximum total energy production of the wind farm is 9.8×10^8 kWh [11]. The corresponding optimal pitch angle and tip speed ratio of WT_1 are 1.8° and 7.0 [11]. At the ambient wind speed of 11 m/s, the

maximum total energy production of the wind farm is 8.7×10^8 kWh [11]. The corresponding optimal pitch angle and tip speed ratio of WT_1 are 5° and 7.2 [11].

Compared with the MPPT method, to maximize the total energy production of the wind farm, the optimized pitch angle and tip speed ratio of WT_1 and the corresponding rotor speed, active power and energy production of WT_1 are shown in Fig. 5.8 [11]. In Fig. 5.8, it can be observed, by increasing the pitch angle and reducing the tip speed ratio of WT_1, the active power of WT_1 is reduced, the lifetime of WT_1 is increased, the energy production of WT_1 is slightly reduced at lower wind speeds, the energy production of WT_1 is respectively increased by 27.1%, 1274.8% and 409.1% at the wind speeds of 9 m/s, 10 m/s and 11 m/s [11].

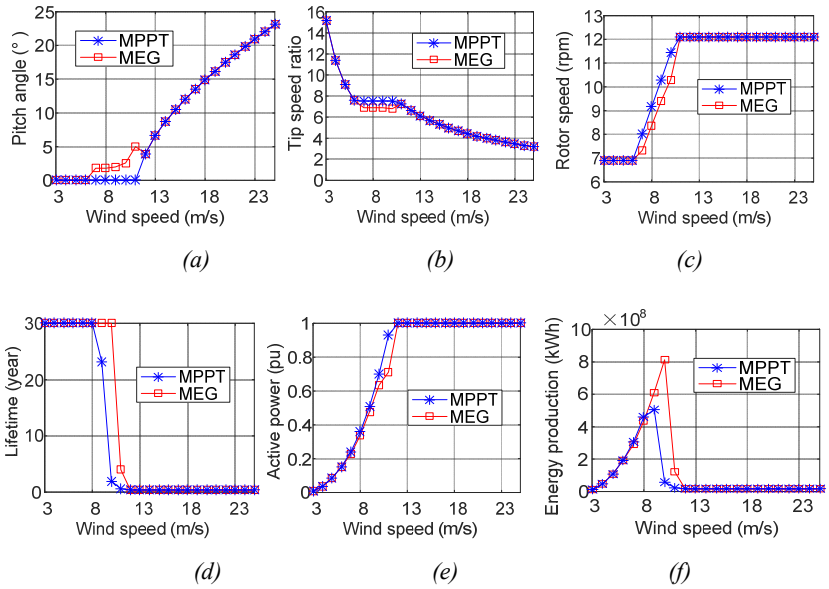

Fig. 5.8. At the wind direction of 270°, comparison between the MPPT method and the proposed MEG method of: (a) Pitch angle; (b) Tip speed ratio; (c) Rotor speed; (d) Active power; (e) Lifetime and (f) Energy production of WT_1 [11].

5.3.4. COMPARISON OF THE WIND FARM ENERGY PRODUCTION BETWEEN THE MPPT METHOD AND THE MEP METHOD

By assuming the constant wind direction of 270° and constant ambient wind speed in all the wind turbine lifespan, with the optimized control curves of WT_1 and WT_2 as shown in Fig. 5.8 and Fig. 5.6 implemented, the energy production of the wind farm is shown in Fig. 5.9(a) [11]. It can be observed, at the constant ambient wind speeds of 9 m/s, 10 m/s and 11 m/s, the wind farm energy production can be increased by 22.7%, 186.3% an 72.5% respectively [11].

Taking into account the wind direction distribution as shown in Fig. 5.3(b) and the wind speed distribution as shown in Fig 5.2(a), compared with the MPPT method, the total energy production of WT_1, WT_2 and the wind farm at all the wind direction and all the ambient wind speed are shown in Fig. 5.9(b) [11]. It can be observed, the total energy production of WT_1, WT_2 and the wind farm are increased by 43.6% 42.1% and 42.9% respectively [11]. This is because the energy production of the wind farm can be increased by the MEP method at all the wind directions including the wind directions that the wind farm has no power loss due to the wake effect [11].

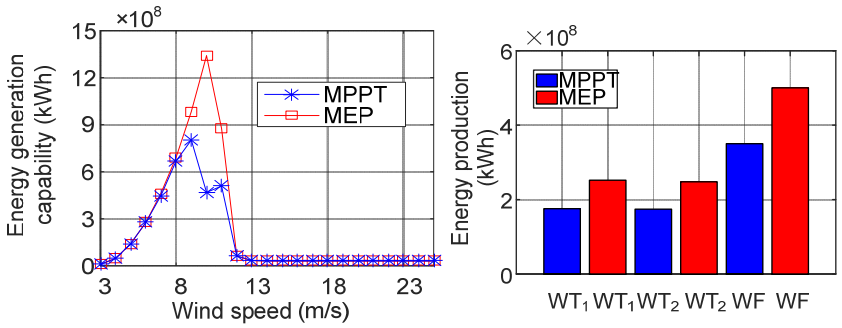

Fig. 5.9. Comparison between the MPPT method and the MEP method: (a) Energy generation of the wind farm at constant wind direction of 270° and constant ambient wind speeds in all the wind turbine lifespan; (b) Energy generation of WT_1, WT_2, and the wind farm with wind speed profile [11].

5.4. SUMMERY

The energy production of the wind farm depends on the active power and lifetime of all the wind turbines in the wind farm. In this chapter, taking into account the wake effect and the wind turbine lifetime, a Maximum Energy Production (MEP) active power control method is proposed to maximize the total energy production of the wind farm in all the wind turbine lifespan by optimizing the pitch angle and tip speed ratio of all the wind turbines. The optimal pitch angle and tip speed ratio of each wind turbine are selected by exhausted search method. By comparison of the total energy production of the wind farm, the maximum total energy production and the corresponding optimal pitch angle and tip speed ratio of each wind turbine can be obtained with a resolution. To implement the optimized pitch angle and tip speed ratio, optimal control curves for each wind turbine are generated.

In this chapter, firstly, the total energy production of the wind farm is compared between the MPPT method and the MPG method proposed in Chapter 4 which optimizes the pitch angle and tip speed ratio of each wind turbine to maximize the total active power of the wind farm considering the wake effect without the

consideration of the wind turbine lifetime. It is found that compared with the MPPT method the total energy production of the wind farm can be increased in some content by the MPG method. However, the maximum total energy production of the wind farm cannot be achieved. Moreover, as the MPG method is just carried out at the wind directions where the wind farm has power loss due to the wake effect, the total energy generation of the wind farm cannot be increased by the MPG method at the wind directions where the wind farm has no power loss due to the wake effect.

In the 2-turbine wind farm, to maximize the total energy production of the wind farm, the optimal pitch angle and tip speed ratio of the downstream wind turbine can be selected separately from the upstream wind turbine. The optimal pitch angle and tip speed ratio of the downstream wind turbine are corresponding to the maximum energy production of the downstream wind turbine at a specific wind speed at the position of the downstream wind turbine. Then, the optimized control curves of the downstream wind turbine can be generated with the optimized pitch angle and tip speed ratio at each wind speed at the position of the downstream wind turbine. With the optimized control curves of the downstream wind turbine implemented, the optimal pitch angle and tip speed ratio of the upstream wind turbine are corresponding to the maximum total energy production of the wind farm.

It is found that, compared with the MPPT method, the energy production of a single wind turbine can be increased by the MEP method proposed in this chapter, which indicates that the energy production of the wind turbine can be increased by the proposed MEP method at all the wind directions including the wind directions where the wind farm has no power loss due to the wake effect. Studied in the 2-turbine wind farm, taking into account a real wind profile, the total energy production of the wind farm can be increased by 42.9% by the proposed MEP method compared with the MPPT method.

CHAPTER 6. OPTIMAL REACTIVE POWER DISPATCH METHOD IN DFIG WIND TURBINE BASED WIND FARM CONSIDERING WAKE EFFECT AND WIND TURBINE LIFETIME

6.1. INTRODUCTION

As presented in Section 2.3, the DFIG wind turbine has some amount of reactive power capability [19] and [20]. The reactive power can be used to support the gird voltage control [18]. Required by the modern grid codes [15] and [16], the wind farm must be equipped with reactive power control function to control the reactive power supply by the wind farm in the point of connection. The reactive power control function can be implemented in individual wind turbine controller or in the wind farm controller. As shown in Fig. 6.1, a typical wind farm controller is provided by [21]. Receiving the reactive power set point from the Transmission System Operator (TSO), the wind farm controller dispatches the reactive power reference of the wind farm to each wind turbine [2], [18] and [21].

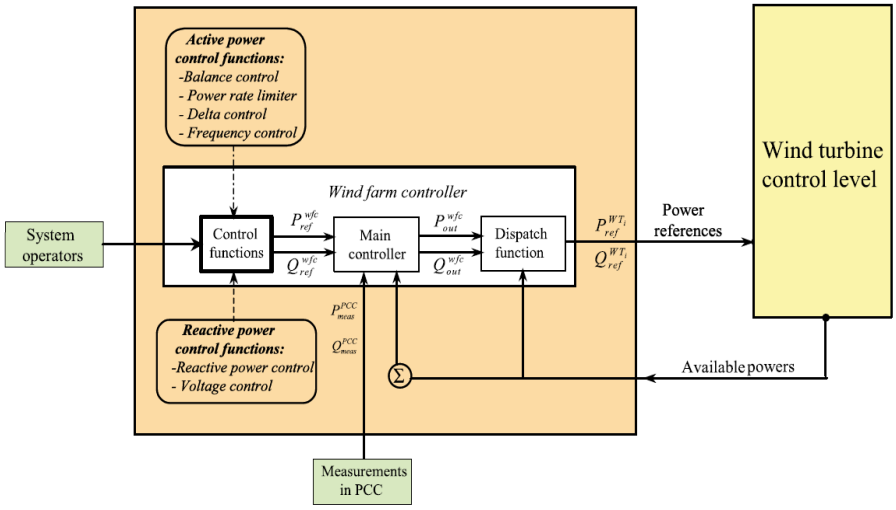

Fig. 6.1. Control functions of the wind farm central controller [21].

As presented in Section 2.3, the wind turbine reactive power capability depends on the wind turbine active power. Due to the wake effect, the wind turbines in a wind farm have different active power, which results in the different reactive power capabilities among the wind turbines [2]. The conventional reactive power dispatch method is to dispatch the reactive power required for the wind farm to each wind turbine in proportion to each wind turbine's reactive power capability [21]. By this method, the stress can be balanced among the wind turbines in some extent [2]. As presented in Chapter 3.4, the wind turbine lifetime is determined by the active power and reactive power of the wind turbine [2]. By the conventional reactive power dispatch method, the lifetime of the upstream wind turbine may be overly short [2]. In this chapter, with the MPPT method implemented for active power control, based on the wind turbine lifetime estimation, an optimal reactive power dispatch method is proposed to improve the lifetime of the wind turbines in the wind farm [2].

As presented in Section 2.3, the reactive power capability of the DFIG wind turbine depends on its stator voltage. The stator voltage is determined by the voltage at the Point of Common Coupling (PCC) and the active and reactive power generation of the wind turbines in the wind farm [2]. In return, the active and reactive power generation of the wind turbines determines the stator voltage of each wind turbine, due to the voltage drop on the wind farm connection cable [2]. The proposed method calculates the stator voltage of each wind turbine by the power flow calculation in the wind farm with the possible active and reactive power generation of the wind turbines [2]. Moreover, the reactive power consumption on the connection cable is taken into account. The proposed method is verified in the 80-turbine wind farm as shown in Fig.3.10 [2].

6.2. PROPOSED REACTVIE POWR DISPATCH METHOD

The proposed reactive power dispatch method maximizes the total lifetime of all the wind turbines in a wind farm. The objective function can be formulated by [2],

$$Max(\sum_{i=1}^{n} \omega_i(L_i) L_i(P_i, Q_i)) \tag{6.1}$$

where n is the number of wind turbines, L_i P_i and Q_i donate the B10 lifetime, active power and reactive power of WT_i.

The wind turbine lifetime is very sensitive to the wind turbine active power and reactive power [2]. With a small change of the reactive power, there will be an extremely large difference of the wind turbine lifetime [2]. Aims to maximize the total lifetime of all the wind turbines may result in the overly short lifetime of the upstream wind turbine and extremely large lifetime of the downstream wind turbine

[2]. As it is important to increase the wind turbine lifetime which is overly short and it is meaningless to increase the wind turbine lifetime which is larger enough, in the objective function (6.1), a weight coefficient ω_i as a function of the wind turbine lifetime is added for each wind turbine to improve the wind turbine lifetime which is overly short by sacrificing the wind turbine lifetime which is long enough [2].

The main principle to design the weight coefficient is to set a large value when the wind turbine lifetime is short and set a small value when the wind turbine lifetime is long [2]. As shown in Fig. 2.12, the B10 lifetime of the NREL 5 MW wind turbine is 11.4 years in case that the wind turbine is operating at the rated active power and 0 reactive power [2]. In the case study in Section 6.3, $\omega_i=(11.4/L_{WTi})^3$ is implemented [2]. In this case, the wind turbine lifetime which is less than 11.4 years will be improved by sacrificing the wind turbine lifetime which is larger than 11.4 years [2].

In (6.1), the wind turbine lifetime is a function of the wind turbine active power and the reactive power [2]. The wind turbine active power is determined by the wind speed and the active power control method [2], [3], [8] and [11]. The wind turbine reactive power is the control variable of the optimization and limited by the wind turbine reactive power capability [2]. The reactive power capability of the DFIG wind turbine depends on the wind turbine active power and stator voltage [19] and [2]. The stator voltage is determined by the voltage at PCC and the active power and reactive power of all the wind turbines due to the voltage drop on the connection cable [2]. Moreover, total reactive power of all the wind turbines should be equal to the reactive power required for the wind farm [2]. The reactive power consumption on the connection cable should be taken into account [2].

The following constraints exist [2]:

$$Q_{i\_drc} \le Q_i \le Q_{i\_urc} \tag{6.2}$$

$$\sum_{i=1}^{n} Q_i - Q_{cons} = Q_{WF} \tag{6.3}$$

$$V_{WT\_\min} \le V_{WTi} \le V_{WT\_\max} \tag{6.4}$$

where Q_{i_urc} and Q_{i_drc} denote the up and down reactive power limit of WT_i, the Q_{cons} denotes the reactive power consumption on the wind farm connection cable, Q_{WF} denotes the required reactive power for the wind farm, and the V_{WT_min} and V_{WT_max} donate the minimum and maximum limit of the wind turbine stator voltage.

In (6.1), the reactive powers of the wind turbines are the control variables of the

optimization [2]. Changing the reactive powers of the wind turbines leads to the changing of the lifetimes of the wind turbines, the reactive power consumption on the wind farm connection cable, the stator voltages of the wind turbines and the reactive power capabilities of the wind turbines [2]. In this chapter, the optimal reactive powers of the wind turbines are selected by the PSO based optimization algorithm [2].

The flow chart of the PSO based optimization algorithm to select the optimal reactive powers of the wind turbines is shown in Fig. 6.2 [2]. In Fig. 6.2, the active

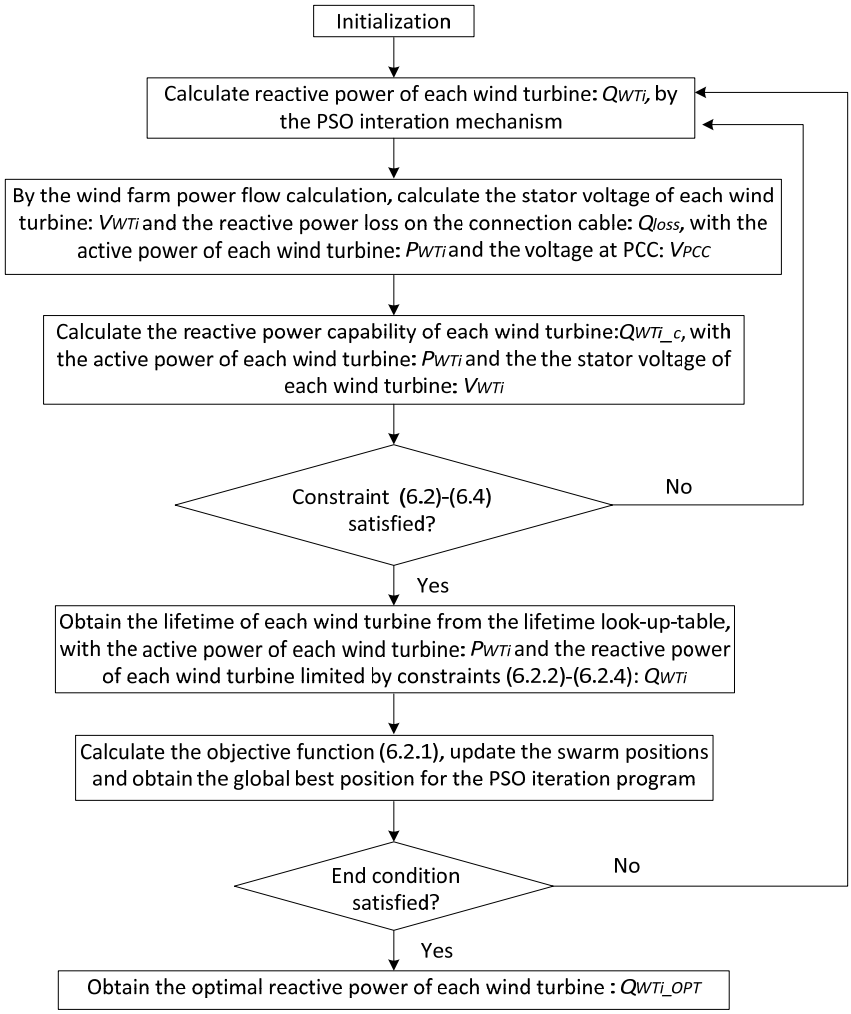

Fig. 6.2. Flow chart of the PSO based optimization algorithm to select the optimal reactive power for each wind turbine [2].

power of each wind turbine is calculated considering the wake effect in initialization. In the iterations, firstly, the reactive powers of the wind turbines are calculated by the PSO iteration mechanism. By the wind farm power flow calculation, the stator voltages of the wind turbines and the reactive power consumption on the connection cable can be calculated [2]. Then, the reactive power capabilities of the wind turbines can be obtained by the method as presented in Section 2.3 [2]. The lifetime of each wind turbine can be obtained by the method as presented in Section 2.4 with the active powers of the wind turbines and the reactive powers of the wind turbines limited by the constraints (6.2)-(6.4) [2]. By the comparison of the objective function (6.1), the optimal reactive powers of the wind turbines in the wind farm can be selected [2].

6.3. STUDY CASE IN AN 80-TURBINE WIND FARM

The proposed reactive power dispatch method to improve the lifetime of the wind turbines in the wind farm is based on the active power difference among the wind turbines due to the wake effect [2]. In the 80-turbien wind farm as shown in Fig. 3.10, with the MPPT method implemented for active power control, the active power difference among the wind turbines appears at the wind directions of around 41°, 90°, 131°, 172°, 221°, 270°, 311° and 352° [2]. Considering the wake effect, the active power generation of each wind turbine in the 80-turbine wind farm is presented in Section 3.3.2 and Section 3.2.3 [2].

In this section, over-excited reactive power of the DFIG wind turbine from the stator side of the generator is assumed, which means the wind turbine just produces the positive reactive power to the wind farm connection cable from its stator side of the generator. The under-excited reactive power from the stator side of the generator, the over-excited and under-excited reactive power from the GSC, and the PMSG wind turbine based wind farm will be studied in the future work. By the method as presented in Section 2.3.2, with the MPPT method implemented for active power control, at the stator voltages of 0.9 pu, 1.0 pu and 1.1 pu, the over-excited reactive power capabilities of the NREL 5 MW DFIG wind turbine from the stator side of the generator in terms of the wind turbine active power are shown in Fig. 6.3 [2], The Fig. 6.3 can be made as the reactive power capability look-up-table of the NREL 5 MW DFIG wind turbine in terms of the active power and stator voltage [2].

At the wind direction of 270°, with the MPPT method implemented for active power control, assuming 1.0 pu voltage at the PCC, the reactive power capabilities of the wind turbines are shown in Fig. 6.4 [2], where the ambient wind speeds of from 3 m/s to 15 m/s with the resolution of 1 m/s are taken into account. It can be observed there is a big difference of reactive power capabilities among the wind turbines at the lower wind speeds [2].

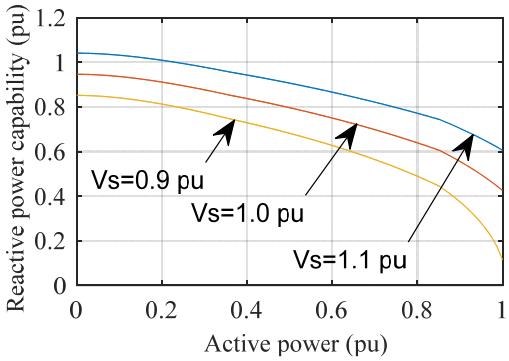

Fig. 6.3. Over-excited reactive power capabilities of the NREL 5 MW DFIG wind turbine from the stator side of the generator in terms of active power, at stator voltages of 0.9 pu, 1.0 pu and 1.1 pu [2].

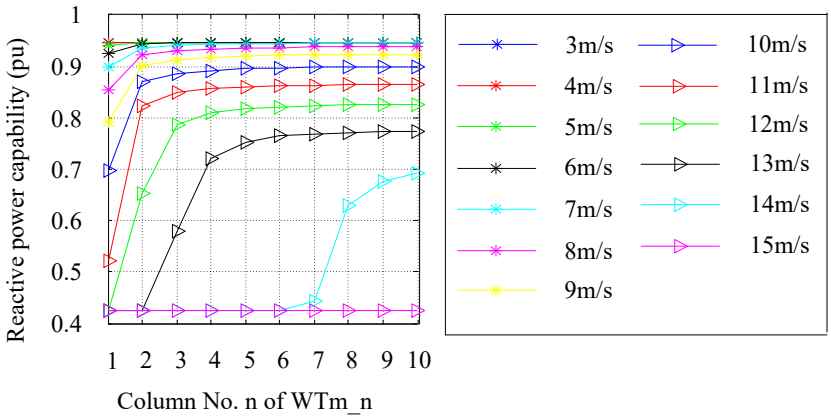

Fig. 6.4. Over-excited reactive power capability of the wind turbine in each column from the stator side of the generator, at 270° wind direction and at the wind speeds from 3 m/s to 15 m/s with the resolution of 1 m/s [2].

The lifetimes of the NREL 5 MW DFIG wind turbine in terms of the active power and reactive power from the stator side of the generator are shown in Fig. 2.12 [11] and [2]. The stator voltages of the wind turbines and the reactive power consumption on the connection cable can be calculated by the power flow calculation in the wind farm with the voltage at the PCC and the active and reactive power generation of the wind turbines known [2]. Assuming the constant voltage at PCC of 1.0 pu, with the weight coefficient $\omega_i=(11.4/L_{WTi})^3$ implemented in the objective function, at the wind direction of 270° and ambient wind speed of 12 m/s, by the PSO based optimization algorithm, the optimized reactive power and lifetime of each wind turbine are shown in Fig. 6.5 [2].

In the 80-turbine wind farm, at the wind direction of 270°, the wind turbine in one row will not cause the power loss to the wind turbines in other rows [2] and [3]. Thus, the wind turbines in the same column have the same active power generation [2] and [3]. As a consequence, as shown in Fig. 6.5, the wind turbines in the same column have the same optimized reactive power and lifetime [2].

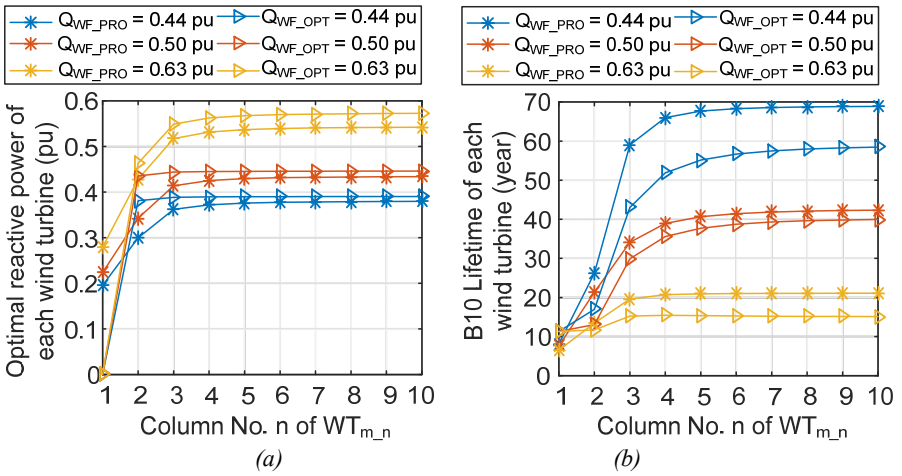

Fig. 6.5. Comparison between the proposed reactive power dispatch method and the conventional reactive power dispatch method: (a) Reactive power of the wind turbine in each column; (b) B10 lifetime of the wind turbine in each column [2].

In Fig. 6.5, compared with the conventional reactive power dispatch method, which dispatches the required reactive power for the wind farm to each wind turbine in proportion to the wind turbine's reactive power capability, the total lifetime of all the power converters are decreased, at the 0.44 pu, 0.50 pu and 0.63 pu reactive powers required for the wind farm [2]. This is because the upstream wind turbines WT_{m_1} which have overly short lifetime has been improved by the weight coefficient in the optimization objective function [2]. In this section, the weight coefficient is set to be $(11.4/L_{WTi})^3$ to improve the B10 lifetime of the wind turbine which is overly short, where 11.4 is the lifetime of the NREL 5 MW DFIG wind turbine operating at the rated active power and with no reactive power generation [2]. As shown in Fig. 6.5(a), the reactive power of the wind turbine in the first column is reduced to 0 compared with the conventional reactive power dispatch method [2]. In consequence, the B10 lifetime of the wind turbine in the first column is increased to 11.4 years, at the 0.44 pu, 0.50 pu and 0.63 pu reactive powers required for the wind farm [2].

The optimization result as shown in Fig. 6.5 is obtained at a specific wind direction and a specific wind speed. It is assumed that the wind direction and the wind speed

are constant in all the lifespan of the wind turbines [2]. By the same method, the optimized reactive power and B10 lifetimes of the wind turbines at other constant wind directions and ambient wind speeds can be obtained [2].

By the proposed reactive power dispatch method and with the annual wind direction and ambient wind speed distribution as shown in Fig. 3.16, the annual lifetime consumptions of the wind turbines are calculated and shown in Fig. 6.6 [2]. In Fig. 6.6, the $WT_{(m-1)*10-n}$ represents the WT_{m_n} in Fig. 3.10. Compared between the proposed reactive power dispatch method and the conventional reactive power dispatch method, the annual total lifetime consumptions of all the wind turbines are separately reduced by 5.01% and 7.15% at the reactive powers required for all the wind turbines of 0.5 and 0.8 times the total reactive power capabilities of all the wind turbines [2]. However the annual lifetime consumption of the wind turbine in the first column which is overly large is reduced [2].

In the optimization, to improve the lifetime of the wind turbine which is overly short has the priority than to maximize the total lifetime of all the wind turbines [2]. This is because it is more meaningful to improve the lifetime of the wind turbine which is overly short than to improve the lifetime of the wind turbines which are long enough [2]. In the case study, the MPPT method is implemented for active power control [2]. The proposed reactive power dispatch method can be implemented in the wind farm with any active power control method implemented [2]. Moreover, the proposed reactive power can be implemented in any wind farm layout and wind profile at the location of the wind farm [2].

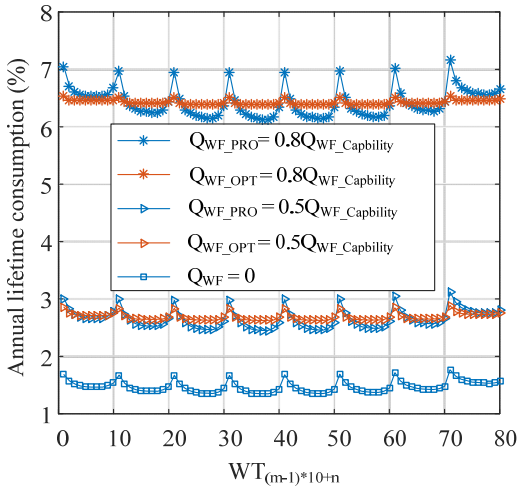

Fig. 6.6. Comparison of the annual lifetime consumption of each wind turbine between the proposed reactive power dispatch method and the conventional reactive power dispatch method [2].

6.4. SUMMARY

The DFIG wind turbine has amount of reactive power capability, which can be used to support grid voltage control. The conventional reactive power dispatch method dispatches the reactive power of the wind farm to each wind turbine in positive proportion to the wind turbine's reactive power capability. By this method, the power loss and stress can be balanced among the wind turbines to some content.

Due to the wake effect, there is a difference of active power generation among the wind turbines in a wind farm. As the wind turbine lifetime is determined by the wind turbine active power and reactive power, optimal dispatch the reactive power of the wind farm to each individual wind turbines, the wind turbine lifetime can be improved. By the conventional reactive power dispatch method, the wind turbine lifetime may be overly short. In this chapter, an optimal reactive power dispatch method is proposed to maximize the total lifetime of all the wind turbines in a wind farm, where the lifetime of the wind turbine which is overly short is improved.

The dispatched reactive power for each individual wind turbine is limited by the wind turbine' reactive power capability. The wind turbine's reactive power capability is determined by the stator voltage and the active power generation, which is controlled with MPPT method. The active power generation of each wind turbine can be estimated considering the wake effect. The wind turbine stator voltage and the reactive power consumption on the connection cable can be calculated by the power flow calculation in the wind farm with the voltage at PCC and the power generations of all the wind turbines known.

Case study in an 80-turbine wind farm is carried out to verify the proposed reactive power dispatch method. Compared with the conventional reactive power dispatch method, the total lifetime of all the wind turbines is reduced by the proposed optimal reactive power dispatch method at the reactive power required for the wind farm of 0.5 and 0.8 times the total reactive power capability of all the wind turbines with a wind profile. This is because the lifetime of the wind turbine which is overly large is increased by the weight coefficient in the optimization objective function. It is more meaningful to improve the lifetime of the wind turbine which is overly short than to improve the lifetime of the wind turbines which are long enough. The proposed reactive power dispatch method can be implemented in the wind farm with any active power control method implemented. Moreover, the proposed reactive power can be implemented in any wind farm layout and wind profile at the location of the wind farm.

In this chapter, the consideration is limited for the DFIG wind turbine based wind farm and over-excited reactive power from the stator side of the wind turbine generator. In the future work, under-excited reactive power from the stator side of

the generator, the reactive power from the GSC, and the PMSG wind turbine based wind farm will be taken into account.

CHAPTER 7. SUMMARY AND OUTLOOK

7.1. SUMMARY

In a wind farm, due to the wake effect, the upstream wind turbine causes wind speed deficit and the power loss to the downstream wind turbine. According to a field investigation from onshore wind farms, the power loss in a wind farm can reach up to approximately 15% of the wind farm power generation. In modern wind farms, the popular and widely installed wind turbines are the variable speed wind turbine, including the DFIG based wind turbine and the PMSG based wind turbine. The DFIG wind turbine has two degrees of freedom for active power control, which are the pitch angle and tip speed ratio. The commonly implemented active power control method in the DFIG wind turbine based wind farm is the MPPT method. Compared with the MPPT method, by changing the pitch angle and tip speed ratio of the upstream wind turbine, the active power of the upstream wind turbine will be reduced, and the wind speed at the position of the downstream wind turbine can be increased, which results in the active power increase of the downstream wind turbine. Overall, the total active power of the wind farm can be increased.

The wind speed at the position of each wind turbine in the wind farm can be estimated by the wake model with the ambient wind speed. In the last few decades, wake models have been developed with different complexity. Generally speaking, the wind speed at the position of each wind turbine can be accurately calculated by the CFD wake model, which calculates the wind velocity throughout the whole wind field by solving the complete N-S equation. Due to the large amount of calculation complexity of the N-S equation, the state-of–the-art engineering solutions all have simplified the N-S equation and its parameters with the boundary layer theory and the momentum conservation theory implemented. In consequence, there is a gap between the engineering solutions and the complete CFD models.

The Katic wake model, which is embedded in the industrial software WAsP, estimates the power loss at the positon of the downstream wind turbine based on the momentum conservation theory. In the Katic wake model, the power loss is represented by the wind speed deficit. Compared with the CFD model, the calculation complexity is reduced significantly. According to a research work, where the accuracy of the state-of-the-art wake models has been compared, it is hard to say which wake model is more accurate than the others. In this PhD thesis, to optimal control each wind turbine just the wind speed at the position of each downstream wind turbine need to be estimated. The wind speed at the position of each downstream wind turbine is estimated by the Katic wake model.

As the first main contribution of this PhD thesis, a Maximum Power Generation (MPG) active power control method is proposed to maximize the total active power of the wind farm considering the wake effect. Firstly, the feasibility to maximize the total active power of the wind farm by optimizing the pitch angle and tip speed ratio of each wind turbine is presented. Then, the optimal pitch angle and tip speed ratio of each wind turbine are selected by the PSO based optimization program. To implement the optimized pitch angle and tip speed ratio, optimized active power, pitch angle and rotor speed curves in terms of the wind speed are generated for each wind turbine. In case of the wind turbine is controlled by the torque control scheme, the optimal torque and pitch angle curves in terms of the rotor speed can be generated from the optimized active power, pitch angle and rotor speed curves in terms of the wind speed.

The computation complexity of the optimization depends on the optimization parameter number, which are two times of the wind turbine number. In a large scale wind farm the optimization computation complexity is large. By the exhausted search method, the total active power generation of the wind farm is compared among all sets of pitch angle and tip speed ratio of all the wind turbines. it is found that, in the wind farm with wind turbines in a line, there is a small difference of the optimized pitch angle and tip speed ratio between the upstream wind turbine and the downstream wind turbine at the same wind speed at the position of the upstream wind turbine and the downstream wind turbine. Moreover, there is a small difference of the total active power of the wind farm in a large range of the pitch angle and tip speed ratio of each wind turbine. Thus, the optimized control curves of the upstream wind turbine in the 2-turbien wind farm can simply be implemented in the wind farm with more wind turbines in a line. As a consequence, in the regular rectangular layout wind farms, the computation complexity can be reduced significantly.

Considering the estimation error of the wake model and the simplification to implement the optimized control curves in the wind farm, the proposed MPG method may not be able to increase the total active power of the wind farm compared with the MPPT method at the wind directions where the wind farm has small power loss. However, the total active power of the wind farm can be increased in a large proportion at the wind directions where the wind farm has large power loss due to the wake effect. The wind farm operator can make a decision at which wind direction to implement the MPG method by trading off between the estimation error and the increased total active power of the wind farm theoretically. In the typical 80-turbine wind farm with rectangular layout, with the MPG method implemented in the wind rose sections of 265°-275°, 85°-95°, 345°-355° and 165°-175°, and with an annual wind profile, the Annual Energy Production (AEP) of the wind farm can be increased by 1.1%.

With the wind farm moving from the onshore to the offshore, the reliability issue became more and more important due to its expensive installation and maintenance. With a filed survey, it is found that the wind turbine electrical system has the largest failure rate compared with the other components, which means the lifetime of the turbine can be represented by the lifetime of the converter. Many research works have been contributed to the B10 lifetime estimation of the power converter modules, which is closely related to the wind turbine operation condition. The B10 lifetime estimation of the power converter is subjected to the operation condition calculation of the wind turbine, the power losses calculation in the wind turbine electricity system, the thermal stress calculation and damage consumption. It can be concluded, at a specific wind speed, the B10 lifetime of the power converter is determined by the wind turbine pitch angle, tip speed ratio and the reactive power generation.

The energy production of the wind farm relates to its active power and operation time. Considering the wake effect, at a specific wind direction and a specific ambient wind speed, the active power of the wind farm is determined by the pitch angle and tip speed ratio of all the wind turbines in the wind farm. In case of the wind turbine doesn't generate the reactive power, the B10 lifetime of the power converter is also determined by the pitch angle and tip speed ratio of the wind turbine.

As the secondary main contribution of this PhD thesis, by assuming the lifetime of wind turbine is represented by the B10 lifetime of the power converter and no reactive power generation of the wind turbines in the wind farm, a Maximum Energy Production (MEP) active power control method is proposed to maximize the total energy production of the wind farm by optimizing the pitch angle and tip speed ratio of all the wind turbines in the wind farm. Compared with the MPPT method, by the MEP method which objects to maximize the total active power of the wind farm, the energy production of the wind farm can be increased in a large proportion both at the wind directions that the wind farm has power loss due to the wake effect and at the wind directions that the wind farm has no power loss due to the wake effect. In the 2-turbine wind farm, with the MEP method implemented, and with an annual wind profile, the total energy production of the wind farm in the whole lifespan of each wind turbine can be increased by 42.9%.

The DFIG wind turbine has some amount of reactive power capability, which can be used to support the grid voltage control. Required by the modern grid codes, the wind farm must be equipped with the reactive power control function, which can be implemented either in wind turbine controller or in wind farm central controller. After receiving the reactive power reference of the wind farm from the Transmission System Operator (TSO), the conventional reactive power dispatch method dispatches reactive power of the wind farm to each wind turbine in proportion to the reactive power capability of each wind turbine. By this method,

the power load and the stress can be balanced among the wind turbines in some extent. As the lifetime of the wind turbine is also determined by the reactive power of the wind turbine, the upstream wind turbine may have overly short lifetime due to its large active power generation in case of the MPPT method is implemented for the active power control.

As the third main contribution of this PhD thesis, considering the wake effect and the lifetime of the wind turbine, an optimal reactive power dispatch method in DFIG wind turbine based wind farm is proposed to maximize the total lifetime of all the wind turbines. The lifetime of the wind turbine which is overly short and the optimized reactive power of each wind turbine are respectively limited by a weight coefficient and the reactive power capability of the wind turbine.

At a specific wind speed, the reactive power capability of the wind turbine is determined by the active power control method and the stator voltage of the wind turbine. The active power of each wind turbine is estimated by the wake model. The reactive power consumption on the connection cable is taken into account. The stator voltage of each wind turbine and the reactive power consumption on the connection cable are calculated by the power flow calculation in the wind farm with the voltage at PCC and the power generations of all the wind turbines.

In the typical rectangular layout wind farm equipped with 80 NREL 5 MW DFIG wind turbines, by assuming the MPPT method is implemented for active power control and the over-excited reactive power from the stator side of the generator, compared with the conventional reactive power dispatch method, the lifetime of the wind turbine which is overly short is increased. The total lifetime of the wind farm is reduced, as it is more meaningful to improve the lifetime of the wind turbine which is overly short than to improve the lifetime of the wind turbines which are long enough. The proposed reactive power dispatch method can be implemented in the wind farm with any layout and with any active power control method implemented.

7.2. MAIN CONTRIBUTIONS

Considering the wake effect and the wind turbine lifetime, in this PhD thesis, optimal active power control methods are proposed in the DFIG wind turbine based wind farm to maximize the total active power of the wind farm and to maximize the total energy production of the wind farm. Moreover, an optimal reactive power dispatch method is proposed in the DFIG wind turbine based wind farm to maximize the total lifetime of all the wind turbines in the wind farm. The main contributions in this PhD thesis are listed as follows:

- Based on the Katic wake model, the wind speed deficit and power losses due to wake effects in typical wind farms are analyzed in detail. The

influence of the wind direction, ambient wind speed, wind farm layout and active power control method are taken into account.

- Considering the wake effect, an MPG active power control method is proposed in the DFIG wind turbine based wind farm to maximize the total active power of the wind farm.
- The B10 lifetime of a single DFIG wind turbine in terms of the active power and reactive power are estimated. Considering the wake effect, the B10 lifetime of all the wind turbines in typical wind farms equipped with DFIG wind turbines are presented.
- Considering the wake effect and the wind turbine lifetime, a MEG active power control method in the DFIG wind turbine based wind farm is proposed to maximize the total energy production of the wind farm.
- Reactive power capability of the DFIG turbine both from the stator side of the generator and the GSC is calculated.
- Considering the wake effect and the wind turbine lifetime, an optimal reactive power dispatch method in the DFIG wind turbine based wind farm is proposed to maximize the total lifetime of all the wind turbines. Compared with the conventional reactive power dispatch method, the lifetime of the wind turbine which is overly short is improved.

7.3. RESEARCH PERSPECTIVES

Based on the wake effect analysis, the wind turbine lifetime estimation and the proposed optimal control methods in this PhD thesis, the following perspectives are listed for further investigation:

- In this PhD thesis, the wind speed deficit in the wind farm is estimated by the Katic wake model. Many institutes and projects are underway of modify and develop CFD wake models to improve the calculation accuracy and to reduce the computation complexity. In case that more accurate and simplified CFD wake model is developed, the optimal control methods proposed in this PhD thesis will be improved.
- In this PhD thesis, the lifetime of the DFIG wind turbine is represented by the B10 lifetime of the RSC. In the future work, the lifetime of the GSC and the other wind turbine components including the mechanical parts will be taken into account.
- In the future work, the lifetime estimation of the PMSG wind turbine will be taken into account, and the proposed optimal active power control method to maximize the total energy production of the wind farm will be extended into the PMSG wind turbine based wind farm.
- The proposed optimal reactive power dispatch method in DFIG wind turbine based wind farm assumes the over-excited reactive power from the stator side of the generator. In the future work, over-excited reactive power

from the GSC, under-excited reactive power both from the stator side of the generator and the GSC will be taken into account.

- The PMSG wind turbine also can provide reactive power from its GSC. Based on the lifetime estimation of the PMSG wind turbine, optimal reactive power dispatch method in the PMSG wind turbine based wind farm will be evaluated in the future work.
- As the wind turbine lifetime is determined by both the active power control method and the reactive power generation, optimal coordinative active power and reactive power control method will be evaluated in the future work.

LITERATURE LIST

[1] 2015 IEA wind annual report. Available online: http://www.ieawind.org (Aug. 2016)

[2] J. Tian, D. Zhou, C. Su, Z. Chen and F. Blaabjerg. "Reactive power dispatch method in wind farms to improve the lifetime of power converter considering wake effect," *IEEE Trans. Sustainable Energy,* Sep. 2016. (E-Pub Ahead of Print)

[3] J. Tian, D. Zhou, C. Su, M. Soltani, Z. Chen and F. Blaabjerg. "Wind turbine power curve design for optimal power generation in wind farms considering wake effect" *Energies*, vol. 10, no. 3, Feb. 2017.

[4] J. R. Kristoffersen and P. Christiansen, "Horns rev off shore windfarm: its main controller and remote control system," *Wind Eng*. 2003, vol. 27, no. 5, pp.351-366.

[5] R. J. Barthelmie, K. Hansen, S. T. Frandsen, O. Rathmann, J. G. Schepers, W. Schlez, J. Phillips, K. Rados, A. Zervos, E. S. Politis, and P. K. Chaviaropoulos, "Modelling and measuring flow and wind turbine wakes in large wind farms offshore," *Wind Energy*, vol. 12, no. 5, pp. 431–444, 2009.

[6] Photo by Christian Steiness / Vattenfall (Horns Rev Offshore Wind Farm, Denmark) Original Image Link: http://i.imgur.com/qruVcnu.jpg.

[7] R. J. Barthelmie, G. C. Larsen, S. T. Frandsen, L. Folkerts, K. Rados, S.C. Pryor, B. Lang and G. Schepers, "Comparison of wake model simulations with offshore wind turbine wake profiles measured by sodar," *J. Atmos Ocean Technol*, vol. 23, no. 7, 888–901, 2006.

[8] B. Wu; Y. Lang; N. Zargari; S. Kouro, Power Conversion and Control of Wind Energy Systems, NJ: Wiley, 2011.

[9] A. Duckworth, and R. J. Barthelmie, "Investigation and validation of wind turbine wake models," *Wind Engineering*, vol. 32, no. 5, pp. 459–475, 2008.

[10] J. Tian, C. Su, M. Soltani, and Z. Chen, "Active power dispatch method for a wind farm central controller considering wake effect, " *in Proc. 2014 40th IEEE Industrial Electronics Society Conf.,* pp. 5450-5456.

[11] J. Tian, D. Zhou, C. Su, F. Blaabjerg and Z. Chen. "Optimal control to increase energy production of wind farm considering wake effect and lifetime estimation," *Applied Sciences*, vol. 7, no. 1, Jan. 2017.

[12] B. Hahn, M. Durstewitz and K.Rohrig, Reliability of Wind Turbines, Experiences of 15 Years with 1,500 WTs. ISET. 2007. Available online: http://renknownet2.iwes.fraunhofer.de/pages/wind_energy/data/2006-02-09Reliability.pdf, 09 Feb, 2006.

[13] Load-Cycling Capability of HiPaks. ABB Application Note. 2004.

[14] D. Zhou, F. Blaabjerg, M. Lau and M. Tonnes, "Optimized reactive power flow of DFIG power converters for better reliability performance considering grid codes," *IEEE Trans. Ind. Electron.*, vol. 62, pp. 1552–1562,2015.

[15] Energinet, "Technical regulation 3.2.5. for wind power plants with a power output greater than 11 kW," Energinet, Fredericia, DK, 2010.

[16] M. Mohseni, and S. M. Islam, "Review of international grid codes for wind power integration: diversity, technology and a case for global standard," *Renewable and Sustainable Energy Reviews*, vol. 16, no. 6, pp. 3876–3890, Aug. 2012.

[17] M. S. El-Moursi, G. Joos, and C. Abbey, "A secondary voltage control strategy for transmission level interconnection of wind generation," *IEEE Trans. Power Electronics*, vol. 23, no. 3, pp. 1178–1190, May, 2008.

[18] N. Qin, H. Abildgaard, P.Lund, E. Dmitrova, T. Lund, P. B. Eriksen, C. L. Bak, and Z.Chen, "Automatic Voltage Control (AVC) of Danish Transmission System-Concept design," presented at the CIGRE US National Committee, 2014 Grid of the Future Symposium.

[19] J. Tian, C. Su, and Z. Chen, "Reactive Power Capability of the Wind Turbine with Doubly Fed Induction Generator," in *Proc. 2013 39th IEEE Industrial Electronics Society Conf.,* pp. 5310–5315.

[20] T. Lund, P. Sorensen, and J. Eek, "Reactive power capability of a wind turbine with doubly fed induction generator," *Wind Energy*, vol. 10, pp. 379–394, Apr. 2007.

[21] D. Hansen, P. Sorensen, F. Iov, and F. Blaabjerg, "Centralised power control of wind farm with doubly fed induction generators," *Renewable Energy*, vol. 31, no. 7, pp. 93.

[22] M. Soleimanzadeh, Wind Farms: Modeling and Control. 2012.

[23] R. J. Barthelmie, K. Hansen, S. T. Frandsen, O. Rathmann, J. G. Schepers, W. Schlez, J. Phillips, K. Rados, A. Zervos, E. S. Politis, and P. K. Chaviaropoulos, "Modelling and measuring flow and wind turbine wakes in large wind farms offshore," *Wind Energy*, vol. 12, no. 5, pp. 431–444, 2009.

[24] N. G. Mortensen, D. N. Heathfield, L. Myllerup, L. Landberg and O. Rathmann, Wind Atlas Analysis and Application Program: WAsP 8 Help Facility. Risø National Laboratory, Roskilde, DK. 335 topics. ISBN 87-550-3457-8, 2005.

[25] J. Jonkman, S. Butterfield, W. Musial, and G. Scott, "Definition of a 5-MW Reference Wind Turbine for Offshore System Development," Golden, CO: National Renewable Energy Laboratory, Tech. Rep. NREL/TP-500-38060, Feb. 2009.

[26] Z. S. Zhang, Y. Z. Sun, J. Lin, and G. J. Li, "Coordinated frequency regulation by doubly fed induction generator-based wind power plants," *IET Renew. Power Gen*., vol. 6, no. 1, pp. 38-47, Jan. 2012.

[27] J. G. Slootweg, S. W. H. de Haan, H. Polinder, W. L. Kling, "General model for representing variable speed wind turbines in power system dynamics simulations," *IEEE Trans. Power Syst*., vol. 18, no. 1, pp. 144-151, Feb. 2003.

[28] G. Abad, J. Lopez, M. Rodriguez, L. Marroyo, G. Iwanski, Doubly Fed Induction Machine, CA: Wiley, 2011, PP. 15.

[29] R. Amro, J. Lutz, and A. Lindemann, "Power cycling with high temperature swing of discrete components based on different technologies," *in Proc, of PESC 2004*, pp. 2593-2598, 2004.

[30] R. J. Templin, An estimation of the interaction of windmills in widespread arrays, National Aeronautical Establishment, Lab. Report LTR-LA-171, Ottawa, 1974.

[31] B. G. Newman, "The spacing of wind turbines in large arrays," *Energy Conversion*, vol. 16, pp. 169-171, 1977.

[32] E. A. Bossanyi, G. E. Whittle, P. D. Dunn, N. H. Lipman, P. J. Musgrove and C. Maclean, "The efficiency of wind turbine clusters," in *Proc. International Symposium on Wind Energy Systems*, Lyngby, pp.401-416, 1980.

[33] S. Frandsen, "On the wind speed reduction in the center of large clusters of wind turbines," *J. Wind Engineering and Industrial Aerodynamics*,; vol. 39, pp. 251-265, 1992.

[34] S. Emeis and S. Frandsen, "Reduction of horizontal wind speed in a boundary layer with obstacles," *Boundary- Layer Meteorology*, vol.64: pp.297-305, 1993.

[35] A. Crespo, J. Hernandez and S. Frandsen, "Survey of modelling methods for wind turbine wakes and wind farms," *Wind Energy*, vol.2, pp.1-24, 1999.

[36] Aerospace Engineering post, Available online: http://aerospaceengineeringblog.com/boundary-layers/ (18 Sep, 2016)

[37] P. B. S. Lissaman, "Energy effectiveness of arbitrary arrays of wind turbines", *American Institute of Aeronautics and Astronautics, 17th Aerospace Sciences Meeting*, New Orleans, 1979.

[38] D. Katic, Højstrup and N. O. Jensen, "A sample model for cluster efficiency," in *Proc. 1986 European Wind Energy Association Conf*., pp. 407-410, 1986.

[39] N. O. Jensen, A note of wind generator interaction, Tech. Rep. Risø-M-2411, 1983.

[40] N. G. Mortensen, D. N. Heathfield, L. Myllerup, L. Landberg and O. Rathmann, Wind Atlas Analysis and Application Program: WAsP 8 Help Facility. Risø National Laboratory, Roskilde, DK. 335 topics. ISBN 87-550-3457-8, 2005.

[41] European Wind Turbine Standards II, Part 1 Sub A, Wind farms – wind field and turbine loading.

[42] G. C. Larsen, J. Hùjstrup, and H. A. Madsen, "Wind fields in wakes," in *Proc. 1996 European Union Wind Energy Conf.,* pp. 764-768, 1996.

[43] P. M. Sforza, W. Stasi, M. Smorto, P. Sheerin, "Wind turbine generator wakes, American Institute of Aeronautics and Astronautics," *17th Aerospace Sciences Meeting*, New Orleans, 1979.

[44] P. A. Taylor, "On wake decay and row spacing for WECS farms," *3rd International Symposium on Wind Energy Systems*, Lyngby, pp.451-468, 1980.

[45] M. K. Liu, M. A. Yocke and T. C. Myers, "Mathematical model for the analysis of wind-turbine wakes,", *J. Energy*, vol.7, pp.73-78, 1983.

[46] A. Crespo, F. Manuel, D. Moreno, E. Fraga and J. Hernandez, "Numerical analysis of wind turbine wakes," in *Proc. Delphi Workshop on Wind Energy Applications*, Delphi, pp.15-25, 1985.

[47] J. F. Ainslie, "Calculating the flowfield in the wake of wind turbines," J. *Wind Eng. Ind. Aerodyn*., vol.27, no.1–3, pp.213–224, 1988.

[48] M. Soleimanzadeh, Wind Farms: Modeling and Control. 2012.

[49] R. J. Barthelmie, K. Hansen, S. T. Frandsen, O. Rathmann, J. G. Schepers, W. Schlez, J. Phillips, K. Rados, A. Zervos, E. S. Politis, and P. K. Chaviaropoulos, "Modelling and measuring flow and wind turbine wakes in large wind farms offshore," *Wind Energy*, vol. 12, no. 5, pp. 431–444, 2009.

[50] J. Tian, D. Zhou, C. Su, F. Blaabjerg and Z. Chen, "Wake effects on lifetime estimation in DFIG-based wind farms," in *Proc. of IEEE International Future Energy Electronics Conf. 2017 - ECCE Asia*, 2017.

[51] M. Steinbuch, W. W. de Boer, O. H. Bosgra, S. Peters, and J. Ploeg, "Optimal control of wind power plants," *J. Wind Eng. Ind. Aerodyn*., vol. 27, nos. 1-3, pp. 237-246, Jan. 1988.

[52] G. P. Corten, P. Schaak, "More power and less loads in wind farms: 'heat and flux'," in *Proc. European wind energy conference & exhibition*, pp.1-10, 2004.

[53] G. C. Larsen, H. Aagaard Madsen, N. Troldborg, T.J. Larsen, P.E. Réthoré, P. Fuglsang, S. Ott, J. Mann, T. Buhl and M. Nielsen, TOPFARM-next generation design tool for optimisation of wind farm topology and operation, Tech. Rep., Risø-R-1805(EN), 2011.

ISSN (online): 2446-1636
ISBN (online): 978-87-7112-942-7

AALBORG UNIVERSITY PRESS